Final Storage of Spent Nuclear Fuel – KBS-3

I General
II Geology
III Barriers
IV Safety

SKBF/KBS

Final Storage of Spent Nuclear Fuel – KBS-3

III Barriers

SKBF/KBS
Swedish Nuclear Fuel Supply Co/Division KBS
MAILING ADDRESS: SKBF/KBS, Box 5864, S-102 48 Stockholm, Sweden
Telephone: 08-67 95 40

TABLE OF CONTENTS

9 BUFFER AND BACKFILL MATERIAL

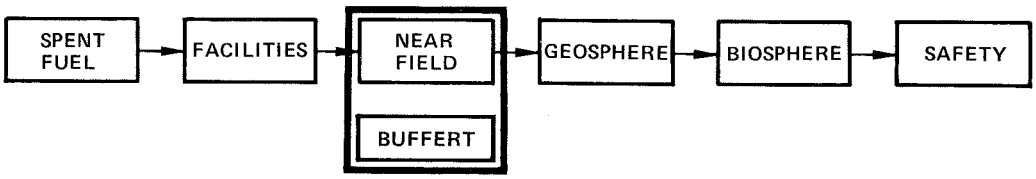

This chapter deals with the clay material, here called buffer material, that is applied between the canister and the rock in the deposition holes, as well as the clay/sand mixture with which tunnels and shafts are backfilled when the repository is sealed.

9.1 GENERAL

The function of the buffer material is to constitute a mechanical and chemical zone of protection around the canister and to limit the inward transport of corrosive substances from the groundwater to the canister surface, and in a later stage to limit the outward transport of leached radioactive substances from the canister.

The function of the backfill in tunnels and shafts is a) to preserve the mechanical stability of the excavated spaces, and b) to restore the hydrological conditions in the area.

Figure 9-1 shows how the buffer material is applied in deposition holes and tunnels.

9.2 PROPERTIES OF THE BUFFER MATERIAL

9.2.1 General

By using pure bentonite of high density, a buffer material is obtained that has very low hydraulic conductivity and diffusivity and otherwise has the following desirable properties:

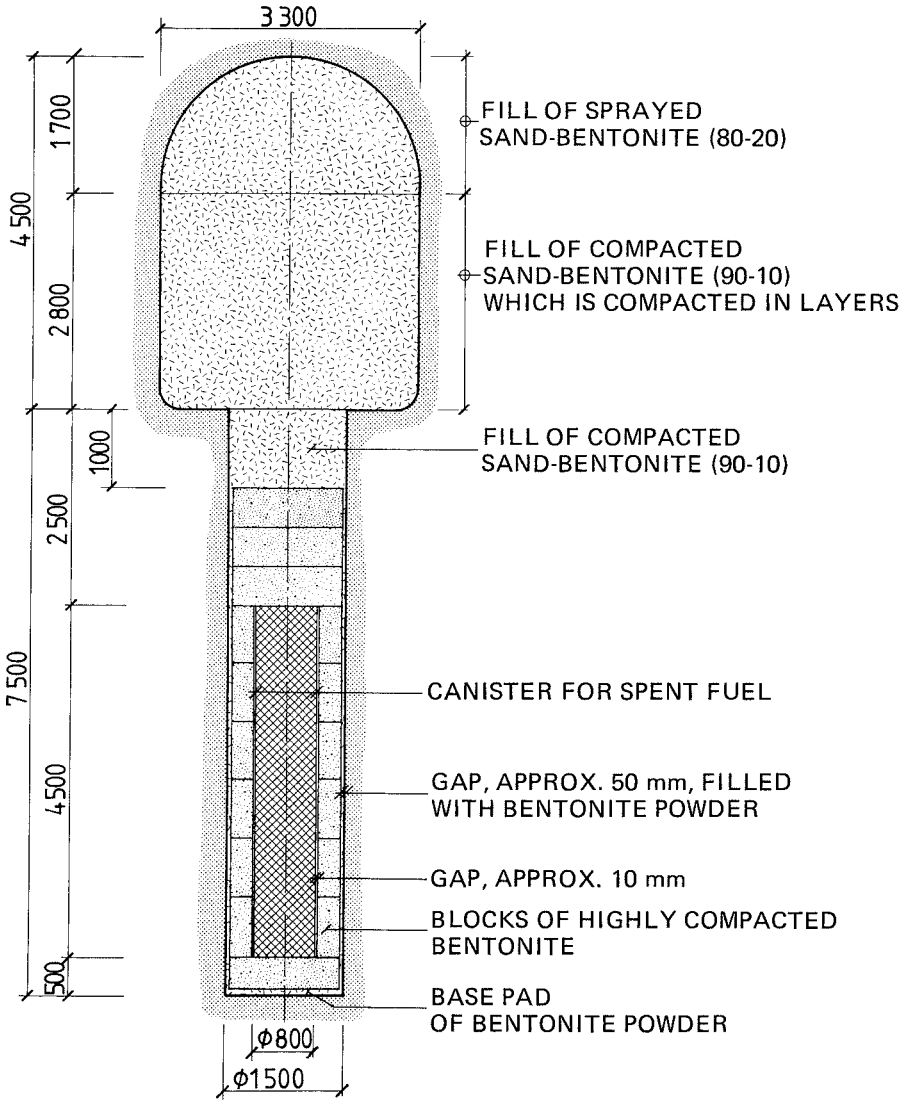

Figure 9-1. Schematic drawing of depostion hole.

- good bearing capacity, so that the canister is held in its position in the deposition hole

- good thermal conductivity, so that the heat given off by the fuel in the canister is transferred to the rock without the canister or the buffer material reaching too high a temperature

- long-term stability, so that the material retains its properties over the very long period of time during which the function of the final repository is to be upheld.

The material should not contain components that can significantly increase the rate of corrosion of the copper canister. A pH-buffering function is desirable from the corrosion viewpoint, and bentonite is favourable in this respect: its pH is about 8-9 in the water-saturated condition. Bentonite also has a good ion exchange capacity, so that any positively charged radionuclides that escape from the canister are retarded.

Bentonite of high density is characterized by the capacity to swell greatly when it absorbs water. If swelling is restrained, a high swelling pressure is instead created /9-1/. This property leads to self-healing and homogenization and prevents water-bearing passages from being created in the material. Owing to the swelling pressure, the bentonite also penetrates into and seals any fractures that may exist in the walls of the storage hole.

Because many of the properties of the buffer material which are fundamental to its function are dependent upon a sufficiently high density being obtained in the storage hole, the bentonite is applied in the hole in the form of highly-compacted blocks. Under the influence of penetrating groundwater, the bentonite swells and fills out the spaces and cavities remaining after the application procedure. The swelling is restrained by the surrounding rock and the fill in the overlying tunnel so that a sufficiently high density is maintained. The bentonite's water absorption proceeds slowly and is also counteracted to some extent by the heat given off by the canister.

Even if a high density of the buffer material is desirable, there is an upper limit, since excessively high swelling pressures can give rise to undesirable stresses in the surrounding rock. The chosen design gives a density of 2.0-2.1 t/m^3, which is judged to be a suitable value in view of the function of the material. Moreover, it allows a relatively simple manufacturing and application procedure.

Figure 9-2. Isostatically pressed bentonite can be formed into blocks of regular shape, which can then be assembled together with good fit.

9.2.2 Composition

Bentonite is the geological name of clays occurring in nature formed from volcanic ashes. These clays are rich in swelling clay minerals, smectites, of which montmorillonite is a common variety. Such clays have numerous applications, both within foundry and oil drilling technology and within construction technology and are commercially available in different forms. A bentonite designated Volclay MX-80, which is mined in Wyoming and South Dakota in the United States has been chosen as a reference material. Other types of natural or synthetic smectite can also be used. MX-80 is a

so-called sodium bentonite consisting of 90% montmorillonite, with sodium as the dominant adsorbed ion. This ion coating provides the best sealing and swelling properties, but bentonite saturated with calcium can also have satisfactory properties /9-2/. Commercially available calcium bentonites produce roughly the same swelling pressures as sodium bentonite at the densities attained in the highly-compacted state. Hydraulic conductivty, however, is approximately five times higher and homogenization capacity poorer than in sodium bentonite. Partial ion exchange from sodium to calcium can occur in the deposition holes, but the resultant increase in hydraulic conductivity is without practical importance /9-3/.

The main chemical components of Volclay MX-80 are silicon and aluminium. The substance also contains smaller quantities of sodium, magnesium and iron as well as calcium and potassium.

The grain size of granulate is about 0.07-0.8 mm and its specific gravity is 2.7 t/m^3. For a more detailed description of the properties and structure of bentonite, see /9-4/.

Bentonite can contain organic matter that can be of importance for canister corrosion, see chapter 10. The organic content of the bentonite should not exceed 200 mg/kg. If this content is exceeded, the bentonite should be purified, which can be done by heating in air at 425^{o}C for 15 hours. Tests have shown that such a heat treatment does not affect the swelling properties of the bentonite.

9.2.3 Density

The bentonite is applied in the storage hole in the form of fitted blocks (Fig. 9-2) that have been pressed under a pressure of about 100 MPa. The gap that must exist between the blocks and the rock in order to permit application is filled with loose bentonite powder. The filling can be varied to provide the desired final density of the water-saturated material. The bulk density of air-dried material is 2.1-2.2 t/m^3 for the blocks and about 1.2 t/m^3 for the powder in the gaps. The mean density, when all bentonite in the storage hole has been water-saturated and swelling has ceased, is 2.0-2.1 t/m^3. It is determined by the increase in volume which

results from the fact that the joints between the blocks are filled up and the bentonite in the gaps (see Fig. 9-1) is compacted, and by the fact that bentonite from the deposition hole displaces and compresses the sand/ bentonite fill in the overlying tunnel to some extent.

9.2.4 Chemical stability

Natural deposits of bentonite which have been exposed to temperatures, groundwater conditions and pressures similar to those that prevail in the final repository show that the smectite mineral can be counted on to remain chemically stable for the periods of time during which the buffer material must retain those of its properties which are vital to the function of the final repository. Thus, it has been shown that the predominant portion of the smectite content will remain chemically intact for more than one million years as long as the temperature does not exceed 100°C /9-4, 9-5/. With this temperature limitation, other undesirable chemical changes, such as cementing through quartz precipitation, will also be negligible /9-4/.

9.2.5 Hydraulic conductivity and diffusivity

The hydraulic conductivity (permeability) of smectite-rich clays as a function of density is well-known from both the literature and extensive laboratory studies with different bentonites /9-3/.

The general relationship is illustrated by the graph in Fig. 9-3. At a density of 2.0 t/m^3, hydraulic conductivity is about 5×10^{-14} m/s. This means that the material is virtually impenetrable by water after full water saturation has been attained.

Owing to this low hydraulic conductivity, diffusion will be the dominant mechanism for the transport of ions through the buffer material. The diffusion properties of highly-compacted bentonite have been determined by means of laboratory tests, whereby it has been shown that variations in its bulk density within the range 1.6-2.1 t/m^3 are of little importance /9-6/. Ion size and charge,

(Diagram, ton/m^3 = t/m^3)

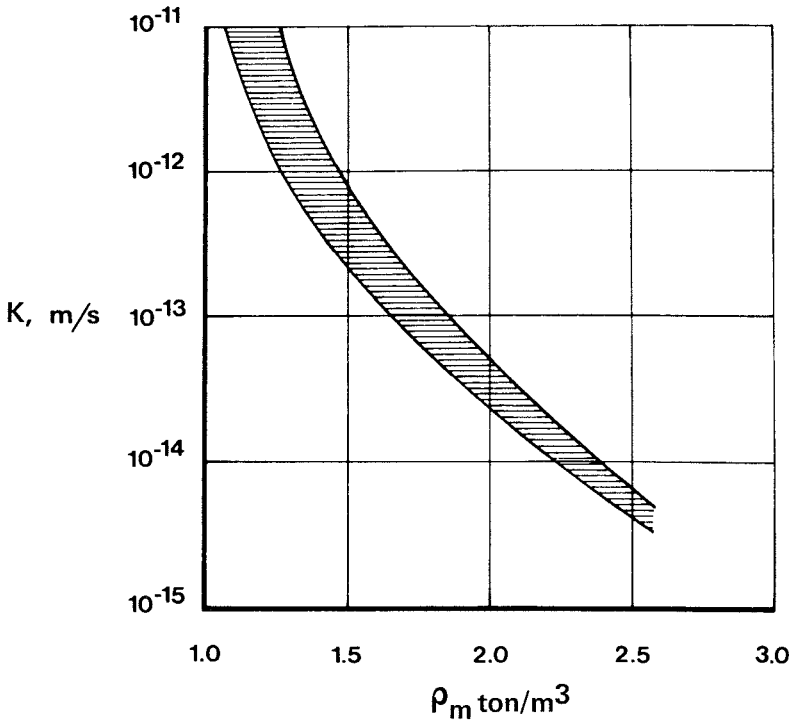

Figure 9-3. The graph illustrates the relationship between hydraulic conductivity (K) and bulk density (ρ_m) for water-saturated sodium bentonite at room temperature. The shaded area between the curves shows the range of variation due to the effects of varying salt content in the pore water and the scatter of experimental measurement data.

on the other hand, play a decisive role in determining the rate at which the ion diffuses /9-7/. Thus, it has been shown that non-sorbing ions (anions), such as iodide and chloride, migrate very slowly. The diffusion coefficients of these ions are less than 6 x 10^{-12} m^2/s.

Cations migrate faster, and here the influence of ion size is clearly evident: the diffusion coefficient for strontium is max. 5 x 10^{-11} m^2/s, while that for cesium is max. 8 x 10^{-12} m^2/s.

9.2.6 Bearing capacity

The blocks of highly-compacted bentonite which are placed in the deposition hole possess very high bearing capacity. In appearance and to the touch, the material resembles talc. Its shear strength is comparable to that of sedimentary rocks. The water ratio of the blocks (i.e. the ratio between the weight of the water and the

weight of the solid material) before application in the deposition holes is about 10%. At full water saturation of the bentonite in the deposition holes, the water ratio is about 25%.

Bearing capacity is a function of the material's density. At the average density the bentonite has in the deposition holes when it is fully water-saturated, 2.0-2.1 t/m^3, the subsidence of the canister caused by gravity after one million years will be less than 10 mm /9-8/. Even at a bulk density of 1.5 t/m^3, the bearing capacity of the bentonite is sufficient to prevent the canister from sinking through the underlying bentonite layer, even over a very long period of time. This means that, even assuming improbably high material losses in the rock, the bentonite will still posses sufficient bearing capacity /9-9/.

Bentonite in contact with water in a fracture in the rock around the deposition hole swells and penetrates out into the fracture. This penetration into the fracture is caused by the fact that the bentonite's swelling pressure in the fracture declines with its distance from the borehole wall. This penetration is counteracted by a flow resistance due to internal forces in the bentonite material and friction against the fracture walls.

If the flow resistance is neglected for all fractures, the penetration rate will only be limited by the water absorption. If the rock around a deposition hole is assumed to have 15 fractures with a maximum width of 0.5 mm, the bentonite will penetrate less than 3 m during one million years. No more than 0.2 m^3 of bentonite can fit into this volume of rock, i.e. about 2% of the bentonite volume in the hole /9-9/.

A calculation with five times more fractures and five times greater fracture width but with flow resistance left in fractures that are smaller than 1 mm gives the result that 3 m^3 of bentonite with a density of 1.5 t/m^3 fills and thereby seals the fractures in the vicinity of the hole. This volume of bentonite corresponds to a density decrease of the bentonite in the storage hole from 2.05 t/m^3 to about 1.9 t/m^3. /9-9/

Flowing groundwater cannot transport away clay particles in such quantity that it will be of importance for the density of the bentonite in the deposition hole. The water velocity in fractures with a width less than 0.5 mm is on the order of 0.1-1 mm/s. This velocity is not sufficient to mechanically dislodge bentonite particles, even in the loosest gel in the groundwaters in question /9-9/.

9.2.7 Swelling pressure

Bentonite that absorbs water under restrained swelling exerts a swelling pressure which is a function of the density of the material. The ratio between swelling pressure and density has been determined by means of extensive tests for MX-80 and compared with theoretical calculations /9-1/. At a bulk density of 2.0-2.1 t/m^3, the swelling pressure is about 10 MPa, which has been verified by large-scale field tests in the Stripa mine. A swelling pressure of this order of magnitude is suitable for the purpose of largely restoring the original state of stress in the rock surrounding the deposition holes as well as providing a sufficiently high swelling potential. Fig. 9-4 shows the general relationship between bulk density and swelling pressure.

9.2.8 Thermal conductivity

The thermal conductivity of air-dried highly-compacted bentonite with a bulk density of 2.1 t/m^3 and a water ratio of about 5-14% has been determined to be about 0.96-1.15 $W/(m \cdot K)$ /9-10/. Corresponding values of heat capacity are 2.02-2.56 $MJ/(m^3 \cdot K)$. Water will penetrate into the bentonite in the deposition holes, causing the thermal conductivity to increase to 1.5 $W/(m \cdot K)$. During a transitional period, thermal conductivity will be lower due to gaps between the bentonite blocks, the canister and the rock as well as some drying-out of the bentonite nearest the canister. Measurements in the laboratory /9-11/ and in field tests in Stripa show that the effective thermal conductivity will be about 0.75 $W/(m \cdot K)$. The maximum temperature of the canisters is estimated to reach 80°C (cf. section 4.5.4), which provides a good margin to 100°C and does not the chemical stability of the smectite minerals /9-4/.

(Diagram, ton/m^3 = t/m^3)

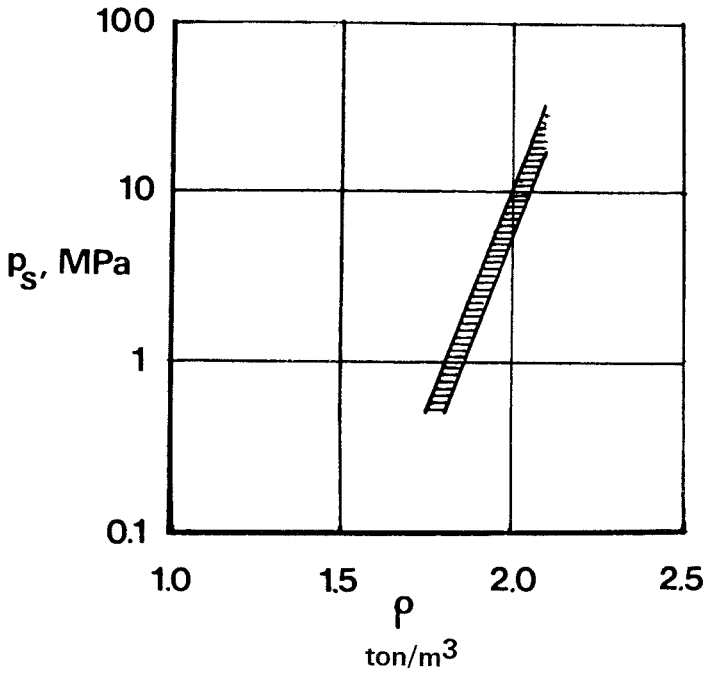

Figure 9-4. The graph illustrates the relationship between swelling pressure (p_S) and bulk density (ρ). The shaded area between the curves shows the range of variation caused by differences in groundwater composition.

9.2.9 Ion exchange capacity

Owing to its high content of the clay mineral montmorillonite, bentonite possesses a considerable capacity to retard certain nuclides through ion exchange. These matters are dealt with in chapter 12.

9.3 FUNCTION OF THE BUFFER MATERIAL

Following deposition, water will penetrate into the deposition holes. Water absorption in the bentonite takes place relatively slowly; in most holes, it will take several years until full water saturation is reached, and in some holes, it may take several tens of years. If surface water in tunnels is prevented from flowing into the deposition hole, there will not be enough time during the period before backfilling of a storage tunnel for water saturation to occur in the normal case. Surface water is kept out by casting a

concrete slab with raised lip before drilling the hole, which is covered after it has been filled with the canister and bentonite. The concrete and the cover are removed just before application of the tunnel fill. Tendencies towards excessively rapid swelling can, if necessary, be kept under control during the interval until tunnel backfill by propping between the cover and the tunnel roof.

In connection with water absorption in the bentonite, so-called wetting heat is generated that leads to some temperature increase. However, the absorption of water simultaneously increases the thermal conductivity of the bentonite, and the influence of the wetting heat can therefore not be distinguished from the influence of the heat from the canister. This is confirmed by the ongoing field tests in Stripa.

When the final repository has been sealed, the original groundwater conditions are gradually restored. Water then enters from the overlying tunnel as well and is absorbed by the highly-compacted bentonite. As the bentonite absorbs more and more water, its hydraulic conductivity decreases, so that water absorption takes place at an increasingly slow rate.

The swelling pressure forces the bentonite into fractures in the walls of the deposition holes, sealing them. The density of bentonite penetrated into a fracture decreases, causing the swelling pressure to decrease rapidly with distance from the hole wall. In the small fissures (width < 0.5 mm) that may open into a storage hole, wall friction causes the penetration of the bentonite to cease after a few decimetres. The outer part of the penetrating bentonite forms a stable gel under the influence of the calcium ions in the groundwater, which means that the transport of bentonite out from fractures by groundwater erosion will be negligibly small /9-9/.

As a result of the swelling, the highly-compacted bentonite in the deposition holes will bulge up a few dm into the sand/bentonite fill in the tunnel above. The previously stated final density of 2.0-2.1 t/m^3 has been calculated taking this volume increase into consideration. This density may be slightly lower in the top part of the storage hole and higher in the bottom part, but the dif-

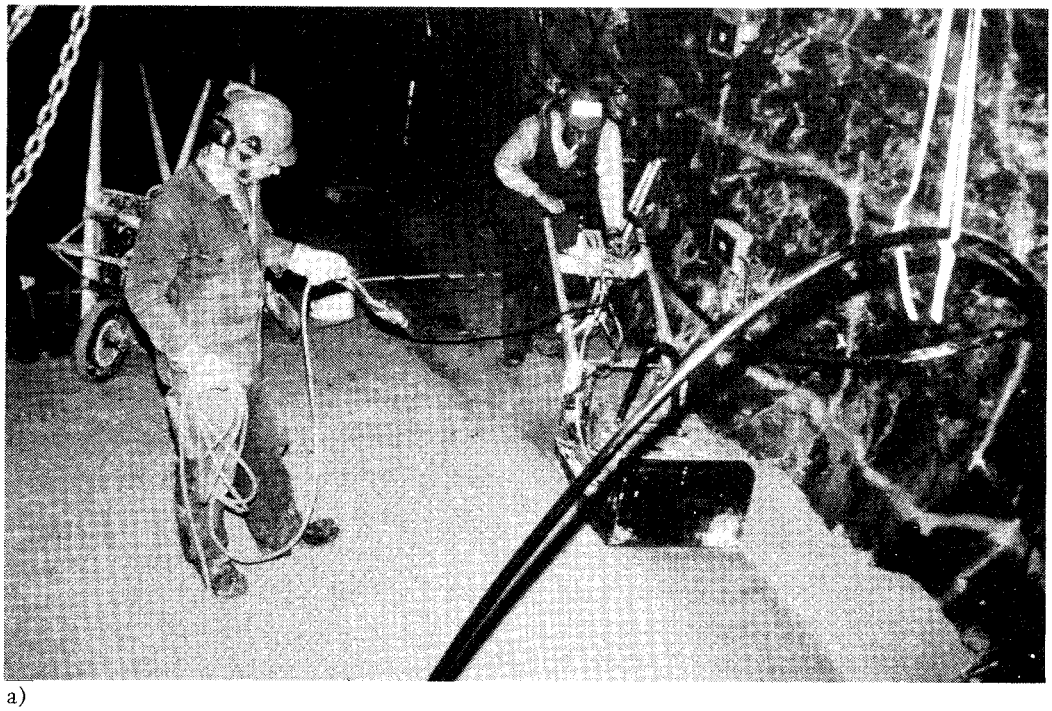

a)

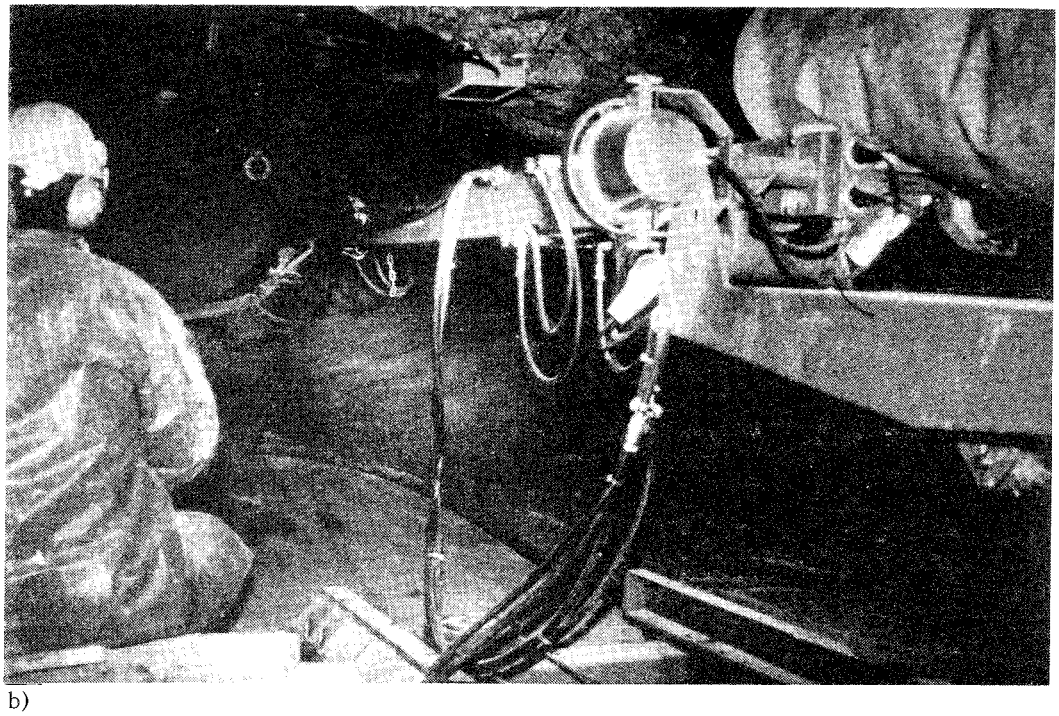

b)

Figure 9-5. Backfilling with sand/bentonite in tunnel in field test in Stripa: a) layer-by-layer compaction by vibration, b) spraying with shotcrete equipment.

ferences will not be great enough to affect the function of the buffer material. The bentonite cannot penetrate into the pores in the sand/bentonite fill in the same manner as it penetrates into fractures, since the pores are too small.

If the original distribution of stresses and orientation of fractures in the rock are unfavourable, the swelling pressure can widen some fractures. But it can be shown that this influence will not extend beyond a few metres in length and will give rise to an insignificant loss of bentonite. The density of the bentonite is therefore affected only marginally /9-9/.

9.4 BACKFILL MATERIAL

The tunnels and shafts in the final repository are backfilled with bentonite-based material whose primary functions are to provide a durable support for the rock and restore the hydraulic conditions in the area. The backfill shall therefore have at least as low hydraulic conductivity as the rock mass it replaces. For this purpose, a homogeneous mixture of 10-20% bentonite powder and the rest sand of a suitable grade shall be used /9-2/. Mixing and homogenizing should preferably be done in large mixers, and the backfill should be applied in layers that are compacted with a number of passes. Nearest the roof, the tunnel is filled by spraying the backfill with shotcrete equipment. Experiences from compactions in field tests in Stripa (see Fig. 9-5) show that a density of 1.8-2.2 t/m^3 is achieved by the first method, with a water ratio of 8-13%, while a density of 1.1-1.8 t/m^3 and a water ratio of 11-22% are achieved with the second method /9-12/.

The hydraulic conductivity of the bentonite-sand mixture amounts to a maximum of 10^{-9} m/s /9-10/.

9.5 PLUGGING OF BOREHOLES AND SEALING OF TUNNELS AND SHAFTS

Even if the final repository is situated in a selected rock formation with low fracture frequency, it must be expected that the tunnels at some places will intersect sections of rock with eleva-

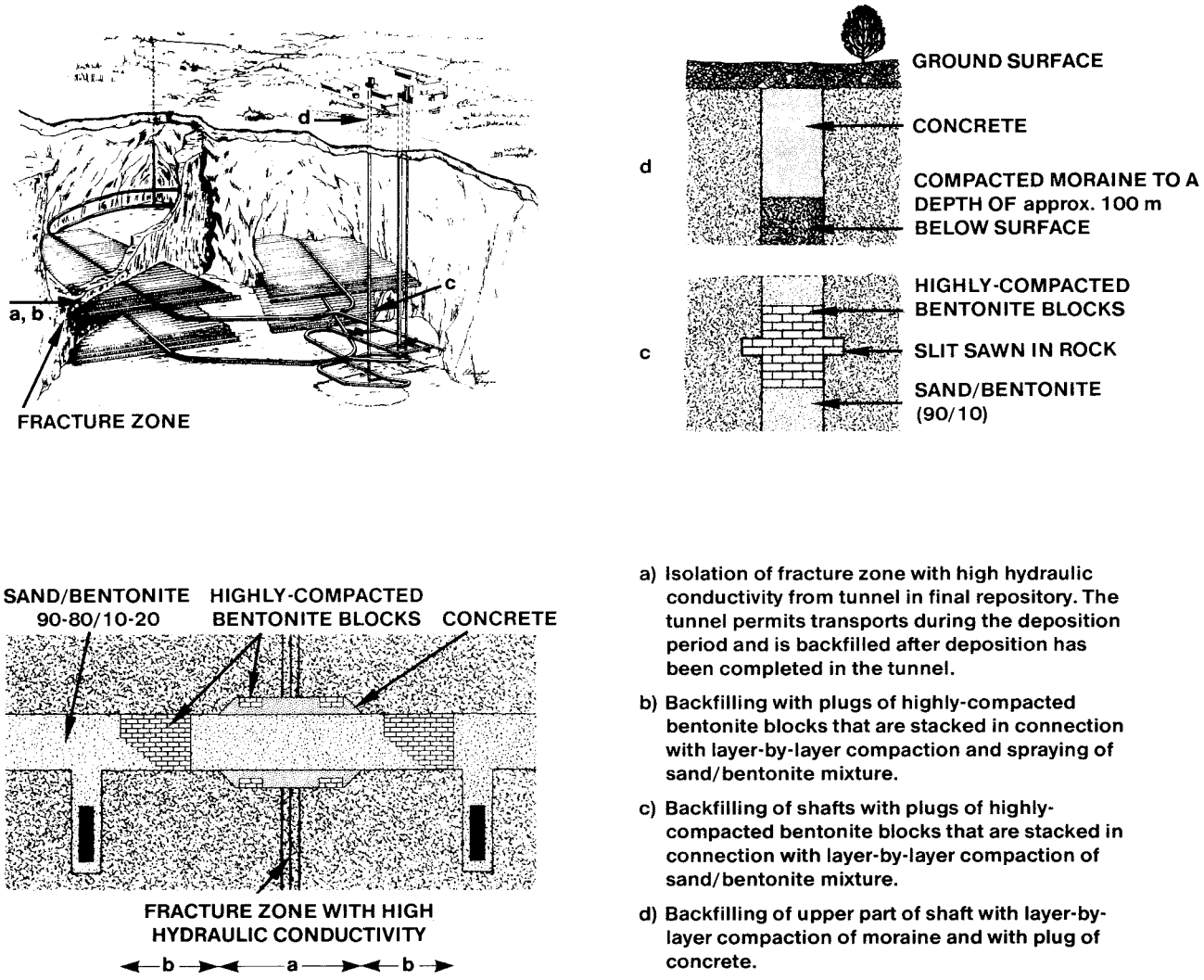

Figure 9-6. Plugs of highly-compacted bentonite in tunnels and shafts in the final repository.

ted groundwater flow. Such sections are not used for waste storage and are isolated from their surroundings in the manner illustrated in Fig. 9-6. The shafts are backfilled for the most part with the same backfill material as the tunnels, except that the upper part is filled with concrete and moraine. Plugs of highly compacted bentonite are used in combination with slits for sealing the rock zone that may have been affected by the blasting. As in the storage holes, the highly-compacted bentonite swells and creates a tight seal with the rock while simultaneously displacing a certain volume of the adjacent fill material, until a state of equilibrium is

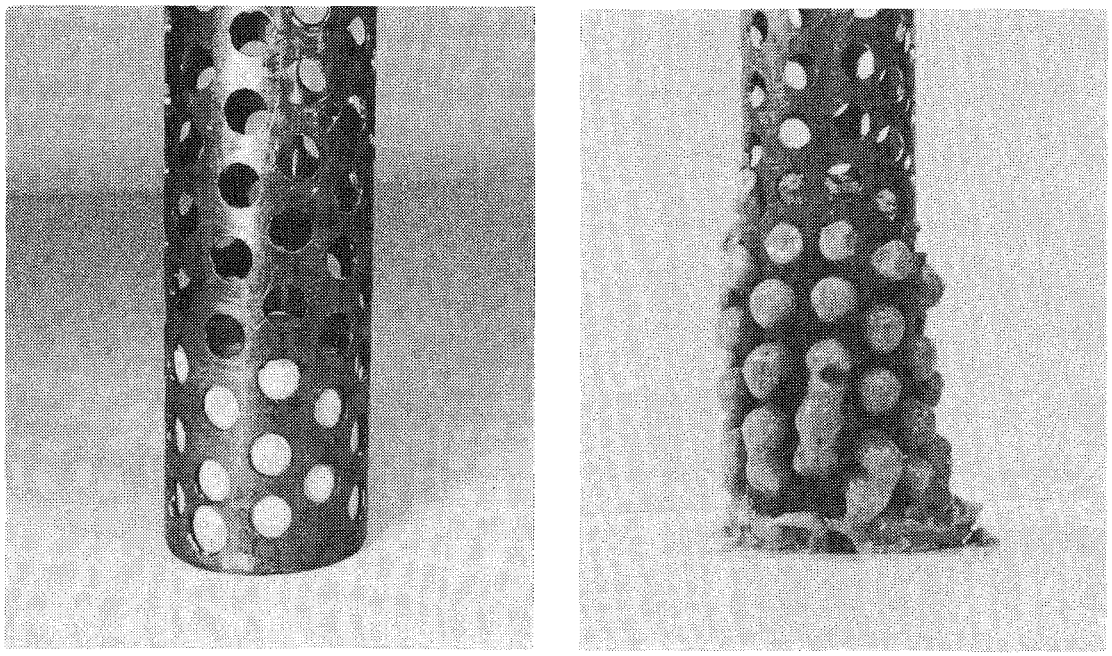

Figure 9-7. Perforated metal tube with pellets of highly-compacted bentonote. At left: Before immersion in water. At right: After 24 hours in water.

achieved. The final density of the highly-compacted bentonite is estimated at 1.9-2 t/m^3, which gives a hydraulic conductivity of 10^{-12} m/s or less, which is equivalent to highly impervious rock.

For the sealing of boreholes that have been drilled in connection with preliminary investigations of various kinds, highly-compacted cylindrical bentonite pellets are placed in the holes. The pellets are applied in tubes, which are joined together and inserted into the holes. About 50% of the surface of the tubes is perforated with holes with a diameter of about 1 cm. On absorbing water, the bentonite swells and fills the borehole in the form of a homogeneous mass with a final density of 1.7-2.0 t/m^3, see Fig. 9-7 /9-13/. Where the boreholes pass through highly fractured rock, where there is a risk of material loss, pellets of sand/bentonite or magnesium oxide can be used. The former type contains coarser grains which block fracture openings. The magnesium oxide is hydrated, swells and forms tightly-sealing stable plugs of $Mg(OH)_2$ (brucite).

9.6 QUALITY CONTROL

Commercial bentonite powder can be used as a starting material for the manufacture of blocks of highly-compacted bentonite. Bentonites containing large amounts of certain minerals - e.g. calcite, graphite and pyrite - should, however, be avoided. The properties that are above all desirable - i.e. low hydraulic conductivity, good swelling capacity and ion exchange capacity - are proportional to the smectite content. It is therefore desirable to use as smectite-rich bentonite as possible. The following criteria and checks should be applied:

1. The clay content (fraction of particles smaller than 2 um) should be at least 80% by weight. This is checked by sedimentation analysis.

2. Smectite minerals should constitute at least 70% of the clay fraction. Mineral identification is done by mans of X-ray diffraction analysis. Continuous delivery inspection is carried out by means of liquid limit determination (W_L > 250%) or an equivalent method.

3. The bentonite's content of sulphides and organic matter shall each be lower than 200 mg/kg (cf. chapter 10). Checked by means of chemical analysis.

The bentonite of type Volclay MX-80 which has been tested within the KBS Project meets these requirements, but heat treatment has been necessary to reduce the content of sulphides and organic matter to the above-specified value.

10 THE CANISTER AND CANISTER CORROSION

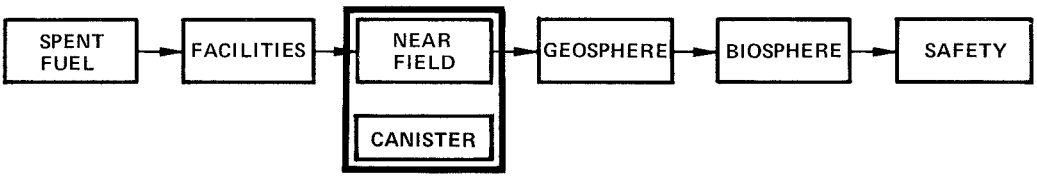

This chapter describes the premises for the choice of canister material, applicable methods for manufacture and quality control and the mechanical and chemical action that can be entailed by final storage. The chapter is concluded with an evaluation of the minimum time it will take for canisters of varying wall thickness to be penetrated.

10.1 FUNCTION OF THE CANISTER

The purpose of the canister is to contain the spent fuel for a long period of time and thereby prevent the dispersal of radioactive substances with the groundwater. Only when the canister has been penetrated through corrosion or if canister failure has been caused by mechanical stresses can such dispersal occur.

The wall thickness of the canister is decisive in determining the earliest point in time at which penetration caused by corrosion can be expected to take place. Variations within a final repository of groundwater flow, groundwater composition and the nature of the corrosion attack lead to a considerable dispersion in time of the individual canister penetrations. In addition to prolonging the life of the canisters, a greater wall thickness also leads to a greater dispersion in time of the individual canister penetrations. These factors, as well as the rate of decay of the radioactive substances in the fuel, serve as the premises for the choice of canister wall thickness.

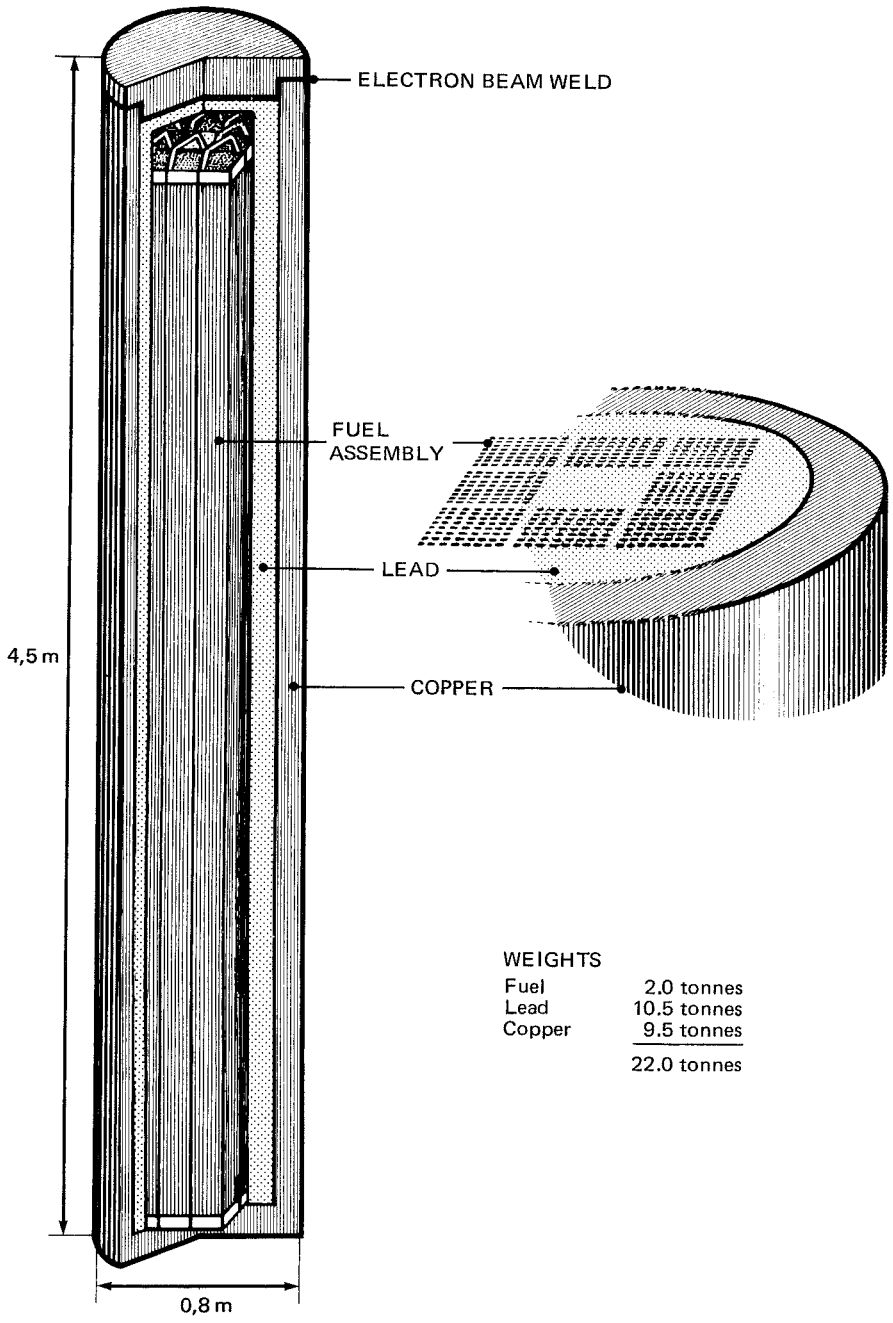

Figure 10-1. Welded copper canister.

10.2 CHOICE OF MATERIAL

In the final repository, canister damage will be determined by the chemical environment prevailing in the storage hole. The composition of the groundwater is of fundamental importance here. Since very high demands are made on canister life, it would be desirable to have access to a canister material that is thermodynamically stable in the environment in question. This would make it unnecessary to evaluate corrosion kinetics data in determining canister life.

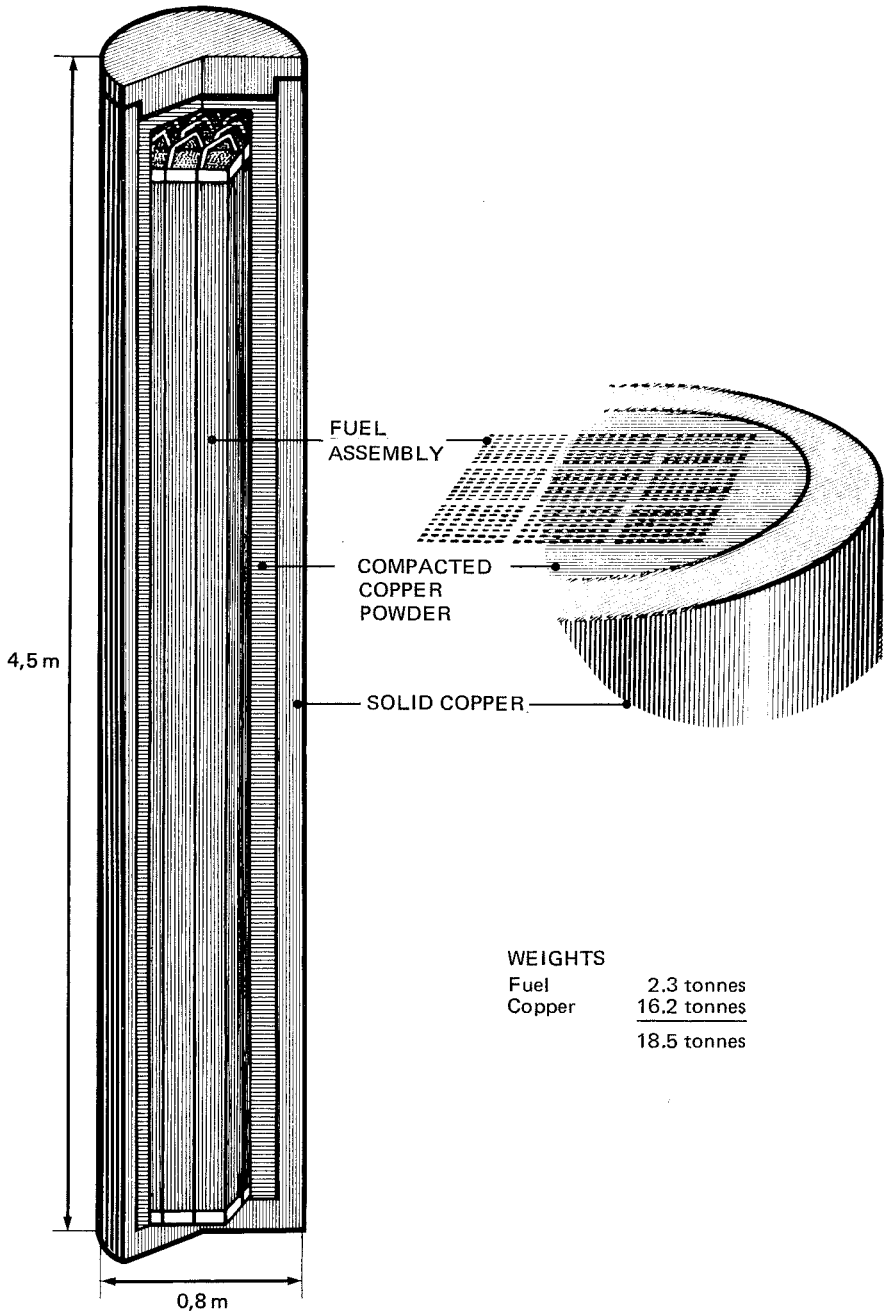

Figure 10-2. Copper canister produced by hot isostatic pressing.

Copper is the noblest (i.e. least reactive) of the common engineering materials. It is thermodynamically stable in pure water. This means that the corrosion of copper in the groundwater will be determined by the supply of corrosive substances dissolved in the water. These substances are primarily dissolved oxygen and, for reducing groundwater conditions, dissolved sulphide.

Unalloyed copper has therefore been chosen as the canister material. For reasons of corrosion resistance and ease of fabrication, two

types of oxygen-free copper have been studied: Oxygen Free High Conductivity Copper (OFHC) and Phosphorous-Deoxidized High Conductivity Copper (PHC).

10.3 METHOD OF MANUFACTURE AND QUALITY CONTROL

As explained in section 4.4, there are two alternative encapsulation procedures: One where the canister is filled with lead and sealed by electron-beam welding and one where the canister is filled with copper powder and sealed by means of hot isostatic pressing (HIP), at the same time as the copper powder is compacted. In both alternatives, the canister is prefabricated of oxygen-free forged copper.

10.3.1 Sealing by means of electron-beam welding

In the electron-beam welding alternative, the space between the fuel assemblies and the copper wall is filled with lead. The quantity of fuel in a canister is determined by the residual heat of the fuel (cf. section 4.4.2). After the top surface of the lead has been face-machined, a lid (see Fig. 10-1) is applied, which is welded on radially by means of electron-beam welding /10-2/.

10.3.2 Sealing by means of hot isostatic pressing

In the hot isostatic pressing alternative, the space between the fuel and the copper canister is filled with copper powder, which is compacted by vibration to a level corresponding to the lower edge of the lid, see Fig. 10-2. The lid is then applied and the canister with lid is placed in a thin-walled container. After the air has been pumped out, the container with canister and copper powder are pressed at 500^{o}C and 150 MPa to a homogeneous body. At whereby the lid is sintered together with the canister /10-1/.

10.3.3 Quality requirements and quality control

In order to ensure safety and operational availability in the encapsulation station and safety in the final repository, effective quality control is required. This control includes quality surveillance of deliveries of raw materials and semimanufactures as well as monitoring of processes and quality control of the final products.

Methods of both manufacture and quality control will be developed and tested in pilot setups in connection with the planning and design of the equipment for canister fabrication.

Inspection and surveillance of finished canisters and raw materials such as copper and lead will be carried out using established quality control methods.

Incoming materials inspection of raw materials can include:

- chemical analysis of stock
- mechanical and metallographical inspection of stock
- visual inspection of surfaces and ultrasonic inspection for internal flaws

Process control can include:

- monitoring and recording of production parameters

Inspection of the canister can include:

- visual inspection of the canister's surfaces and joints
- dimension inspection
- ultrasonic inspection of joints

Recorded deviations from normal process parameters shall occasion more comprehensive inspection and possible rejection of the final product, i.e. the incorrectly performed process is redone.

The most critical step in canister manufacture is sealing of the canister. Inspection of the seal is planned to be carried out in

the form of visual inspection in order to make sure that the external surface of the joint is smooth and pore-free and ultrasonic inspection of the deeper parts of the joint.

The inspection method is tailored to the joining method employed in order to detect the most probable defects. In the case of a hot isostatically pressed joint, the most probable defects are defective bonding (lamination) between two plane surfaces. An electron-beam welded joint is mainly expected to have defects in the form of pores, either of nearly spherical shape or in the shape of elongated (cylindrical) cavities /10-2/.

Tests with ultrasonic inspection have shown that it is possible to detect pores (cavities) with a diameter less than 2 mm through 100 mm thick copper and by means of immersion testing with focussed ultrasound /10-3/.

10.4 MECHANICAL ACTION ON THE CANISTER

Mechanical stresses will exist in the body of the copper canister whose origin may be traced to fabrication and handling or conditions in the final repository. Depending on the method of manufacture, these mechanical stresses vary somewhat between the welded canister and the hot isostatically pressed canister.

10.4.1 Residual stresses from manufacture

By means of stress relief annealing, the starting material, i.e. the empty canister and the lid, can be rendered stress-free prior to filling and sealing. During hot isostatic pressing, however, the compaction of the copper powder together with the differences in thermal expansion between the copper and the fuel assemblies, will give rise to residual stresses in the surface of the canister after cooling to equilibrium temperature. These stresses are so large that it must be assumed that the copper will be deformed plastically. Calculations have shown that the canister will have annular stresses of 45-105 MPa, while the axial stresses will be about 120 MPa /10-1/, i.e. well below the ultimate strength of copper

(for fully annealed copper about 225 MPa, for cold-drawn copper about 450 MPa).

In the case of the welded canister, residual stresses can arise in connection with welding-on of the lid. It is reasonable to assume that these stresses are so large that the copper is deformed plastically in the weld zone and that the size of the stresses is comparable to those obtained in hot isostatic pressing.

10.4.2 External forces

Water absorption and swelling of the bentonite, together with the hydrostatic pressure at the repository depth, give rise to a nearly isostatic pressure of a maximum of 15 MPa. In the case of the isostatically pressed canister, which has been subjected during manufacture to a considerably higher pressure (about 150 MPa), this external pressure will more likely reduce the tensile stresses in the copper and therefore scarcely leads to higher mechanical stresses on the canister.

The welded, lead-filled canister must be assumed to have pores in the lead fill, partly due to incomplete lead filling and partly due to the fact that a space must be left between the top surface of the lead and the bottom of the lid in order to permit problem-free lid application and welding. The external pressure then causes the lead to fill these pores by creep, with the result that the copper canister can be deformed. The stresses caused by external forces are judged to lie well below the ultimate strength of copper.

10.4.3 Internal forces

During the final storage period, an internal pressure of helium will be built up due to alpha decay in the fuel rods. This helium pressure will, in the most unfavourable cases (PWR fuel 45 MWd/kgU /10-4/), amount to about 16 MPa after 10^6 years. This is approximately the same pressure as the external pressure on the canister from the bentonite and the hydrostatic pressure at a depth of about 500 m. In other words, the evolution of helium in the fuel will not

give rise to stresses in the canister that exceed the initial canister stresses caused by hot isostatic pressing or electron-beam welding.

10.5 CHEMICAL ACTION ON THE CANISTER

10.5.1 Chemical environment

Since copper is stable in pure water, corrosion can only be caused by substances dissolved in the groundwater. The corrosion environment of the canister is defined by the chemical composition of the groundwater that comes into contact with the canister as well as the composition of the buffer mass. Other parameters that can affect corrosion are temperature and pressure conditions in the repository.

The heat which is generated by the waste gives rise to an elevated temperature next to the canister. The maximum temperature, about 80°C, is reached 50-400 years following deposition, depending on the design of the repository. After several thousand years, the temperature has dropped to about 50°C.

The hydrostatic pressure corresponding to a groundwater depth of 500 m is about 5 MPa. This shall be added to the swelling pressure of the surrounding buffer mass of 5-10 MPa.

The composition of the water in contact with the canister is determined by the composition of the regional groundwater in the repository area and by the composition of the buffer mass. At a canister thickness of several centimetres, radiolysis of the water will not have any significant effect /10-5/.

The composition of the groundwater that has been used in the corrosion evaluations is given in table 10-1. These values are based on analysis results from water samplings of the investigated sites, see chapter 7.

Table 10-1. Assumed composition of deep granitic groundwaters (concentrations in mg/l)

pH	7-9
Eh(V)	0-(-0.45)
HCO_3^-	90-275
SO_4^{2-}	0.5-15
NO_3^-	0.01-0.05
Cl^-	4-15[1)]
HS^-	0-0.5
Ca^{2+}	10-40
Fe^{2+}	0.02-5
Fe (tot)	1-5
NH_4^+	0.05-0.2
TOC	1-8

1) An evaluation has also been done for chloride concentrations of up to 35 000 mg/l.

10.5.2 Corrosion processes, general

Corrosion is a redox process where metals are oxidized. The reaction can take place either electrochemically or through direct chemical attack. Copper is thermodynamically stable in pure water, since hydrogen ions are not a sufficiently strong oxidant.

However, hydrogen ions can serve as an oxidant under the provision that copper ions formed are bound in a compound with a very low free energy (lower than that of the copper oxide). Such a compound is copper sulphide. If sulphide ions are present, copper corrosion can therefore take place to an extent corresponding to the supply of sulphide.

The review of the prerequisites for corrosion reactions at the copper surface which is presented in /10-5/ shows that free oxygen and sulphide are the only substances that can cause corrosion in practice. Thermodynamically, sulphate can also act as an oxidant

with the formation of copper sulphide, if the reaction is coupled to an oxidation of e.g. bivalent iron to trivalent iron. However, geological evidence indicates that this reaction does not take place at all in practice (it is kinetically inhibited). The latter also applies to another thermodynamically possible oxidant, namely nitrate. Moreover, the concentration of nitrate is so low that this oxidant should not have to be taken into consideration /10-5/.

Since the flow of water through the very impervious buffer material is negligible, material transport takes place solely through diffusion.

In addition to these general corrosion phenomena, certain kinds of localized corrosion can also occur. These types of corrosion have been identified as crevice corrosion, stress corrosion cracking and pitting.

10.5.3 Oxygen corrosion

Free oxygen is virtually absent from the groundwater in rock at great depths. This is related to the presence of bivalent iron in minerals in the rock. The maximum concentration of dissolved oxygen in the groundwater around the repository has been conservatively estimated at 0.1 ppm. With a flow of 1 $l/(m^2.year)$, this gives a maximum quantity of copper oxidized through oxygen of less than 3 kg in a million years.

In addition to the quantity of oxygen supplied with the groundwater, relatively large quantities of atmospheric oxygen become entrapped in the pores of the buffer material when the final repository is sealed. By far most of this oxygen is present in the bentonite-sand mixture in the tunnel above the deposition holes. This oxygen will react with Fe(II) in the rock. The oxygen migrates more readily to the tunnel wall and diffuses a few mm into the rock than it diffuses 2.5 m through compacted clay in the hole to the canister. Calculations show that only a few per cent of the oxygen in the tunnel (a few moles of O_2) will reach the copper canister. This amount can oxidize less than 0.5 kg of copper /10-5/.

Another contribution to the supply of oxidant comes from the radiolytic decomposition of water caused by the gamma radiation emitted by the waste. Due to the radiation shielding provided by the copper canister and recombination reactions, however, this effect is relatively limited. In the presence of iron(II), the quantity of copper oxidized due to radiolysis would be less than 10 kg in a million years for a canister with a wall thickness of 60 mm. If the wall thickness is increased to 100 mm or more, the oxidation caused by radiolysis is completely negligible.

When the canister has been penetrated, the alpha radiation can also give rise to radiolysis. However, after the first penetration, the canister is not credited with any barrier function.

10.5.4 Sulphide corrosion

As in the case of oxygen corrosion, the corrosion caused by sulphide can be divided into two components: Sulphide supplied through the groundwater and sulphide from buffer material and tunnel fill. As for oxygen, however, the supply of sulphide in deep groundwaters is limited, among other things through the presence of iron, which binds the sulphide in the form of practically insoluble iron sulphide /10-6/.

In addition to the sulphide supplied by the groundwater and the buffer mass, sulphide can theoretically be formed by the microbiological reduction of sulphate in groundwater and bentonite. This reduction requires the presence of degradable organic matter, which could conceivably be supplied through the groundwater, but is also available in the buffer mass (conservatively estimated at maximum 200 mg/kg). The total quantity of sulphide that can be made available through direct supply and microbial activity corresponds to a corrosion of about 25 kg of copper per canister and million years.

After a possible oxidizing heat treatment, the buffer material contains very small quantities of sulphide: about 200 mg/kg, mainly in the form of practically insoluble pyrite. This quantity of sulphide can corrode a maximum of about 3.5 kg of copper.

The total maximum contribution to copper corrosion from sulphide from tunnels, storage holes and the groundwater flow would amount to 30 kg in one million years.

10.5.5 Chloride corrosion

Hydrogen ions can oxidize copper in the presence of Cl^- at low pH. Such corrosion can conceivably occur in certain crevices and pores, where it is known as crevice corrosion. This can be avoided by making sure that there are no external crevices or pores in the canister design. The gap that exists between the buffer mass and the canister wall is not expected to lead to crevice corrosion, since the buffer mass prevents low pH in this gap.

10.5.6 Oxidation with sulphate

Studies have shown that the reduction of sulphate to sulphide in the absence of a catalyst proceeds so extremely slowly at temperatures below 200°C that the oxidation is negligible even during geological periods of time. Sulphate has therefore been judged to be an improbable oxidant under repository conditions. Moreover, the reaction is limited by the supply of bivalent iron. Under the apparently improbable assumption that this reaction takes places, corrosion can be reduced by means of a granite plug in the mouth of the hole in order to limit the diffusion area from the tunnel, or by the choice of a sulphur-poor bentonite grade.

The only known catalyst for sulphate reduction is microbiological catalysis. However, the micro-organisms require a supply of organic matter for their life processes. With an excess of sulphate, the supply of organic matter will then be the determining factor for the extent of the corrosion, which has been taken into consideration in 10.6.4.

10.5.7 Stress corrosion cracking

Studies of susceptibility to stress corrosion cracking employing the constant strain method have shown that both OFHC copper and PHC copper have a certain susceptibility to stress corrosion cracking in nitrite-bearing aqueous solutions /10-7/. The groundwaters that will be present around the final repository do not contain significant nitrite concentrations. Stress corrosion cracking is therefore judged to be improbable for canisters of OFHC copper or PHC copper under the specified disposal conditions.

10.5.8 Form and growth of attack

Owing to the low supply of oxidants to the canister, only local corrosion attacks are of decisive importance for the life of the canister. The most important local corrosion is pitting.

On the basis of experience, the relationship between pit depth (P) and time can be expressed with the equation /10-5/

$$P = A(t-t_0)^n$$

where t_0 is the incubation time before pitting begins
A is a constant
n is a constant with a value of between 0 and 1.

This equation shows that the growth rate of a pit decreases with time.

The time for corrosion breakthrough increases sharply with wall thickness, and with a sufficiently thick wall, the growth of the corrosion pit is expected to virtually cease with time. The continued attack then consists of existing pits growing in width and new pits being initiated. With extremely thick walls, the attack most nearly resembles a corroded surface zone with variations in depth.

The ratio between pit depth and mean corrosion rate is called the pitting factor, and the largest value of the pitting factor that has been observed in connection with exposure of copper in soil is

25. This value can be regarded as very conservative and studies of archaeological material, native copper and earth electrodes for lightning conductors have shown that a probable maximum value of the pitting factor is 5 /10-5/.

On the basis of the available copper surface area on each canister and the supply of oxidants, the mean corrosion rate on each copper canister has been calculated as a function of the exposure time. The maximum corrosion depth has been calculated from the mean corrosion rate by multiplying by the pitting factor. The calculations have been carried out for a probable case with a maximum pitting factor of 5 and an unfavourable case with a maximum pitting factor of 25. The results are shown in table 10-2.

Table 10-2. Maximum pit depth (mm) at different times and for different canister thicknesses.

Exposure time (years)	10^3		10^4		10^5		10^6	
Pitting factor	5	25	5	25	5	25	5	25
Canister thickness	Pit depth (mm)							
10 mm	0.6	3.0	0.7	3.3	1.1	5.8	5.5	penetrated
60 mm	0.6	3.0	0.6	3.0	0.9	4.5	3.6	18
100 mm	0.6	3.0	0.6	3.0	0.9	4.5	3.5	17
200 mm	0.6	3.0	0.6	3.0	0.9	4.5	3.4	17

10.6 CANISTER LIFE AND DISTRIBUTION OF PENETRATIONS IN TIME

The expert group that has studied canister corrosion has summarized the results of its calculations, which are presented in table 10-3.

Corrosion breakthrough will not take place simultaneously for all canisters. Rather, a considerable dispersion in time can be expected due to variations in the fracturing of the surrounding rock, tunnel fill, bentonite purity, groundwater composition etc.

Table 10-3. Canister life for different wall thicknesses according to /10-5/.

Wall thickness (mm)	Time to first penetration (years)	
	Probable case	Unfavourable case
10	$>10^6$	10^5
60	$>10^6$	$>10^6$
100	$>10^6$	$>10^6$
200	$>10^6$	$>10^6$

11 FUEL AND FUEL DISSOLUTION

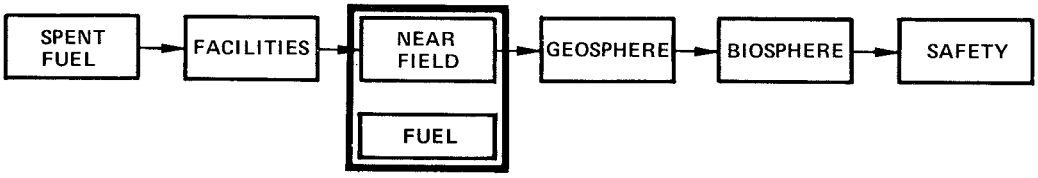

Mechanisms and properties that affect the dissolution of radioactive substances in the spent nuclear fuel if the fuel comes into contact with groundwater are discussed in this chapter.

11.1 IMPORTANCE OF FUEL DISSOLUTION

The spent fuel itself constitutes the innermost of the barriers included in the final repository's barrier system. If the copper canister is penetrated, the low solubility of the fuel matrix (uranium dioxide) constitutes a limitation of the rate of dispersal of the long-lived radionuclides, chiefly the actinides.

11.2 CHARACTERIZATION OF THE FUEL MATRIX AND THE DISTRIBUTION OF NUCLIDES IN THE FUEL

After irradiation in the reactor, the fuel pellets are heavily fissured. During reactor operation when the fuel was subjected to a high temperature (1 200-1 300^{o}C), gaseous fission products may have migrated to the grain boundaries and formed bubbles. In some cases, this can also give rise to open porosity. Cesium, iodine and even e.g. tellurium may accompany the fission gases to some extent and become enriched in the fuel's pores or the gap between the pellet and the cladding.

Certain related metals - such as technetium, molybdenum, ruthenium, rhodium and palladium - can form metallic inclusions, mainly at the grain boundaries, but sometimes also in connection with pores. The quantity of these inclusions is unknown, but their formation is believed to be dependent on factors such as operating temperature, burnup and the oxygen-metal ratio in the fuel.

The actinides occur in solid solution in the UO_2 matrix, with an enrichment towards the surface of the fuel pellet. This is because the actinides are formed for the most part by absorption of epithermal neutrons and because the flux of these neutrons is greatest at the surface of the fuel pellet. The highest concentration of actinides is therefore present in a narrow zone in the periphery of the pellet.

11.3 EXPERIMENTAL INVESTIGATIONS

Relatively few studies of corrosion/leaching of spent nuclear fuel have been conducted. Besides the Swedish research /11-1, 11-2/, studies have been conducted by the AECL, the Whiteshell Nuclear Research Establishment, Canada /11-3 to 11-6/, Battelle, Pacific Northwest Laboratory, USA /11-7, 11-8/ and the Los Alamos Scientific Laboratory, USA /11-9/. These studies have been of two kinds: more fundamental studies of the corrosion of UO_2 under oxidizing conditions /11-10, 11-11/, and pure leaching/corrosion tests on spent nuclear fuel, under both oxidizing /11-1, 11-2, 11-3, 11-4, 11-7, 11-8/ and reducing conditions /11-2, 11-6/. The results of these tests, which were conducted under rather varying conditions otherwise, show essentially the same tendencies.

11.3.1 Cesium and iodine

Cesium, which has partially segregated to the gap between the fuel pellets and the zircaloy cladding, is leached selectively, and in the case of undamaged fuel from normal operation, one or several per cent of the entire cesium inventory in the fuel can have leached out in a few weeks /11-2, 11-3, 11-6/. A small fraction of the BWR rods from normal operation have been found to have a higher release of fission gases, and experience shows that the release of cesium and iodine follows the fission gases. These rods could therefore release up to 10% of their cesium and iodine inventory in a few weeks. In the case of PWR fuel, up to 30% of the cesium and iodine inventory can be rapidly accessible for a small number of the fuel rods.

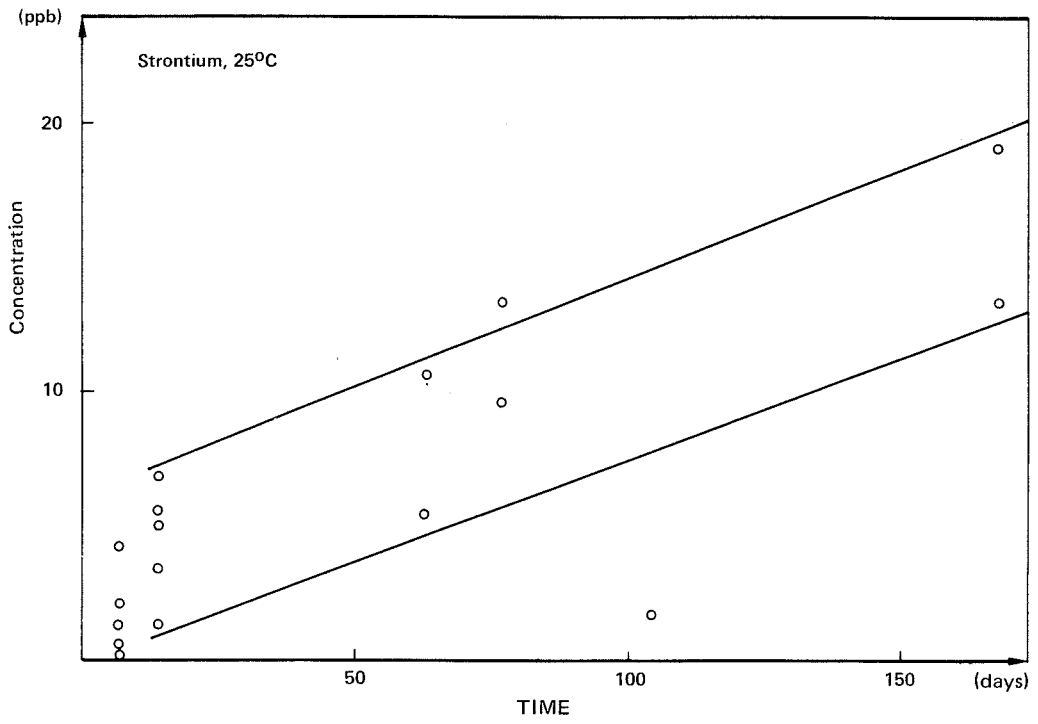

Figure 11-1. Concentration of dissolved strontium in leach water (groundwater) as a function of contact time. (From data from /11-2/).

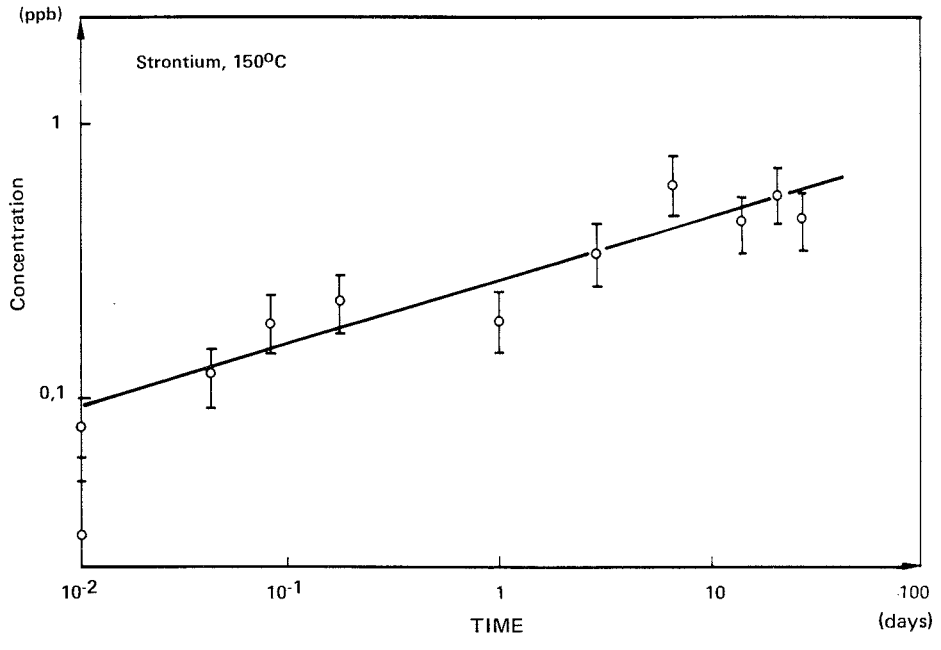

Figure 11-2. Concentration of dissolved strontium in leach water (groundwater) as a function of contact time. (From /11-6/).

11.3.2 Strontium and other fission products

Strontium is released at a slower rate than cesium and iodine. The concentration of strontium in the leachant solution increases with time, see figures 11-1 and 11-2. The leach rate in the Swedish tests is around 3×10^{-6} d^{-1} as a fraction of the inventory leached per day /11-2/. Typical leach rates in the Canadian studies are 1×10^{-7} d^{-1} for most of the fission products /11-6/. The results from Battelle and Los Alamos /11-7, 11-8, 11-9/ are reported in units that are difficult to convert to "fraction of inventory per day", which makes a comparison difficult. However, an approximation shows that these results also lie within the same interval as the Swedish and Canadian values. Discrepancies of one to one and a half orders of magnitude between the results from different laboratories can be explained on the grounds of dissimilarities between the fuel samples, such as e.g. burnup, specific area etc.

Strontium appears to have a relatively homogeneous distribution in all uranium dioxide fuel and strontium leaching, with the exception of an elevated initial leach rate, has therefore been proposed as a measure of the dissolution rate for the fuel matrix /11-2, 11-6/.

11.3.3 Uranium and other actinides

Uranium and the actinides exhibit irregularities where leaching is concerned. The leach rate declines with time and a state of saturation is reached at relatively low concentrations /11-2, 11-9, 11-11/. The leach rates for uranium that have been observed in the Swedish tests lie below 10^{-7} d^{-1} and for plutonium around 10^{-9} d^{-1} /11-2/. The Canadian studies show leach rates for uranium of around 5×10^{-8} d^{-1} and for plutonium around 10^{-8} d^{-1} /11-6/. For Battelle and Los Alamos, here as well it is difficult to compare the results directly due to other units, but an approximation once again shows that the results are of the same order of magnitude /11-7, 11-8, 11-9/.

The studies that have been conducted on fuel under reducing conditions show that the dissolution rate for spent fuel is lower in a reducing environment /11-2, 11-6/. Measured as the leach rate for

^{90}Sr, the dissolution rate decreases by a factor of 30 /11-2/. The concentration of uranium in solution lies around a few tens of ppb. This is a higher concentration than can be expected on the basis of thermodynamic considerations, but it indicates that under reducing conditions, fuel dissolution will proceed at a much slower rate than under the oxidizing conditions given above.

11.4 MODELS FOR FUEL DISSOLUTION

11.4.1 Matrix dissolution based on measured leach rates

Under oxygen-free (reducing) conditions, UO_2 is very stable and practically insoluble in water. The mechanisms for reaction between UO_2 and water under oxidizing conditions that have been proposed entail an oxidation and dissolution with precipitation of new solid uranium(VI)compounds /11-6, 11-10/. If this should also apply for the dissolution of spent fuel in contact with groundwater, this means that substances contained in the uranium dioxide matrix could be released continuously as the matrix is converted from tetravalent oxide to new solid uranium(VI)compounds, even if the concentration of uranium in solution doesn't increase. This conversion is then controlled by, among other things, the supply of oxidant necessary to oxidize uranium(IV) to uranium(VI). In addition to oxidants supplied with the groundwater, the possibility cannot be excluded at the present time that some oxidizing substances will be supplied due to radiolysis of the water that comes into contact with exposed fuel.

The release of ^{90}Sr, which should be relatively evenly distributed in the fuel matrix, can be used as a measure of matrix conversion in leach tests. In principle, other nuclides can also be released simultaneously with the dissolution of the original uranium(IV) oxide matrix, but in reality, a considerable coprecipitation will be obtained with the new uranium(VI)compounds. This applies especially to the actinides, which are chemically very like uranium. This has been verified experimentally for the coprecipitation of plutonium in uranium /11-12/. Hence, in the case of those substances which, like the actinides, tend to be coprecipitated with

uranium, their release to the solution is controlled by the net dissolution of uranium itself, as long as these substances do not actually have a much lower solubility than uranium itself. The dissolution of the solid uranium matrix, whether it has been converted or not, will be called matrix dissolution in the following and is controlled by uranium solubility. Other substances are thereby assumed to be uniformly distributed in the solid uranium phases and are released at the same rate as the net dissolution of uranium. However, the possibility of a more rapid release of highly soluble substances with a low tendency to be bound in solid uranium phases cannot be ruled out.

The strontium leach rates that have been measured for high-burnup fuel (approx. 40 MWd/kg U) under oxidizing conditions and relatively short experiment times are around 3×10^{-6} d^{-1}. This corresponds to a conversion time of about 1 000 years for the total quantity of fuel in one canister. However, long-term experiments (up to 900 days /11-5, 11-8/) show a progressively declining leach rate for strontium during the first 300 days of the experiment. After about 300 days, the leach rate for Sr is approximately one 100th of the starting value, which gives an accordingly longer conversion time for the total quantity of fuel. The leach rates that have been measured for uranium give a dissolution time of about 30 000 years, while the leach rates for plutonium and americium would lead to complete leaching-out of the plutonium and americium inventory in 200 000-300 000 years. However, this presupposes free access to water, and in view of the fact that the rate of water turnover in the repository is very low, 0.2-1.6 l per canister and year (cf. chapter 13), the concentration of uranium and actinides in the water will rapidly reach saturation at this rate of dissolution.

11.4.2 Matrix dissolution based on measured concentrations in leachant solutions

The solubility of uranium under oxidizing conditions is largely determined by the concentration of carbonate, which is the most important complexing agent in the groundwater (see chapter 12).

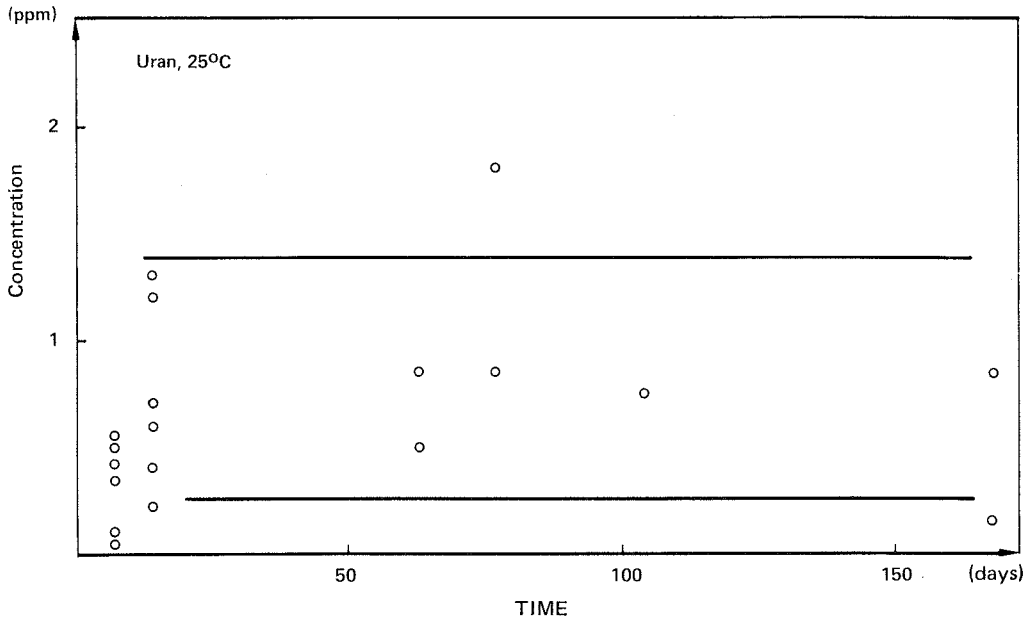

Figure 11-3 Concentration of dissolved uranium in leach water (groundwater) as a function of contact time (From data from /11-2/).

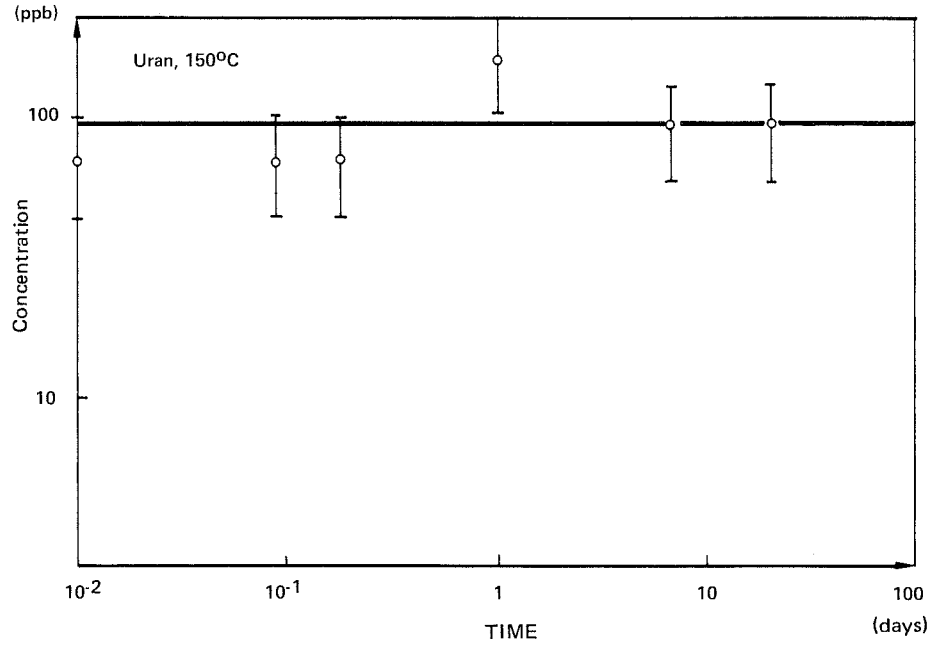

Figure 11-4. Concentration of uranium in leach water (groundwater) as a function of contact time (From /11-6/).

In the studies of fuel leaching that have been conducted, in no case have the results come close to the theoretical solubility

limit (360 mg/l at a total carbonate concentration of 275 mg/l) for uranium /11-2, 11-4, 11-6, 11-9, 11-11/. The concentrations that have been measured at room temperature have been in the range 0.5-10 ppm. Moreover, there are indications that the concentration of uranium in solution is constant or even decreases with long contact times between groundwater and uranium /11-2, 11-6/ (see figures 11-3 and 11-4). This low apparent solubility may be due to sorption phenomena, with reprecipitation of uranium and actinides on fuel pellets and the zircaloy cladding, or to an actual reduction of the solubility in groundwater due to the formation of sparingly soluble uranate phases. Calculations where such phases ($Na_2U_2O_7$) have been assumed to exist lead to solubilities on the order of those that have been observed /11-13/. This assumption is verified by geological evidence, where the low uranium concentrations in superficial, oxidizing groundwaters have been explained by the presence of sparingly soluble, hexavalent weathering minerals from uraninite.

If these observed low uranium concentrations in the leach samples are representative of the situation in the final repository, they would lead to dissolution times of over 10^8 years for uranium and the nuclides that are bound to the dissolution of uranium.

11.5 DISCUSSION AND CONCLUSIONS

The two models for inerpretation of measurement data from fuel leaching tests that have been described in the preceding section give very different dissolution times for the total quantity of fuel in a canister: a few tens of thousands of years based on measured leach rates and 10^8 years based on measured uranium concentrations in the leach samples.

The rate of water flow in the final repository is very low. The leach rate for the uranium dioxide matrix will therefore be determined by the supply of water and the solubility of uranium in the water in question, see chapter 13. Leach rates from leach tests with a plentiful supply of water are therefore not applicable to evaluations of the fuel dissolution rate in the final repository.

12 RADIONUCLIDE CHEMISTRY IN THE GROUNDWATER ENVIRONMENT

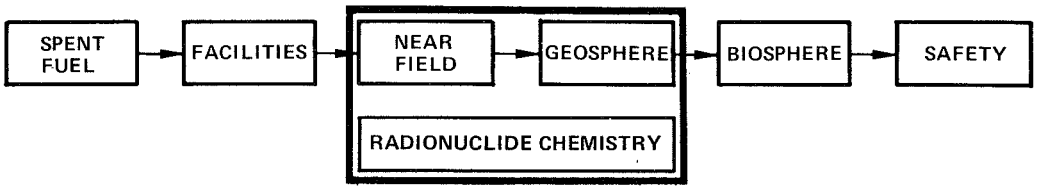

This chapter deals with the chemical properties of the radioactive substances in the groundwater environment. Solubility and sorption data are discussed, along with the formation of colloids and complexes.

12.1 CHEMISTRY OF THE ACTINIDES

The actinides comprise their own group of elements in the periodic table. As can be seen in table 12-1, U, Np and Pu can all be expected to exist in several oxidation states in the groundwater environment.

The chemical properties of different oxidation states of the same actinide are completely different. Different actinides in the same oxidation state, on the other hand, have very similar properties. In other words, no significant differences exist in this context between Pu(III), Am(III) and Cm(III), nor within the group U(IV), Np(IV) and Pu(IV). As a rule, generally applicable conclusions concerning chemical properties can be drawn from model tests with e.g. Am(III) (or any element in the lanthanide group, e.g. Ce(III), Nd(III), Eu(III) etc.), representing trivalent actinides, U(IV) (in some cases also Th(IV)), representing tetravalent actinides, Np(V), representing pentavalent actinides and U(VI), representing hexavalent actinides /12-1/.

The actinides form strong complexes with oxygen ligands (oxides, hydroxides, carbonates, phosphates, sulphates, humic acids etc.) as well as with fluoride. Different oxidation states of the actinide atoms produce complexes of different strengths. The hydroxide, phosphate and fluoride complexes, as well as the oxides, are highly insoluble as a rule.

Since all of the complexing ions mentioned above are commonly occurring components in groundwater systems, the behaviour of the actinides, and thereby also their mobility and transport properties, are heavily dependent on the groundwater composition. An analysis of relevant complexing constants and groundwater compositions shows, however, that complexing is almost completely dominated by hydroxide and carbonate complexes, as well as possibly by organic compounds /12-2, 12-3/. Formation constants corresponding to the formation of 1,1-complexes (one ligand per actinide atom) as well as solubility products are presented in table 12-2 /12-4/.

Expected actinide species in the groundwater environment have been compiled in table 12-3 and are discussed separately for each element below. Total calculated solubilities are presented in table 12-6.

Table 12-1. Oxidation states of actinides in aqueous solution.

Element	Oxidation state III	IV	V	VI	VII
Th		+			
Pa		(+)	⊕		
U		⊕	⊕ [b]	⊕ [b]	
Np	(+)	⊕	+	(+)	(+)
Pu	⊕	⊕	+	+	(+)
Am	⊕	(+)	(+)	(+)	
Cm	+				

[a] + = can exist in aqueous solution at pH 7-9.

(+) = extreme conditions are required for existence at pH 7-9.

⊕ = expected state in undisturbed deep groundwaters in crystal rock (cf. chapter 7).

[b] at high carbonate concentrations.

12.1.1 Thorium

Thorium exists in the tetravalent state, regardless of the redox potential in the groundwater. Hydrolysis products dominate and total solubility is limited by the solubility of the oxide $ThO_2(s)$ /12-5/.

12.1.2 Uranium

Under oxidizing conditions, uranium exists solely in the hexavalent state with oxides or possibly silicate or phosphate complexes as solubility-limiting solid compounds. However, total solubility is dominated by anionic complexes of the type $UO_2(CO_3)_x^{2-2x}$ at pH levels of 5-6 or more at the carbonate concentrations that can be expected in the groundwater systems in question /12-6, 12-7/.

Under reducing conditions, the solubility of $UO_2(s)$ is limited. Hexavalent carbonate complexes can still dominate at pH above 6-8, although with a low total concentration. At lower pH, tetratvalent hydroxide complexes, as well as pentavalent UO_2^+, can be expected.

Table 12-2. Complex formation constants and solubility products published during the past ten years for the actinides U, Np, Pu and Am in different valence states (III-VI).

$An + L = AnL$, $[AnL]/[An][L] = K_1$
$xAn + yL = An_xL_y(s)$, $[An]^x[L]^y = K_s$

Ligand	log K_1 ($-\log K_s$) III	IV	V	VI
OH^-	5-7 (22-25)	12-14 (>47)	4-5 (8-9)	8-9 (22-25)
CO_3^{2-}	5-6 (31-33)		~5	10-11 (14)
F^-	3-4 (10)	8-9 (24-28)	4	5-6
Org[a]	7-9	13-16		7-9

[a] Humic or fulvic acid; pH-dependent binding constants.

In deep groundwaters, tetravalent uranium dominates at low potentials (lower than 0.24-0.06 pH) and/or low total carbonate concentrations. These conditions are not unusual in deep waters. At higher potentials and/or high carbonate concentrations, hexavalent uranium ($UO_2(CO_3)_3^{4-}$), dominates, but with UO_2(s) as the solubility-limiting solid phase (cf. figure 12-1).

Table 12-3. Dominant inorganic actinide species in solution (Groundwater system, pH 7-9).

Element	Reducing conditions, Fe(II)	Oxidizing conditions, O_2
Th	$Th(OH)_4$	As for red
Pa	Pa(V)-hydrolysis product[a]	As for red
U	$U(OH)_4$, UO_2^+	$UO_2(CO_3)_x^{2-2x}$, x=1-3
	$UO_2(CO_3)_x^{2-2x}$, x=1-3	$(UO_2)_3(CO_3)_6^{6-}$
Np	$Np(OH)_4$	NpO_2^+
		$NpO_2(CO_3)_x^{1-2x}$, x=1-3
Pu	$Pu(CO_3)_x^{3-2x}$, x=1-3	$Pu(OH)_4$
	$Pu(OH)_y^{3-y}$, y=1,2	PuO_2^+
	$Pu(OH)_4$	
Am	$Am(CO_3)_x^{3-2x}$, x=1-3	As for red
	$Am(OH)_y^{3-y}$, y=1,2	
Cm	b	b

[a] Possibly some Pa(IV).

[b] Analogous to Am.

12.1.3 Neptunium

The tetravalent oxide $NpO_2(s)$ is the solubility-limiting solid phase under both oxidizing and reducing conditions. In oxidizing systems, pentavalent carbonate complexes of the type $NpO_2(CO_3)_x^{1-2x}$ dominate, along with NpO_2^+.

Reducing conditions give hydrolysis products, mainly $Np(OH)_4$.

12.1.4 Plutonium

Under oxidizing conditions, $PuO_2(s)$ is the solubility-limiting solid phase with $Pu(OH)_4$ as the dominant species in solution at pH 6-9. At lower pH, the pentavalent PuO_2^+ is probably dominant. An oxidation to Pu(VI) requires a high pH, high carbonate content and the presence of a relatively strong oxidant /12-4/.

Under reducing conditions, plutonium is trivalent, possibly with some tetravalent species present at high pH. The solubility-limiting solid phase is $Pu_2(CO_3)_3(s)$ at low pH values and $PuO_2(s)$ at high pH values. Carbonate complexes of the type $Pu(CO_3)_x^{3-2x}$ dominate in solution.

12.1.5 Americium

Only trivalent americium species can exist in groundwater with $Am_2(CO_3)_3(s)$ as the solubility-limiting phase, and possibly also $Am(OH)_3(s)$ at high pH. The solution chemistry is dominated by cabonate complexes of the type $Am(CO_3)_x^{3-2x}$ (cf. figure 12-1).

12.2 CHEMISTRY OF THE FISSION PRODUCTS

Table 12-4 presents the oxidation states of some fission products, and expected species in the groundwater environment are given in table 12-5 /12-8, 12-9/.

12.2.1 Cesium

Cesium can only exist as non-complexed Cs^+ in the groundwater environment.

12.2.2 Strontium, radium

Both strontium and radium exist almost completely in the form of Sr^{2+} and Ra^{2+}. At very high pH values and carbonate concentrations, a

Table 12-4. Oxidation states of fission products and activation products in aqueous solution.

Element	Oxidation state[a]					
	I	II	III	IV	V	Others
Ni		+				
Sr		+				
Zr				+		
Nb				(+)	⊕	
Tc				⊕		+ [d]
Pd		+				
Sn		⊕		+		
I						⊕ [e]
Cs	+					
Lanthanides[b]			⊕	(+)[c]		
Ra		+				

[a] Symbols as in table 12-1
[b] e.g. Nd, Sm, Eu
[c] Ce
[d] VII; dominant oxidation state in aerated water
[e] -I, O

small fraction of carbonate complexes of the type MCO_3 can be obtained, as well as MSO_4 at high sulphate concentrations. Solubility-limiting solid compounds are usually $SrCO_3(s)$ and $RaSO_4(s)$.

12.2.3 Lanthanides

As in the case of americium, it is the carbonate complex $M_2(CO_3)_3(s)$ and, at high pH, $M(OH)_3(s)$ as well that are solubility-limiting solid phases. The solubility chemistry is dominated by carbonate complexes. This is similar to the americium system.

12.2.4 Zirconium, niobium, nickel

The chemical properties of zirconium and the tetravalent actinides are similar in some respects. The dioxide $ZrO_2(s)$ is the solubility-limiting phase, just as for thorium. The dominant species in solution are the hydrolysis products $Zr(OH)_4$ and $Zr(OH)_5^-$.

Niobium is pentavalent under both oxidizing and reducing conditions and exists in the form of hydroxides or of NbO_4^{3-} or NbO_3^-. The solubility-limiting solid phases are $NaNbO_3$ or $Ca(NbO_3)_2$, and possibly Nb_2O_5. A reduction to the tetravalent state is improbable /12-10/.

Nickel is bivalent under the expected conditions. The formation of hydrolysis products is negligible at pH below 9. Several potential solubility-limiting complexes can exist in the groundwater environment, e.g. NiO, $NiCO_3$, $Ni_3(PO_4)_2$ and NiS /12-11/.

12.2.5 Technetium

Under oxidizing conditions, technetium exists as TcO_4^- in groundwater systems. A potentially solubility-limiting solid phase is Tc_2S_7, but it can hardly be expected, since the sulphide concentration under oxidizing conditions is generally too low.

Under reducing conditions, technitium is predominantly tetravalent (probably as a hydrolized product) with $TcO_2(s)$ as the solubility-limiting phase. A reduction to the elementary state is thermodynamically possible in reducing groundwater environments /12-12/.

12.2.6 Iodine

Under mildly oxidizing or reducing conditions, I^- is the most stable state in solution. An oxidation to I_2 or to IO_3^- can be obtained, however /12-13/.

Iodide forms sparingly soluble complexes with certain transition elements, e.g. copper, silver, mercury, lead etc.

Table 12-5. Dominant inorganic species in solution for some fission products and activation products (Groundwater system, pH 7-9).

Element	Reducing conditions, Fe(II)	Oxidizing conditions, O_2
C	HCO_3^-, CO_3^{2-}	As for red
Ni	Ni^{2+}	As for red
Sr	Sr^{2+}	As for red
Zr	$Zr(OH)_x^{4-x}$, x=4,5	As for red
Nb	NbO_4^{3-}, NbO_3^- Nb(V)-hydrolysis product	As for red
Tc	$Tc(OH)_4$	TcO_4^-
Pd	$Pd(OH)_2$	As for red
Sn	$Sn(OH)_2$ etc.	$Sn(OH)_2^{2+}$ etc.
I	I^-	I^-, I_2, IO_3^-
Cs	Cs^+	As for red
Lanthanides	$M(CO_3)_x^{3-2x}$, x=1-3 $M(OH)_y^{3-y}$, y=1,2	As for red (also $Ce(OH)_4$)
Ra	Ra^{2+}	As for red

12.2.7 Tin, palladium

Tin is tetravalent under oxidizing conditions with SnO_2 as the insoluble phase. Hydrolysis products dominate in the neutral pH range.

Tin can form soluble alkyl compounds in natural waters, but even these are highly hydrolyzed at pH values greater than 4.

Under reducing conditions, tin is bivalent. Hydrolysis products dominate at pH values above 5, and the solubility-limiting solid compound is SnO.

Palladium is bivalent under the conditions in question. Strong complexes are formed with e.g. chloride, but hydrolysis reactions dominate at pH above 5-6, except at extremely high chloride concentrations. Both $Pd(OH)_2$ and PdO are highly insoluble.

12.3 COLLOID FORMATION

Many cations have a tendency to form polynuclear hydroxide complexes. This applies in particular for trivalent and tetravalent ions, e.g. among the actinides (Am(III), Pu(III), Pu(IV), Th(IV) etc.). Polymerized hydroxide complexes can form aggregates with high molecular weights and particulate properties. High residual charges prevent these aggregates, which are usually called true colloids, from growing further and precipitating due to electrostatic repulsion. As a result, the thermodynamic solubility product can temporarily be considerably exceeded /12-14, 12-15, 12-16 and 12-17/.

Polymeric colloidal hydroxide species that are formed in acid or neutral solutions carry a positive residual charge. These colloids therefore tend to be strongly sorbed on e.g. exposed silicate or oxide surfaces, which often have a negative net surface charge. This type of colloidal species represents a metastable state. A fresh colloidal hydroxide precipitate of e.g. a tetravalent hydroxide of plutonium or thorium gradually changes from an amorphous to a crystalline state and a slow growth in particle size can be

observed. This process can largely be regarded as a stage in a spontaneous precipitation process. Stability and growth of colloidal hydroxide aggregates are highly pH-dependent.

The precipitation and crystallization of neutral hydroxide species is a reversible process from a thermodynamic point of view, even though the kinetics are slow. Hence, a precipitated actinide hydroxide should dissolve if the total concentration of the actinide in the water is reduced. However, the fresh hydroxide precipitate of e.g. a tetravalent actinide ($Pu(OH)_4$, $Np(OH)_4$ etc.) undergoes a slow gradual dehydration, and the oxide which is then formed (PuO_2, NpO_2 etc.) has a solubility that is many orders of magnitude lower than that of the primary hydroxide phase.

The formation of polynuclear hydroxide species at low pH and high total metal concentrations, e.g. for thorium and plutonium in the tetravalent state, is not always reversible, however. A formation of thermodynamically stable high-molecular-weight aggregates can take place in connection with the partial neutralization of a strongly acidic highly concentrated solution. The conditions necessary for such a process do not exist in a waste repository, where a slow dissolution of radionuclides takes place at a high pH, limited by the thermodynamic solubility of the uranium oxide and the slow kinetics of the dissolution process.

The strong tendency of the hydroxide colloids to be sorbed on solid surfaces and particles in the solution as well as the complicated kinetics of the conversion from metastable aggregates with a high surface charge to thermodynamically stable species have, in many systems, made detailed quantitative studies of the properties of colloids impossible.

Sorption of colloidal hydroxide species on geologic materials as well as sorption and desorption of radionuclides on naturally occurring colloidal aggregates (e.g. clay particles) are discussed in section 12.8.

12.4 ORGANIC COMPLEXES

High-molecular-weight humic and fulvic acids are potential metal complexing agents which form complexes with the actinides comparable to the hydroxide and carbonate complexes in strength (see table 12-2) /12-18, 12-19/. Deep groundwaters contain organic substances, usually in the concentration range 1-8 mg/l. A smaller portion of the organic fraction consists of humic acids and high-molecular-weight fulvic acids. The total capacity of these potential complexing agents can be on the order of 10^{-5}-10^{-6} eq/l which is comparable to the total carbonate content of groundwater at pH 7.5-8 and below (see chapter 7).

For actinides in the tetravalent and hexavalent state, hydrolysis reactions and carbonate complex formation, respectively, probably dominate over the formation of humic and fulvic acid complexes in the groundwater environment. In the case of the trivalent actinides, on the other hand (americium, as well as plutonium under strongly reducing conditions and low pH), a considerable fraction of the soluble species can exist in the form of organic complexes, especially at a pH of 7 or below /12-3, 12-18 and 12-19/.

12.5 SOLUBILITY

The total concentration of actinides and fission products in the groundwater is determined by solubility-limiting solid phases and the concentration of potential complexing agents in the water. Solubility data for the actinides and technetium calculated from thermodynamic data (figure 12-1) are presented in table 12-6.

If the metastable 1,4 hydroxide ($Th(OH)_4$, $U(OH)_4$, $Np(OH)_4$ and $Pu(OH)_4$) is assumed to be the solubility-limiting solid phase, total solubilities that are several orders of magnitude greater than the values in table 12-6 are obtained (see also section 12-9) /12-3/. When metal hydroxides precipitate, a coprecipitation of other metals with similar ionic radii can be expected, despite the fact that the solubility product for the corresponding hydroxide is not exceeded. Thus, a coprecipitation of Pu(III) takes place together with $U(OH)_4$ far below the solubility product for insoluble Pu(III) compounds.

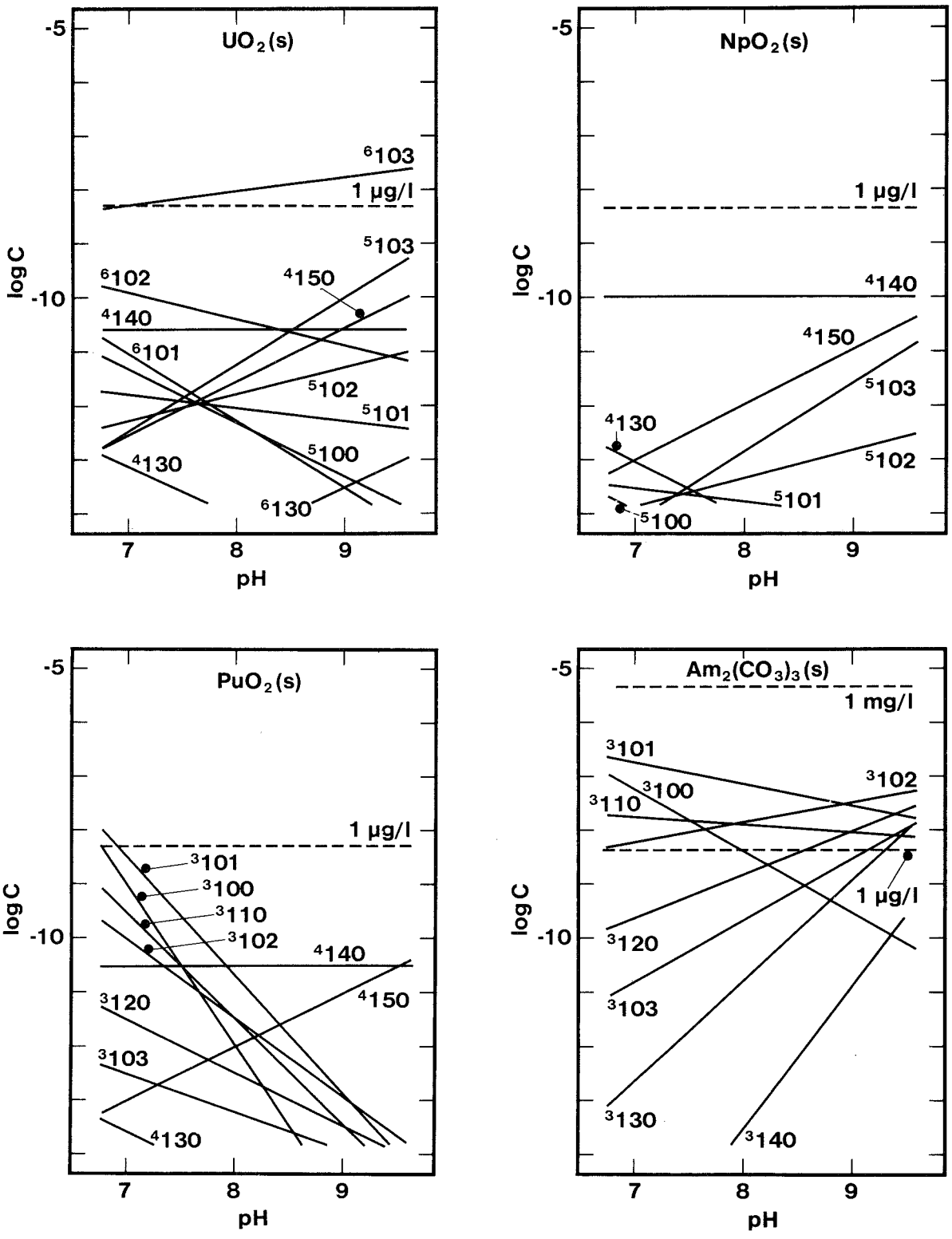

Figure 12-1. Calculated solubilities and chemical composition for uranium, neptunium, plutonium and americium in reducing carbonaterich groundwater (data from section 7.6). – (In the formula ^{n}abc, n denotes the oxidation number, a the number of metal atoms, b the number of hydroxide groups and c the number of carbonate groups in the complex).

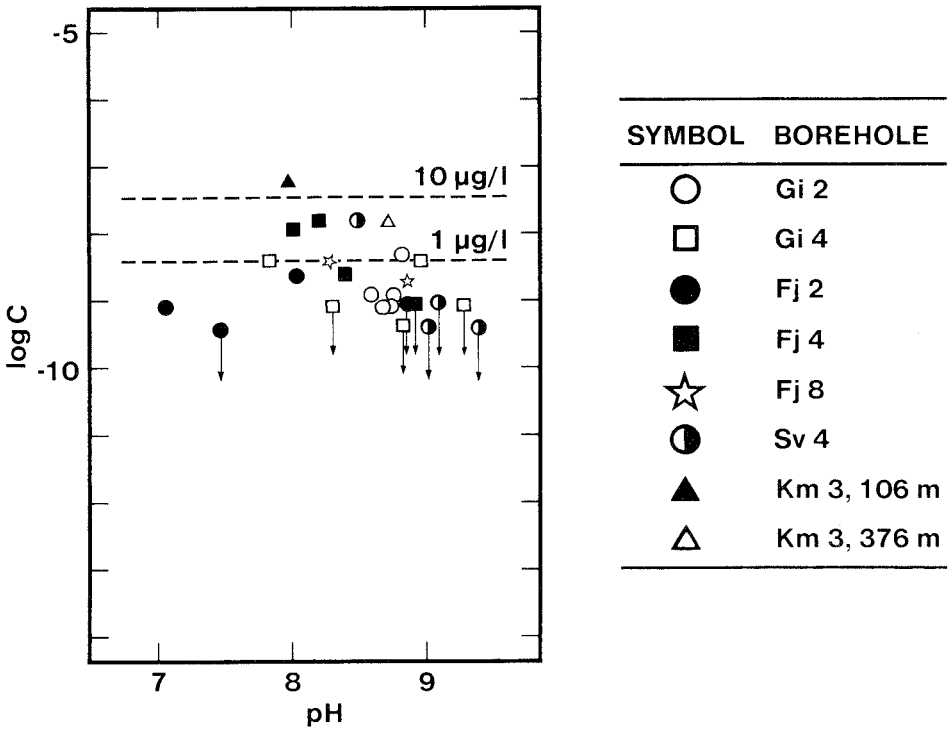

Figure 12-2. Measured uranium concentrations in deep Swedish groundwaters. Concentrations equal to or below the detection limit are marked with an arrox. ▲ represents data from Kamlunge, 106 metres deep (three measurements): the redox potential on this level is positive.

Of particular interest is the uranium system, since the dissolution of the UO_2 oxide in the spent fuel also controls the dissolution of other actinides and fission products from the fuel. Measurements of total concentrations and uranium isotope distributions in natural waters show that the solubility of the uranium under reducing conditions is generally lower than 1 µg/l /12-1/. Concentrations of this order of magnitude have also been measured in deep Swedish groundwaters, see figure 12-2, where saturation probably exists with respect to UO_2(s). The conditions here are strongly reducing (see chapter 7).

Uranium is a common element occurring in granitic bedrock. Concentrations on the order of 5-10 mg/kg can be expected. Solubilities for uranium calculated from thermodynamic data under the conditions in question show acceptable agreement with the measured concentrations as given in figure 12-2. (Cf. Figure 12-1.)

Table 12-6. Calculated solubilities for actinides and technetium in groundwater. The solubility-limiting solid compound is given within parentheses (see also table 12-8).

Element	Maximum concentration µg/l	
	Reducing conditions, Fe(II)	Oxidizing conditions, O_2
Tc	0.2(TcO_2)	(High)[a]
Th	0.4(ThO_2)	0.4(ThO_2)
U	10 (UO_2)	b
Np	1 (NpO_2)	c
Pu	10 (PuO_2), $Pu_2(CO)_3$)	1[d] (PuO_2)
Am	10^2($Am_2(CO_3)_3$)	10^2($Am_2(CO_3)_3$)

a So high that solubility is not limited in relation to the rate of dissolution of the uranium oxide.

b The solubility-limiting solid phase in nature can be a phosphate or silicate compound, or possibly an oxide phase. Reliable thermodynamic data for these compounds are lacking, however. Maximum concentration, limited by the supply of carbonate in the water, is 360 mg/l calculated for $UO_2(CO_3)_3^{4-}$ and 275 mg/l total carbonate concentration.

c The solubility-limiting solid phase is probably a compound of the type $Na_{2x-1}NpO_2(CO_3)_x$, where x = 0.8-1 /12-20/. At high sodium concentrations, solubility is limited to tens of mg/l. The maximum concentration, limited by the supply of carbonate in the water is 360 mg/l, calculated for $NpO_2(CO_3)_3^{5-}$ and 275 mg/l total carbonate concentration.

d A solubility minimum is obtained under mildly oxidizing conditions.

12.6 SORPTION PROCESSES

Interaction between dissolved substances in e.g. an aqueous phase and solid substances in contact with the water is a general phenomenon that generally leads to a partial sorption of the dissolved substance on the solid phase.

A number of different mechanisms can be distinguished for these sorption processes, whose net result is that the quantity of dissolved substance is reduced in a static system, or that the transport velocity for dissolved components is reduced in a dynamic system /12-22, 12-23/.

12.6.1 Physical adsorption

Physical adsorption of trace elements on solid surfaces is caused by non-specific forces of attraction between the dissolved substance and the solid phase. Similar forces act between molecules in all solution systems. This adsorption process is generally rapid, reversible and relatively independent of the temperature, but also independent of the concentration of the trace element (at low total concentrations), and in many cases also the mineralogical composition of the solid sorbent. Several consecutive molecule layers can form on the sorbent, and a gradual transition from adsorption to precipitation can take place, if the concentration of trace element increases.

12.6.2 Electrostatic interaction

Attraction between electrically charged surfaces and ions in solution with opposite charges leads to sorption phenomena. The most common is substitution, when an ion from the aqueous phase is substituted for an ion with the same charge that has been sorbed on the surface of the solid phase (ion exchange). As a rule, ion exchange equilibria are heavily dependent on the concentration of the trace element, as well as on the total salt content of the water, but are also dependent on the chemical composition of the solid sorbent phase. Electrostatic interactions are usually reversible.

12.6.3 Chemisorption

In some systems, specific chemical forces are obtained between the dissolved component and the solid surface, which leads to a sorption reaction that resembles chemical bonding. These sorption processes are concentration-dependent, often strongly temperature-dependent and can be slow and partially irreversible.

12.6.4 Substitution

In some systems, a substitution can take place between species in solution and corresponding elements in the solid phase. This is a slow, concentration-dependent and often partially irreversible process that can lead to a permanent fixation and mineralization of the substituted substance.

12.6.5 Precipitation - mineralization

Precipitation reactions cannot be strictly regarded as sorption processes, but the result is the same, i.e. a dissolved component is fixed on a solid surface. Precipitated insoluble hydroxides (e.g. $Ph(OH)_4$, $U(OH)_4$, $Np(OH)_4$ etc.) can be dehydrated and converted to oxide phases, which can be considered to be a largely irreversible mineralization process.

12.6.6 The distribution coefficient concept

The distribution coefficient for a substance, defined as (total concentration in solid phase)/(total concentration in aqueous phase), is a parameter that is often used to quantify the sorption of a trace element in a system under given conditions /12-23/. The distribution coefficient can easily be calculated from model experiments and also modified or converted so that it can be used to calculate the retardation in transport processes (see chapter 14). However, it must be emphasized that measured sorption characteristics for a trace element are related to a large number of chemical and physical parameters, such as:

- composition of the aqueous phase (radionuclide concentration, concentration of other anions and cations, pH, redox potential)

- composition of the solid phase (mineralogy-chemistry, surface properties, crystallinity, surface/volume ratio etc.)

- other parameters (temperature, contact time).

In general, the distribution coefficient increases with the contact time, due in part to the fact that new surfaces become available for sorption in the solid phase as the dissolved components penetrate into pores and microfissures.

Hence, two different reaction processes can be distinguished. A rapid surface reaction is followed by a slower, diffusion-controlled volume-dependent reaction process.

Distribution coefficients determined in model experiments constitute the sum total of all contributions from different sorption processes and are therefore not element-specific quantities. Laboratory tests under simulated natural conditions have, however, given acceptable agreement in cases where field observations concerning trace element transport are available /12-24, 12-25/.

12.7 RADIONUCLIDE SORPTION ON GEOLOGIC SYSTEMS

The distribution coefficients that are given below for individual radionuclides apply under the following conditions:

- Aqueous phase: Groundwater, with composition according to expected interval in table 7-4; in cases where the redox potential, high salt contents or the presence of specific components directly influence the sorption process, this is discussed separately.

- Radionuclide concentration: Low (10^{-6}-10^{-7} M) or below maximum concentrations determined by the solubility of sparingly soluble phases (e.g. PuO_2, UO_2 etc.). In cases where the radionuclide concentration significantly influences the sorption reaction, this is discussed separately.

- Temperature: 20-25°C; an increase in temperature of a few tens of degrees does not lead to any drastic changes in the sorption processes. As a rule, the distribution coefficient increases by up to a factor of 2 when the temperature increases from 25 to 50-75°C /12-26, 12-27/.

- Solid phase: Mineral and fracture-filling products representative of granite-granodiorite (see chapter 7).

12.7.1 Trivalent and tetravalent actinides - lanthanides

In general, hydrolyzed metal ions are sorbed on e.g. oxide or silicate surfaces through physical adsorption. In the case of the actinides in the lower oxidation states (III and IV) as well as the lanthanides (III) and zirconium (IV), the metal ion is hydrolyzed at low pH, i.e. hydroxide complexes form through reactions with the water. In the case of the trivalent actinides, the hydrolysis reactions begin become substantial at pH above 4-5, and in the case of the tetravalent actinides (uranium, neptunium, plutonium) at pH above 0-1.

The sorption process qualitatively reflects the hydrolysis process in that sorption and degree of hydrolysis increase along with pH. In the case of the trivalent and tetravalent actinides, a sorption maximum is reached in the pH range 6-10, which also corresponds to the formation of hydroxide complexes which have low charge or are uncharged.

The most important sorption-determining parameter is thus pH, together with the redox potential in reduction oxidation-sensitive systems, while the water's total salt content, the total actinide concentration (below the solubility product) and even the ion exchange properties of the mineral phase are less important.

The sorption of trivalent and tetravalent actinides (americium and plutonium, respectively, plutonium being primarily tetravalent under the experimental conditions in question) on a total of 30-35 minerals is illustrated in figure 12-3 /12-28, 12-29, 12-30/.

12.7.2 Pentavalent and hexavalent actinides

Just as in the case of trivalent and tetravalent elements, a correlation can be observed between sorption properties and degree of hydrolysis for the actinides in the pentavalent and hexavalent states, with sorption beginning at pH above 8-9 and 3-4, respectively. However, the hexavalent actinides in particular form very strong negatively charged carbonate complexes (e.g. $UO_2(CO_3)_3^{4-}$ in the uranium system, figure 12-1), resulting in a greatly reduced sorption tendency. The sorption of pentavalent neptunium on geologic material is illustrated in figure 12-3.

12.7.3 Cesium, strontium

The sorption of cesium and strontium on solid geologic material takes place mainly through ion exchange reactions. Important parameters for the sorption process are the ion exchange capacity of the solid mineral phase, figure 12-4, as well as the radionuclide concentration (especially for cesium) and the total salt content of the water (competing positive ions) /12-30, 12-31/.

12.7.4 Technetium

Technetium, in the form of pertechnetate, TcO_4^- (oxidizing environment), is sorbed very poorly on most common geologic materials. However, in the presence of iron(II)-bearing minerals and of iron(II) in the water, technetium will exist in the tetravalent state. Tc(IV), like the tetravalent actinides, forms strong hydroxide complexes, which, when the solubility product is exceeded, can be converted to the oxide TcO_2(s) /12-30, 12-32/.

12.7.5 Iodine

Iodide (I^-) is sorbed considerably by minerals that contain metal ions which themselves form strong metal-iodide complexes, e.g. lead(II), copper(I) etc. Minerals with high anion exchange capacities can also sorb iodide considerably, but such minerals are

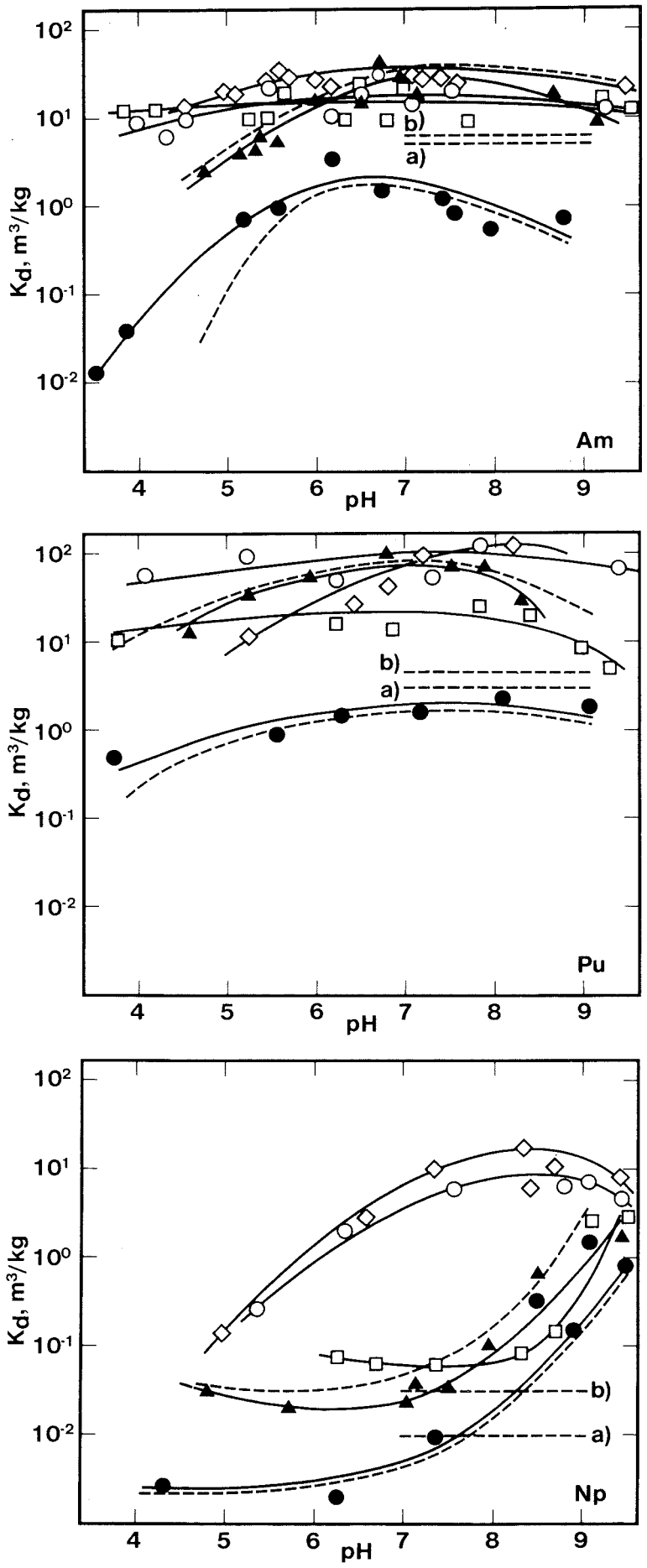

Figure 12-3. Distribution coefficients for americium (III), plutonium (mainly (IV)) and neptunium (V) as a function of pH in the mineral-groundwater system. The dashed lines indicate the range within which the majority of the measured values for the 30–35 mineral systems studied fall. Also plotted are levels for granitic rock corresponding to a. Values used, b. Best estimate according to table 12-7.

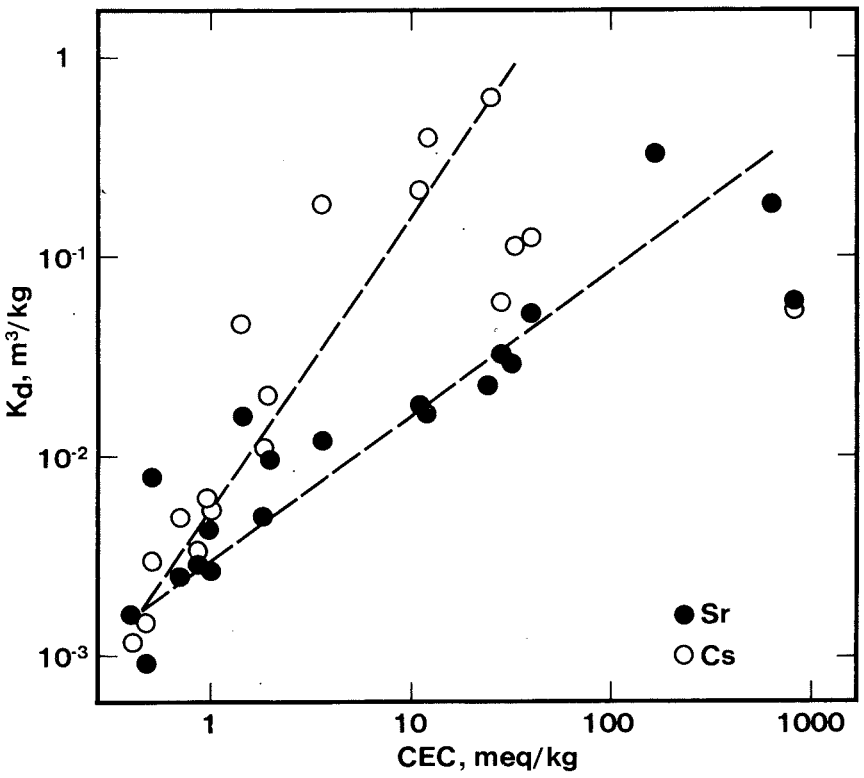

Figure 12-4. Distribution coefficients for cesium and strontium on common granitic essential minerals and fracture-filling products as a function of ion exchange capacity (CEC).

uncommon. Iodide sorption on solid geologic materials is insignificant in most groundwater environments /12-13, 12-30/.

12.7.6 Distribution coefficients

Experimentally determined but conservatively chosen distribution coefficients are presented in table 12-7. These values are measured under conditions representative of deep groundwaters (reducing conditions and a water with a low or intermediary salt content, i.e. up to 1 000 mg/l total salt content). A set of probable "best estimates" are included for the actinide systems. A similar estimate has not been made for e.g. cesium and strontium, for which the total salt content of the water, as well as the mineral content of the water-bearing fractures etc., can greatly affect the values. Values for the redox-sensitive elements under oxidizing conditions

(equilibrium with air) are given within parentheses. The best estimate values for the actinide systems pertain to a quartz-rich granite with a low content of biotite and hornblende, pH 8-8.5, and a carbonate-rich groundwater. Most of the rock species in question have a higher proportion of mica and amphiboles, which means higher distribution coefficients than the estimated values. The values that have been used in the safety analysis are lower than "Best estimate" in order to include extremely quartz- and feldspar-rich rocks as well. Consistently higher experimental values have been obtained for the approximately five different granites studied.

Naturally, the distribution coefficient is not an element-specific constant, as table 12-7 might seem to imply. For the actinides as well as for cesium and strontium, empirical relationships have been derived that define the distribution coefficient as a function of significant parameters e.g. pH (for the actinides), nuclide concentration and ion strength (for cesium and strontium), mineral composition, ion exchange capacity (for cesium and strontium and to some extent for the actinides) etc. For cesium and strontium in particular, which are sorbed on solid materials through ion exchange processes, total salt content is an important parameter. As a rule, variations of these parameters give values that are higher than those given under "Values used" in the table /12-28, 12-31/.

12.8 SORPTION OF COLLOIDAL SPECIES AND MACROMOLECULES

12.8.1 True colloids

The nuclides with the greatest tendency to form colloidal species are the trivalent and tetravalent elements (e.g. Am(III), Pu(III), Pu(IV), Th(IV) etc.) and possibly the hexavalent actinides (e.g. U(VI)) in a carbonate-free environment.

The tendency to form colloids is, as a rule, negligible for other elements of primary interest in the context of waste storage (e.g. Np(V), Cs(I), Sr(II), Ra(II), Tc(VII) etc.)

Table 12-7. Distribution coefficients for radionuclides in granitic bedrock-groundwater systems. (Low salt content, reducing conditions.) Values for oxidizing conditions are given within parentheses for the redox-sensitive elements.

Element	Distribution coefficient, m^3/kg Values used	Best estimate
Co	0.2	
Ni	0.2	
Sr	0.004[a]	
Zr	4	
Nb	4	
Tc	0.05 (0.0002)	
I	0	
Cs	0.05[a]	
Lanthanides	5	
Ra	0.1[a]	
Th	5	13[b]
Pa	5	23
U	5 (0.01)	>13[b] (0.06)[c]
Np	5 (0.01)	>13[b] (0.03)
Pu	5 (3)	6 (4.3)
Am	5	6

[a] Considerably higher values can be obtained for high-capacity minerals, and even lower values for some low-capacity minerals, e.g. quartz. The distribution coefficient can be assumed to decline in proportion to the concentration of competing positive ions in the water, which can give lower values in waters with high salt content (higher than 1 000 mg/l).

[b] Pertains to tetravalent uranium and neptunium; the value for thorium has been postulated as the minimum value.

[c] Pertains to hexavalent uranium: At very low uranium contents (below 10^{-10} M), values up to one order of magnitude higher can be obtained.

True colloids consisting of metal hydroxide aggregates exhibit the same general sorption patterns as molecular hydroxide species, i.e. physical adsorption on most silicate minerals for non-anionic species /12-14, 12-15 and 12-17/. At high pH, when anionic species can be expected, the negative charge leads to reduced sorption on many geologic materials, both for molecular and colloidal species.

Since the hydroxide colloids are not thermodynamically stable, the properties of the colloidal particles change with time (aggregate size, crystallinity, surface charge etc.). In general, these ageing phenomena, which increase with higher temperature and/or higher ion strength, appear to increase sorption on available solid surfaces. No irreversible formation of non-sorbing and thereby mobile colloidal fractions has been observed for the trivalent and tetravalent actinides /12-17/.

12.8.2 Pseudocolloids

Colloidal particles in natural waters can arise through precipitation in supersaturated solution, e.g. of metal cations + silicate, phosphate, carbonate, hydroxide etc. Colloids can also form through dispersion, e.g. in connection with the weathering of rock and the associated suspension of small particles and/or new formation of minerals.

Natural colloids in groundwater usually consist of clay minerals, hydrated oxides and hydroxides of Si, Fe, Mn and Al etc., as well as organic macromolecules.

Colloidal aggregates can serve as radionuclide sorbents and are then called pseudocolloids. The sorption of dissolved radionuclides on colloidal particles does not differ phenomenologically from sorption on macrosurfaces. Around a colloidal particle with a negative net charge on its surface, water molecules orient themselves with their positive ends pointing towards the particle surface. Hydrated metal ions are oriented in a similar manner and can be sorbed through the formation of hydrogen bonds to localized charge centres, or adsorbed directly on the particle surface, but without the hydrate water.

On contact between a radionuclide-bearing pseudocolloid and new solid sorbents, new sorption equilibria appear to establish themselves, where the total available sorbent surface area is the parameter that chiefly determines the distribution of the radionuclide between aqueous phase, solid sorbent phase and pseudocolloid phase. In aqueous systems with a high flow velocity and a high concentration of natural colloidal particles, trace element transport via pseudocolloids should play a decisive role, especially in cases when the particle fraction consists of clay minerals with high ion exchange capacity /12-33/. In e.g. deep granitic groundwater systems, where the flow velocities are low and the concentration of particles is low, the pseudocolloid transport is probably of no practical importance for the following reasons:

- Available sorbent surface area on the surfaces of the water-bearing fractures and microfissures in the rock is several orders of magnitude larger than the surface area on mobile particles in the water.

- Low flow velocities permit long contact times, which enables equilibrium to be established between species in solution and available surfaces areas.

- Transport through narrow material-filled water passages reduces particle flows due to filtration effects.

The transport of colloidal actinides species (Am(III) and Pu(IV)) through crushed rock and clay has been studied in model experiements, both for true hydroxide colloids and for pseudocolloids with iron hydroxide, silicic acid or clay mineral as the carrier. Provided that the flow is slow, i.e. the contact time long, no rapidly migrating colloidal fractions are obtained.

On the other hand, a rapidly migrating fraction has been observed in e.g. transport studies in columns or fractures when the flow has been rapid and the contact time thereby short.

Nor have observations been made to indicate that an irreversible formation of colloidal radionuclide species would take place under the expected repository conditions.

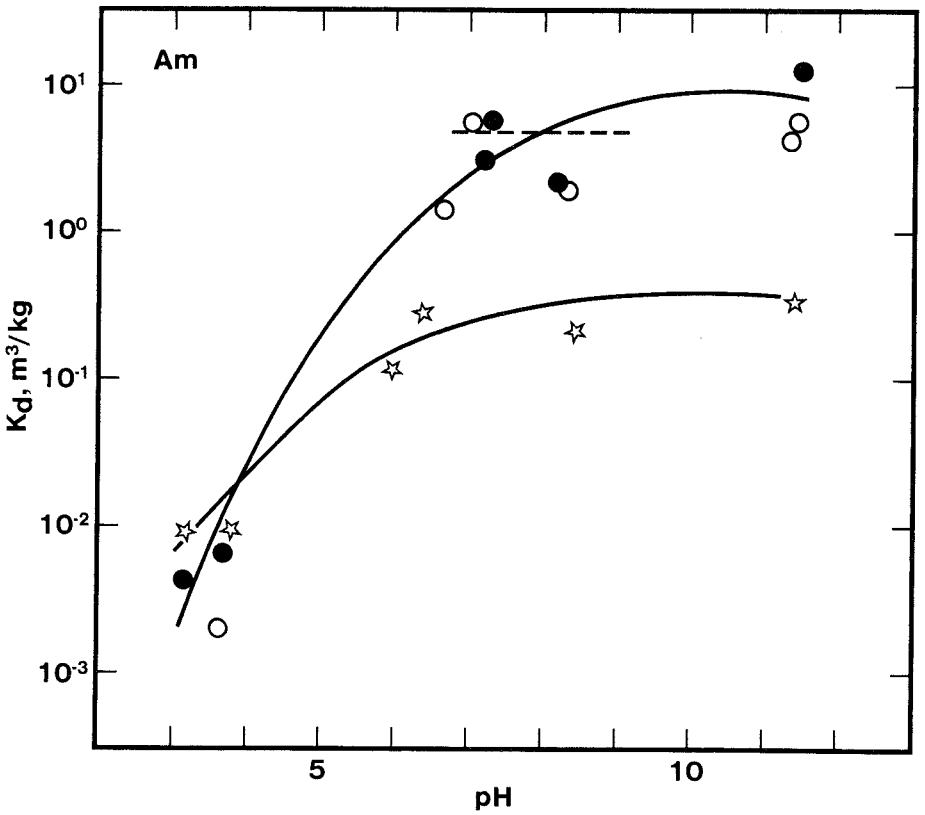

Figure 12-5. The distribution coefficient for americium as a function of pH in the granite-groundwater system in the presence of a strongly complexing humic acid, o without humus, ● 0.1 mg/l humus, ☆ 10 mg/l humus.
The level corresponding to the value used according to table 12-7 is plotted in the figure.

Hence, when the aqueous phase with residual non-sorbed fraction of e.g. Am(III) in a granite-groundwater system comes into contact with a new solid phase, this fraction will interact in a new distribution equilibrium after a certain period of time (days).

12.8.3 Humic and fulvic acid complexes

The actinides form strong complexes in all oxidation states with certain of the high-molecular-weight humic and fulvic acids, which can be encountered above all in shallow waters (see section 7.2.4). In the case of the trivalent actinides in particular, complexes can be expected that constitute a dominant fraction of all soluble molecular species at relatively low pH, when carbonate complexing does not dominate. (See equilibrium constants in table 12-2.) The presence of high levels of complexing humic acids can impede the

sorption of a trivalent actinide on a crystalline mineral phase, which is illustrated in figure 12-5 /12-18/.

Complexing with thorium at high humus concentrations appears to have an insignificant effect on migration properties in nature, however /12-34/.

Fallout plutonium from nuclear weapons tests has been found to have a very low migration tendency in shallow soils with substantial contents of humic and fulvic acids, in other words where a considerable plutonium fraction could be expected to exist in the form of humic and fulvic acid complexes /12-35/. Similar conclusions have been drawn from studies of the mobility of plutonium in humus-rich water near shallow waste repositories etc. Despite the fact that a large fraction of the plutonium (Pu(IV) and Pu (III)) is associated with organic matter, its migration tendency is low /12-36/.

Laboratory tests have also shown that neptunium (Np(V)), as well as both americium and curium, is sorbed strongly on soil particles with a varying organic matter content (up to 3-4%) /12-33/.

In summary, the following can thus be concluded:

- At low total concentrations of humic and fulvic acids, a significant fraction of trivalent actinides can exist in the form of organic complexes; for other oxidation states, hydrolysis and carbonate complexing dominate. This corresponds to the conditions that exist in a deep rock repository. In e.g. shallow soils and in waters with high contents of organic acids, however, humic and fulvic acid complexes can dominate completely.

- The presence of humus in high concentrations reduces the distribution coefficients of the trivalent actinides in the granite-groundwater system.

- Actinides in the form of humic or fulvic acid complexes have little tendency to migrate in nature. This may be due to the fact that the organic complexes are sorbed in turn on geologic materials (albeit with lower distribution coefficients than equivalent hydrolysis products).

- In systems with high water flows and high particle concentrations, actinide transport in particulate form is of greater importance than the transport of soluble complexes; these particles can be soil with a high content of organic complexing agents. This transport mechanism is of no importance in deep groundwaters with low water flows, low particulate contents and large rock surfaces available for sorption (see chapter 14).

12.9 REFERENCE DATA

The data given in table 12-8 have been used in calculating solubility.

The values in column a, corresponding to the formation of a metastable solubility-limiting hydroxide phase, have been used. Equivalent data under the assumption of the formation of an oxide phase are given in column b (cf. table 12-6).

Table 12-8. Radionuclide solubility in groundwater.

Element	Maximum concentration, µg/l			
	Reducing conditions, Fe(II)		Oxidizing conditions, O_2	
	a	b	a	b
Tc	0.2	(0.2)	High	(High)
Th	0.4	(0.4)	0.4	(0.4)
U	10	(10)	3.6×10^5	(3.6×10^5)
Np	8	(1)	High	(3.6×10^5)
Pu	3×10^3	(10)	8	(1)
Am	6×10^3	(10^2)	6×10^3	(10^2)

The distribution coefficients under the heading "Values used" in table 12-7 have been used to calculate retardation as a consequence of radionuclide sorption.

A distribution coefficient of 0.5 m^3/kg is used for Am and Pu under reducing conditions and in the presence of humic substances.

13 NUCLIDE DISPERSAL IN THE NEAR FIELD

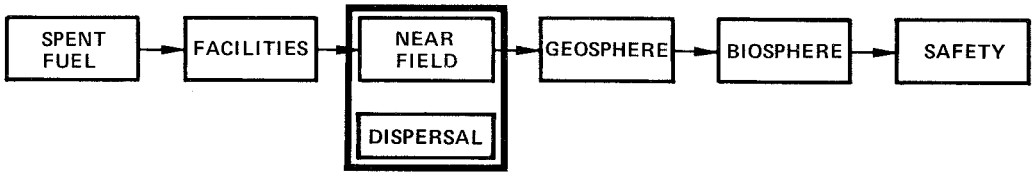

This chapter deals with the processes that control the dissolution and outward transport of radionuclides from the near field in the event of canister penetration. The transport processes that occur in the near field are of importance for canister corrosion as well, and this aspect is also dealt with here. The further dispersal of radionuclides in the geosphere is described in chapter 14.

13.1 GENERAL

By "near field" is meant here the area around the canister where the repository and its components directly influence the dispersal of nuclides after the canister has been penetrated. This influence can be of a chemical, hydrological or mechanical nature. The extent of the near field varies in time and cannot be defined exactly, but can in practice be regarded as extending up to a distance of around 10 m from the canister.

The sequence of events in the near field can be divided into two fundamentally separate stages. In the first stage, the canisters are still intact and no nuclide dispersal to the surroundings takes place. Processes during the first stage are dealt with in chapter 10. In this chapter, the conditions during the second stage are described, when the canister is assumed to have been corroded through. This is assumed to occur at the earliest after 100 000 years. The groundwater thereby comes into contact with the fuel and a process of dissolution and dispersal can begin.

The fuel consists 95% of sintered uranium dioxide crystals in the form of centimetre-long pellets. Other radionuclides are incorporated in the crystals, where they were generated. Exceptions are the noble gases, hydrogen, iodine and cesium, which have to some extent diffused out to the surface of the pellets during reactor operation at high temperature. Other substances are released to the water as the uranium dioxide dissolves. The dissolution rate for the uranium dioxide will therefore essentially determine the rate of release of other nuclides as well.

The uranium dioxide dissolves to the equilibrium concentration of the uranium in the water nearest the surface of the pellets. If there were no outward transport of the uranium, the dissolution would cease. However, dissolved uranium is transported away by diffusing out through the canister's porous corrosion products, further through the clay buffer and out to the groundwater in the fractures in the rock. The other liberated nuclides are transported out in the same manner. Some of the nuclides, including plutonium, have such low solubility, however, that they do not go into solution at the same rate as the uranium. They are therefore transported away more slowly than the uranium.

The diffusion through the very narrow water-filled pores in the clay is a slow process. Moreover, most nuclides (all cations) have a high affinity for the surfaces of the clay particles. They are sorbed (adsorbed or ion-exchanged) on the very large inner surface area (about 1 000 m^2/g) of the clay. The passage of the radionuclides will therefore be retarded, since the sorption sites in the clay must be filled up to equilibrium before the nuclides can migrate further. Some nuclides with relatively short half-lives will decay appreciably during the slow transport through the clay barrier. The long-lived actinides will not be affected appreciably. Some nuclides thus eventually reach the flowing water and are transported further in the fracture system in the rock.

The ionizing radiation that remains when the canister has been penetrated splits the water into hydrogen gas on the one hand and oxidizing substances on the other to such an extent that this process may be of importance for the chemical environment in the vicinity of the canister. The water in the near field then becomes oxidizing, whereby some long-lived nuclides - including U, Np and Tc - become considerably more soluble in the water. These nuclides migrate out through the clay and disperse downstream as well as perpendicular to the direction of flow to some extent. When they reach the border of the unaffected chemical environment, where the water is reducing, they precipitate, since their solubility in reducing conditions is many times lower than in oxidizing conditions. Their solubility can drop a thousand-fold or more. In a reducing environment, these nuclides will therefore be transported further at very low concentrations. The front between oxidizing and reducing conditions moves downstream, but will only move a few metres over a time span of one million years.

There are several possible transport processes that can alter the picture presented above to some extent. The nuclides can themselves form colloids or be sorbed on particles (pseudocolloids), which are transported with the velocity of the water. Some organic substances that are naturally present in the water can also bind radionuclides strongly in organic complexes, as a result of which the nuclides are retarded less.

In the following, the transport mechanisms mentioned above will be described in greater detail and calculations will be presented of the rate at which the radionuclides can be transported away from the repository.

13.2 TRANSPORT THROUGH CORROSION PRODUCTS AND CLAY BARRIER

Most of the canister consists of copper. In the welded version of the copper canister, lead has been cast around the fuel rods, which are made of zircaloy tube and contain the fuel pellets. In the hot isostatically pressed (HIP) canister, there is no lead. The entire canister consists of copper.

The copper canister corrodes by reaction with oxygen and sulphide dissolved in the water. These substances are transported to the canister from the slowly flowing water by means of diffusion through the water nearest the hole and through the clay. This transport is described in greater detail under section 13.2.2.

As the various materials corrode, they form metal salts or oxides, all of which form very low-solubility compounds with ions present in the water /13-1/. The corrosion products copper(I)sulphide and oxide have a density of 5.6 and 6.0 g/cm^3, respectively, while metallic copper has a density of 8.92 g/cm^3. Copper(II)oxide has a density of 6.40-6.45 g/cm^3. The corresponding lead compounds are also of lower density than metallic lead. The densities of the oxide, the sulphide, the sulphate and the carbonate are approximately half that of the lead /13-2/.

When corrosion occurs, the corrosion products must therefore expand 50-100%. This takes place against the swelling pressure of the bentonite, which is more than 5 MPa (cf. section 9.2). The mechanical constraint exerted by the bentonite on the corroding canister will limit the porosity of the corrosion products. No sizable cavities can form, since the corrosion products stay in place due to their poor solubility, and expand. At present, however, there is no reliable way to judge how impervious the corrosion products will be. No consideration is therefore given in the calculations to the fact that they might constitute a barrier to the nuclide transport.

The highly-compacted bentonite clay that surrounds the canister possesses very low permeability to water. Its hydraulic conductivity, K_p, is less than 10^{-13} m/s, cf. section 9.2.5, i.e. on the same order of magnitude as that of unfractured rock. The flow of water will therefore be extremely slow and diffusion will be by far the dominant mechanism for the transport of dissolved substances through the clay. Diffusion measurements in compacted bentonite have been carried out in a number of independent tests for some 15 or so substances. These include dissolved gases, H_2, CH_4 /13-3/, high-molecular-weight compounds /13-4, 13-5/, the fission products Cs^+, and Sr^{2+}, the anions HS^-, Cl^-, Br^- /13-6, 13-7/ and a number of actinides as well as technetium /13-8, 13-9/.

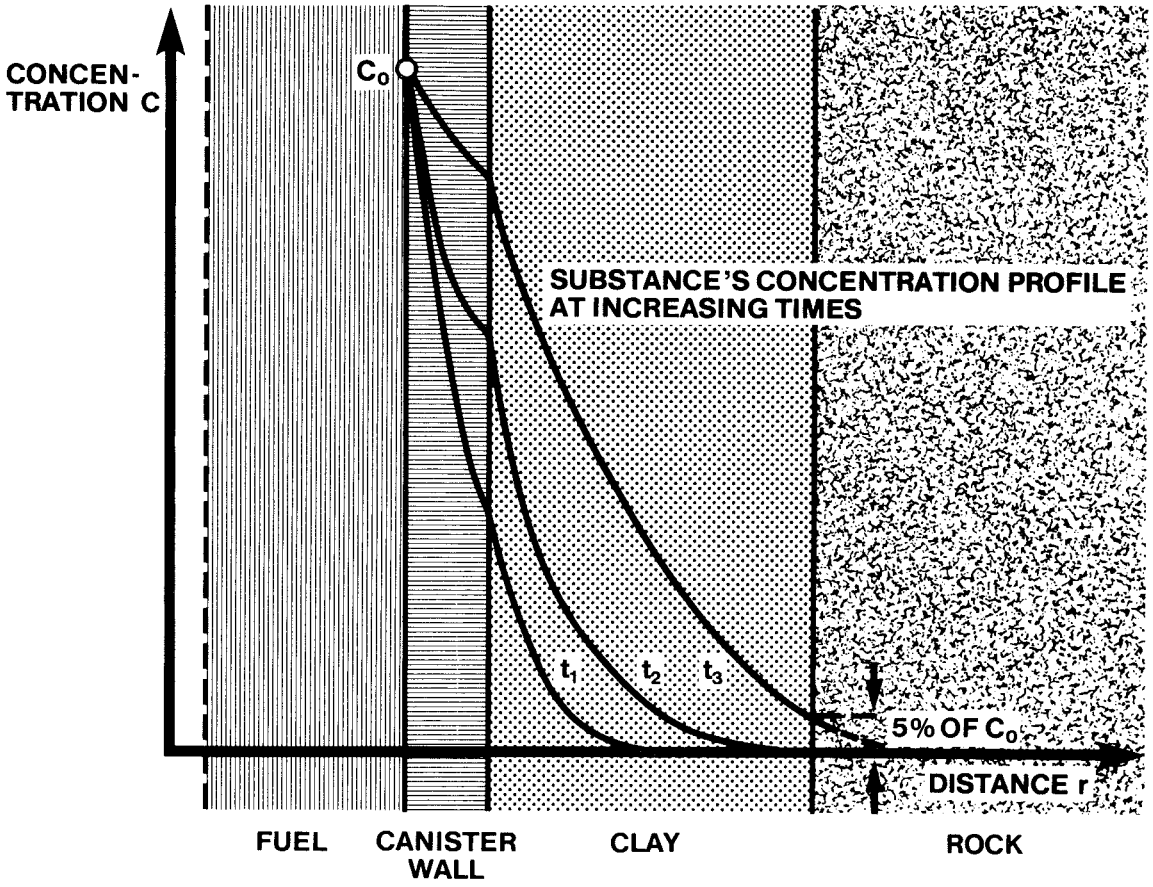

Figure 13-1. The diagram shows how a substance with concentration C_0 at the fuel surface diffuses out through the corroded-penetrated canister wall and the clay. The concentration profile has reached 5 % of the concentration at the fuel surface at time t_3 at the rock-clay interface.

An anlysis and evaluation of the importance of diffusivity has been carried out and is published in /13-10/.

13.2.1 The unsteady-state phase

Most of the nuclides are metals and usually exist in the form of cations in aqueous solutions. Cations have a strong tendency to be sorbed on the surface of the clay particles. Cesium and strontium are sorbed on the clay to a concentration that is about 2 000 times higher than in the water with which the clay is in contact. Many of

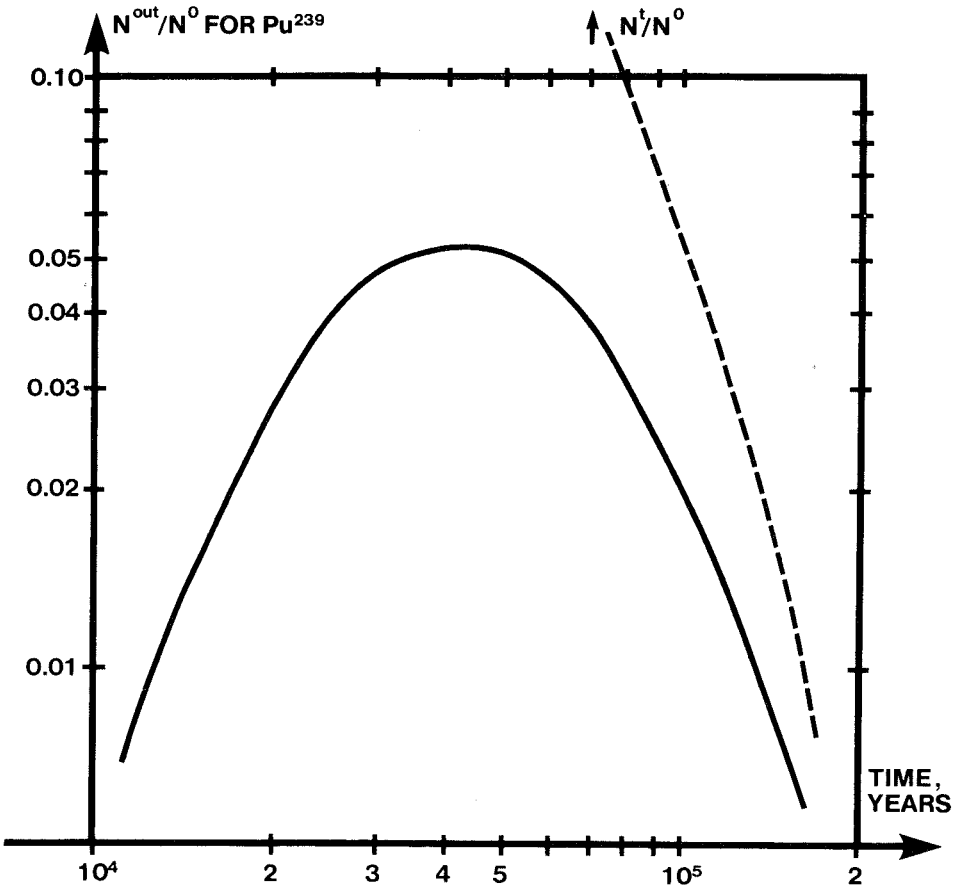

Figure 13-2. The solid curve shows how much ^{239}Pu is released on the outside of the buffer N^{out} in relation to how much was leached N^0 at time 0. The curve shows the combined effect of decay in the fuel and in the buffer. The dashed curve shows how much is leached N^t at time t in relation to the leach rate N^0 at time 0. It shows the effect of decay in the fuel and thus how the release would have been if the clay had not had a retarding effect.

the actinides - U, Pu, Np, Am etc. - are sorbed to concentrations that are tens of thousands of times higher in the clay than in the water (see section 12.5). A nuclide that starts diffusing into the clay will therefore migrate very slowly, since most of the molecules that get into the pore water are sorbed on the surface of the clay particles. Not until equilibrium has been reached does the nuclide migrate further in the pore water. The time before the first traces of a nuclide emerge on the outside of the clay barrier can be tens of thousands of times longer for a sorbing nuclide than for a non-sorbing nuclide.

The time to canister penetration and the time for transport through the clay determine the degree to which the radionuclides decay before they reach the groundwater in the rock fractures.

The results can be graphically illustrated in the following manner. The penetration time for a nuclide through the clay is defined here

as the time it takes for the nuclide on the outside of the clay to reach 5% of the concentration the nuclide has on the inside of the clay barrier. Figure 13-1 illustrates this process graphically. The penetration time determines the number of half-lives the nuclide has undergone on its passage through the clay barrier. At 30 half-lives, the nuclide has decayed to 10^{-9} of its original quantity. Those nuclides that have a penetration time that is longer than 30 times the half-life of the nuclide will come through at such a low concentration that they no longer affect the environment to any appreciable degree. Some nuclides will penetrate through the clay buffer, but in reduced quantity. For the first nuclide in a chain, the flow N_i^{out} from the outside of the buffer can easily be related to the inflow to the buffer if the leach rate is constant. The ratio between outflow and inflow in the buffer for nuclide "i" N_i^{out}/N_i^t has been calculated for a number of nuclides /13-10/.

Table 13-1 shows data for the nuclides and their penetration times in years as well as in number of half-lives. These calculations have been carried out for a clay barrier of compacted bentonite that occupies the space between the canister, with a diameter of 0.75 m, and the storage hole, with a diameter of 1.5 m. The thickness of the barrier is thus about 0.38 m.

Table 13-1, column 6, shows the highest release ever - N_i^{out} - from the outside of the buffer if leaching starts at time t with inflow N_i^t to the buffer. N_i^{out}/N_i^t shows the maximum amount that will be left after the nuclide's migration and decay in the buffer. Column 8 shows how much the inflow term decreases if leading begins after 10^5 years instead of "immediately". Column 9 shows the combined effect on the release of decay in the buffer and long (100 000 years) canister life.

Figure 13-2 shows N_i^{out}/N_i^o for ^{239}Pu calculated for the highest measured value of the diffusivity $D_a = 3 \times 10^{-14}$ m^2/s. The maximum release with initial canister damage is 5.4% of what would have been obtained without retention in the buffer. For other nuclides, the buffer reduces the release to a maximum of 1% for ^{137}Cs, 5.4% for ^{90}Sr, 0.66% for ^{240}Pu and 0.13% for ^{243}Am. Of the fraction of ^{229}Th that is originally present in the fuel, the buffer reduces the release to max. 0.029%, but since ^{229}Th is a daughter in a

Table 13-1. Diffusion data, penetration times and maximum relative outflows to the far field for some important nuclides.

Column 1	2	3	4	5	6	7	8	9
						Canister penetration at 10^5 years		
Nuclide	$D_a \times 10^{12}$ m^2/s	$t_{1/2}$ years	$t_{0.05}$ years	$t_{0.05}/t_{1/2}$	max N_i^{out}/N_i^t	$\frac{10^5}{t_{1/2}}$	N_i^5/N_i^o	max N_i^{out}/N_i^o for D_a max
^{129}I	9	1.6×10^7	53	0	1	0	1	1
^{99}Tc	53	2.1×10^5	9	0	1	0.5	1	1
^{137}Cs	1-8	30	60-480	2-16	9×10^{-6}-1×10^{-2}	>100	0	0
^{135}Cs	1-8	3×10^6	60-480	0	1	0	1	1
^{90}Sr	2-25	29	19-240	0.7-8.5	2×10^{-4}-5×10^{-2}	>100	0	0
^{226}Ra*	2-25	1.6×10^3	19-240	0	1	63	0	0
^{229}Th*	5-9$\times10^{-3}$	7.3×10^3	56-100$\times10^3$	7.7-14	2×10^{-5}-3×10^{-4}	13.6	8×10^{-5}	2×10^{-8}
^{231}Pa	1	3.3×10^4	478	0	1	2.8	0.14	0.14
^{234}U								
^{235}U	1		478	0	1	0	1	1
^{236}U								
^{238}U								
^{237}Np	0.2-0.4	2.1×10^6	1.2-2.4$\times10^3$	0	1	0	1	1
^{239}Pu	7-30$\times10^{-3}$	2.4×10^4	16-69$\times10^3$	0.7-2.9	5×10^{-3}-5×10^{-2}	4.2	0.055	3×10^{-3}
^{240}Pu	7-30$\times10^{-3}$	6.6×10^3	16-69$\times10^3$	2.4-10.5	7×10^{-5}-7×10^{-3}	15.1	3×10^{-5}	2×10^{-7}
^{241}Am	4-14$\times10^{-3}$	433	32-120$\times10^3$	69-260	0	>100	0	0
^{243}Am	4-14$\times10^{-3}$	7.9×10^3	32-120$\times10^3$	4.3-16.2	8×10^{-6}-1×10^{-3}	13.5	9×10^{-5}	9×10^{-8}

N_i^o = the nuclide flow from the fuel if it started being leached at time 0.

N_i^5 = the nuclide flow from the fuel if it started being leached at time 10^5 years.

N_i^t = the nuclide flow from the fuel if it started being leached at time t years.

N_i^{out} = the nuclide flow from the outside of the buffer to water flowing by.

* = only that fraction of the nuclide that is originally present in the fuel.

$t_{0.05}$ = the time it takes for the concentration on the outside to rise to 5% of the concentration on the inside.

D_a = diffusivity.

decay chain, this is of no practical importance. For other important nuclides, retardation in the buffer is of no importance. The calculations for 100 000-year-old fuel show that the transport through the buffer gives approximately the same decay for some nuclides (^{229}Th, ^{239}Pu, ^{240}Pu, ^{243}Am) as a decay time of 100 000 years (column 8). The reported decay in the buffer is not credited in the following treatment.

Doubling the thickness of the buffer would increase $t_{0.05}$ by a factor of four. This would have a significant effect on ^{137}Cs, ^{90}Sr and the two plutonium isotopes as well as ^{243}Am. However, since all of these except ^{239}Pu decay considerably during the life of the canister (100 000 years), only ^{239}Pu is actually affected. The release of this nuclide is reduced by about a factor of ten.

13.2.2 The steady-state phase

The nuclides that do not decay to an appreciable extent during the unsteady-state phase migrate further from the clay and out into the water, which is moving slowly in the rock fractures. The nuclide diffuses out into the water and builds up a concentration profile in the water in a similar manner as during its unsteady-state diffusion through the clay. When a given volume of water has flowed past the canister, it has been in contact with the buffer, which gives off nuclides, for a certain period of time. The concentration profile that has developed in the water during this time determines the quantity of nuclide that the water is able to transport further downstream when the water leaves the buffer. Figure 13-3 shows how the concentration profile develops during the water's passage of the canister.

Transport to the canister of corrosive substances dissolved in the water such as oxygen and sulphide takes place in fundamentally the same manner. The water that flows around the clay is progressively depleted as it passes by the hole due to the fact that the substances diffuse up to the canister wall and react there.

The mass transport under steady-state conditions has been modelled and calculated /13-11, 13-12/. These calculations have taken into

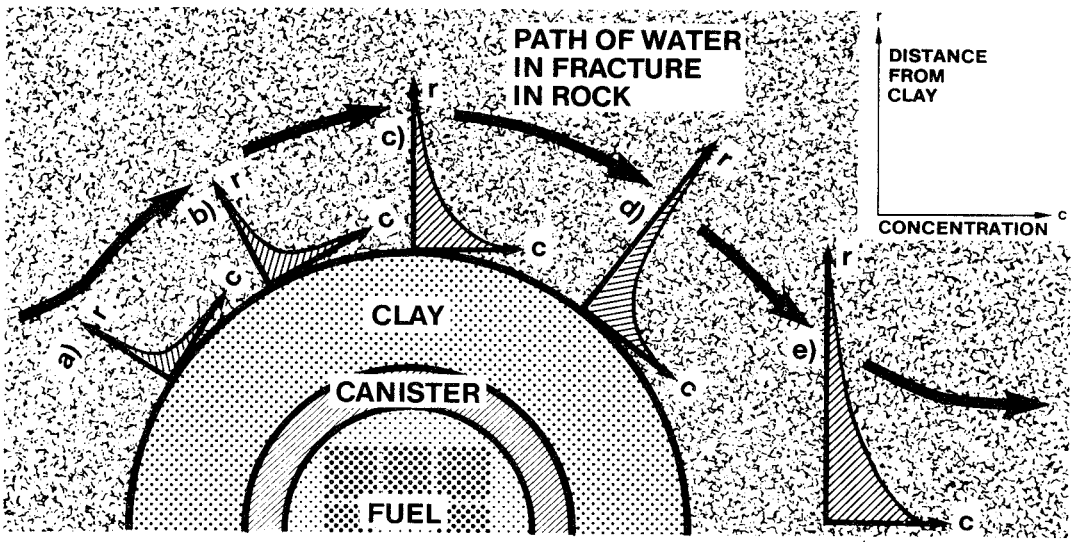

Figure 13-3. When the water first comes into contact with the clay a) from which the nuclide diffuses, the nuclide reaches a short distance out into the water. During the progressively longer contact time b), c), d), the nuclide reaches farther and farther out into the water. When the water has passed the canister e), it does not take up any more nuclide.

consideration both the diffusion in the clay barrier and the diffusion in the water in water-bearing fractures. The diffusion into the rock matrix around the hole is negligible, except during the very first stage. The model also takes into consideration the fact that the rock near the canister may be disturbed due to the excavation work and thereby have higher hydraulic conductivity. The transport in the clay is described as a three-dimensional diffusion transport from the surface of the fuel to the fracture openings in the rock. The transport into the flowing water is described as diffusion in flowing water between two plane parallel fracture walls. The water flow in the rock is determined to a large extent by regional flow conditions and has been calculated to be 0.01-0.1 $l/(m^2 \cdot year)$ (see chapter 6). The flow in the immediate vicinity of the canister can, at most, double if the rock near the canister has acquired a considerably higher hydraulic conductivity as a result of the rock excavation work /13-11/. The transport is also affected by the number of fractures that intersect the storage hole, as well as the width of these fractures. The frequency of

water-bearing fractures has been studied (see chapter 6) in deep boreholes in the study areas. A water-bearing fracture every 5th-10th metre is common in the studied areas.

Fractures that lie parallel to the tunnel can be widened during the tunnelling work. In the calculations, it is assumed that there is one fracture per metre in the near field. The width of the fractures can be determined by assuming that the flow resistance stems from the friction between two plane-parallel plates /13-13, 13-14/. For a fracture spacing of 1 m and a hydraulic conductivity of 10^{-10} m/s, a fracture width of 0.005 mm is obtained. Since the fractures sometimes contain fracture mineralization and fracture-filling material, a fracture width of 0.1 mm is chosen as a value for the calculations.

Since fracture width, fracture frequency and water flow are known, the dissolution rate of the nuclides can be determined by means of the previously described model. The calculations show /13-11, 13-12, 13-15/ that most of the transport resistance arises in connection with the diffusion of the nuclides in the water in the thin fractures. The diffusion resistance of the clay constitutes only about 5-30% of the total resistance, due to the fact that the cross-sectional area for the diffusion of the nuclides is much larger - about 1 m of clay height for every 0.1 mm of fracture width.

Since the diffusivities of the nuclides in water do not differ appreciably from each other and are of the same order of magnitude as for other small dissolved ions, they will be transported equally fast with the same driving force (concentration difference). This is the difference between the concentration at the fuel surface C_o and the concentration in the water far away, where it is 0. The nuclide transport can therefore be written:

$$N_i = \frac{1}{R} \cdot (C_{oi} - 0) \qquad (13.1)$$

where N_i is the quantity of nuclide "i" that is transported at a concentration difference of C_{oi} - 0. The parameter R is equal to the sum of the transport resistances in clay and in fractures. R is determined with the aid of the model described above and is little dependent on nuclide type.

The equation (13.1) can also be interpreted in the following manner: 1/R is the equivalent water flow, Q_{eq} that arrives at the canister with the concentration 0 and leaves it with the concentration C_{oi}.

$$N_i = Q_{eq} \cdot C_{oi} \qquad (13.2)$$

Q_{eq} has been calculated for the 5 m long canister. Table 13-2 below gives values of Q_{eq} at different water flows U_o in the rock.

The transport of corrosive substances to the canister is described with the same equations as those used for the nuclide transport out from the fuel. The diffusivities of oxygen and sulphide in the water are of the same order of magnitude under steady-state conditions as the diffusivity of the nuclides. The sulphide's diffusivity in clay is lower and may reduce Q_{eq} for this substance somewhat in practice. In the present calculations, the values in table 13-2 have been used for oxygen and sulphide transport as well.

The outward transport of uranium will determine the dissolution rate for the uranium dioxide matrix. The concentration of uranium at the surface of the pellets is determined in part by its solubility in the waters in question and in part by whether the dissolution rate is large enough to supply the water at the surface of the pellet with new uranium at the same rate as it diffuses away. Since no reliable data are available on the dissolution rate of spent fuel, it is assumed to be rapid, i.e. it is not limiting. The concentration at the surface will then be equal to the solubility of the uranium. This is determined primarily by the water's carbonate content and pH and by the water's redox potential Eh. The redox potential in surrounding water in the rock is negative, but can be positive at the surface of the pellet due to radiolysis. At positive Eh, the solubility of the uranium is determined by the concentration of carbonate ions. At the highest carbonate contents HCO_3^- = 275 mg/l in Swedish groundwaters in crystalline rock, the solubility of the uranium = 360 mg/l. With Q_{eq} = 0.57 l/canister and year, and with C_{oU} = 360 mg/l, equation (13.2) gives:

N_U^{out} = 0.57 x 360 = 205 mg U/year and canister.

Table 13-2. Q_{eq} at different water flows U_o in the rock for a 5 m long canister.

U_o $l/(m^2 \cdot year)$	Q_{eq} 1/year
0.01	0.19
0.03	0.32
0.1	0.57
0.3	0.94
1	1.57
3	2.41

Each canister contains 1.4 tonnes of uranium, which means that it takes about 7 million years to dissolve the canister's uranium content. This also presumes that the production of oxidizing species via radiolysis is sufficient to oxidize the uranium at the same rate as it is carried away.

The nuclides contained in the uranium dioxide crystals are liberated as the crystals dissolve. They will have a concentration on the surface of the pellets that is proportional to their concentration in the pellets. Thus, nuclide "i" will have the concentration:

$$C_{oi} = C_{uranium,\,sol} \cdot X_i \qquad (13.3)$$

where X_i = the fraction of nuclide "i" in the pellet and $C_{uranium,sol}$ is the solubility of uranium. The nuclide "i" is transported out to the water in the same manner as the uranium. The flow is as before $N_i = Q_{eq}\ C_{oi}$. If the nuclide "i" can dissolve in the water in the concentration C_{oi}, it will be transported out at the same relative rate as the uranium.

Some nuclides, e.g. Th and Pu, have solubilities that are lower than C_{oi}. They therefore precipitate on the surface of the pellets and are only transported away to a small extent. This is determined by the solubility of the individual nuclide. Thus, if the solubility $C_{i,\,sol}$ is smaller than C_{oi} according to (13.3), the outward transport of nuclide "i" will be determined by:

$$N_i = C_{i,\,sol} \cdot Q_{eq} \qquad (13.4)$$

The outward transport of plutonium and thorium is greatly restricted by their low solubility.

Some cesium and iodine has been enriched at the surface of the pellets during reactor operation. This fraction of the cesium and iodine is assumed to be immediately available for leaching (see section 11.3). ^{137}Cs will decay during the life of the canister. ^{135}Cs and ^{129}I reach the water outside virtually unaffected by the buffer. However, since the canisters are penetrated at varying times and spread out over a very long time span, the accessible portion of these nuclides will, on the average for the repository on the whole, be released at a rate that is determined by the rate of canister penetrations. The majority of these nuclides as well will be released when the uranium dioxide dissolves. Since the dispersion in time of the disintegration of the canisters is comparable to the leach time for the uranium, the releases of these nuclides do not differ appreciably from those of the others.

13.3 CONSEQUENCES OF RADIOLYSIS AND HYDROGEN FORMATION

The ionizing radiation can split the water into hydrogen and oxidizing compounds such as oxygen and hydrogen peroxide. The γ radiation can penetrate the canister wall and other solid materials and act at a distance of several decimetres from the canister. It is, however, greatly attenuated on its passage through the solid materials, and its intensity on the outside of the canister is very weak /13-16/. The β and α radiation has a very short range in solid materials and cannot have any effect until the water has come into direct contact with the uranium dioxide matrix. The effective range of the α radiation in water is about 0.03 mm. When the canister has been penetrated and water has got in to the surface of the pellets, α radiolysis can take place. Calculations have been carried out by Christensen and Bjergbakke /13-17/. They have assumed that the entire surface of the uranium dioxide pellets is covered by a layer, 0.03 mm thick, in which the energy from the α radiation is spent. In each canister, approx. 4.2 l of free water could then be subjected to α radiolysis. This is greatly exaggerated, since

the corrosion products from the canister material and the uranium dioxide occupy a larger volume than the original materials, so that even if this volume exists in the gap between the uranium dioxide pellets and the zircaloy cladding when the canister is intact, it is greatly reduced after a corrosion attack. Table 13-3 shows the radiolysis at different points in time expressed as equivalent generated quantity of hydrogen peroxide and hydrogen. These quantities of radiolysis products are probably greatly exaggerated. Radiolysis on this scale has not been observed at OKLO /13-18/, where a natural reactor has been active for some 300 000 years. Radiolysis there has been 100-500 times lower, figured for a comparable quantity of fuel and burnup, than the theoretically maximum figures. Even low levels of iron dissolved in water catalyze the reverse reaction between hydrogen peroxide and hydrogen. This can reduce the net production of hydrogen and hydrogen peroxide by a factor of several hundred /13-17/. The consequences of maximum radiolysis are explored below. However, the radiolysis is expected to be no more than 1/100th of the reported maximum values due to limitations in water supply caused by expansion of the corrosion products, hydrogen outflow and catalyzed reverse reaction.

Table 13-3. Theoretical maximum hydrogen and hydrogen peroxide production from α radiolysis in 1.4 tonnes of uranium according to /13-17/. The radiation is spent in 4.2 l of water spread out in a 0.03 mm layer on the uranium dioxide surface.

Time after discharge from reactor (years)	H_2O_2 and H_2 production (mol/y)	H_2O_2 and H_2 produced in the time interval (mol)
100	4.6	780
300	3.2	750
600	1.8	620
1 000	1.31	7 400
10^4	0.34	16 200
10^5	0.025	15 800
10^6	0.009	
Total produced during 10^6 years		41 550

13.3.1 Influence on canister and fuel

The hydrogen peroxide produced by radiolysis is a powerful oxidant which can attack both the copper canister material and the lead and zircaloy that surround the uranium dioxide pellets. In the presence of certain substances, hydrogen peroxide can spontaneously decompose to oxygen and water. The oxygen will thereby act as an oxidant in the same manner as the hydrogen peroxide. The fuel's metal oxides can also be oxidized to higher valence states. The uranium, which is tetravalent in the fuel, can be oxidized to hexavalent. Other nuclides can also be oxidized, the most important being plutonium, neptunium and technetium. Uranium, neptunium and technetium become many times more soluble in the groundwater at the higher oxidation state. When the uranium dioxide in which the other nuclides are contained is oxidized, these nuclides can be released. They can then be transported out from the repository.

Calculations have been carried out of the course of the radiolysis /13-19/, where the simultaneous outward transport of radionuclides to the mobile water outside the canister has also been taken into account. The calculations are based on the assumption that chemical equilibrium always exists in a given volume of water, which is determined by the water content of the clay. The hydrogen peroxide formed according to table 13-3 and water with its content of carbonate and other dissolved species enters this volume. The same water flow carries away the reaction products. The water flow Q_{eq} is determined as before by the design of the near field (see section 13.2.2).

The outward transport is determined in part by how much of the radionuclides have had time to be oxidized to the more easily soluble forms and in part by the supply of carbonates in the groundwater. The latter constitute complexing agents for uranium and neptunium. Calculations show that the copper in the canister - if it is accessible - will be preferably oxidized and prevent the fuel from being affected almost completely. Since the growth of the corrosion products makes it improbable that the copper will always be accessible for oxidation, the calculations were also carried out under the assumption that the copper does not react at all. In this case, the uranium dioxide is oxidized first.

Table 13-4 illustrates this process and how much uranium, plutonium, neptunium and thorium has been transported out at different points in time. The total carbonate content has been set at 122 mg/l (2 mmol/l) in the calculations. The large change in the quantity of Np and Pu dissolved in the time interval 960-9 960 years stems from the fact that the strongest reductant $UO_2(s)$ has been consumed after approximately 2 500 years. These calculations show what happens for the case of initial canister damage. A canister that has been penetrated after 100 000 years and where no copper, lead or zirconium react with the hydrogen peroxide, and where no hydrogen peroxide leaves the system either, will have all its uranium dioxide oxidized to hexavalent after an additional 250 000 years, if the maximum possible radiolysis is assumed to prevail. If the radiolysis is limited to 1/100th of this, only about 50 kg of uranium will be oxidized in one million years. The oxidation times calculated above are exaggeratedly short due to the fact that no lead, zirconium or copper is assumed to react and that the surface of the pellets is assumed to be covered with a uniform layer of water. The canister materials will be oxidized to a not insignificant extent. The oxidation of uranium dioxide will then be reduced accordingly. The corrosion products from both the fuel and the canister materials have a larger volume than the original materials. They will therefore fill the original volume that had been available for water. The porosity of the corrosion products must be small, since the canister and the surrounding clay and rock exert a powerful restraint on expansion. These effects should limit the effects of radiolysis greatly, which is supported by the conditions in the OKLO reactor where, after 1.8 billion years, only a very small fraction of the uranium dioxide has been dissolved /13-18/.

Only a very small portion of the oxidized hexavalent uranium leaves the canister, see table 13-4. By far most of it remains in the form of crystals of higher uranium oxides/hydroxides /13-19/.

During the recrystallization, the nuclides that do not fit into the uranium oxide's crystal structure are released. The most important of the released nuclides are cesium, strontium, iodine and technetium. These have high solubility and can be transported away at the rate at which they are released from the fuel.

Table 13-4. Dissolution of nuclides from a canister under the influence of radiolysis as per table 13-3, Q_{eq} = 1 l/year and the canister materials are inert. The total carbonate content is 2 mM. From reference /13-19/.

Years after deposition	Dissolved quantity, g, in the time interval		
	U	Np	Pu
0-1	0.12	2.4×10^{-11}	10^{-12}
1-260	24	7.5×10^{-9}	2.4×10^{-10}
260-960	95	2.1×10^{-8}	7.2×10^{-10}
960-9 960	286	2 000	10^{-3}
9 960-10^5	10^4	2 500	0.012
10^5-10^6	1.1×10^5	-	0.024

The radiolysis products can at most oxidize the uranium at approximately the same rate as that at which the water flow in the rock is able to transport it away from the canister. This outward transport (section 13.2.2) is about 200 kg/10^6 years, provided that enough uranium exists in the hexavalent form, while the generation of hexavalent uranium is about 50 kg during the first million years. The release of the aforementioned nuclides is assumed in the further calculations to take place at the rate at which the uranium can be transported out.

Of the actinides, thorium and plutonium have such low solubility under the conditions that prevail in the vicinity of the fuel that they precipitate in the form of solid phases and are only transported away from the canister to a very small extent. This process has been described previously in section 13.2.2.

13.3.2 Influence of radiolysis on nuclide migration in clay and rock

Some of the hydrogen peroxide and other oxidation products, such as hexavalent uranium, may leave the canister and reach the clay and the rock outside the clay. Both the clay and the rock contain bivalent iron compounds, which are readily oxidized to trivalent

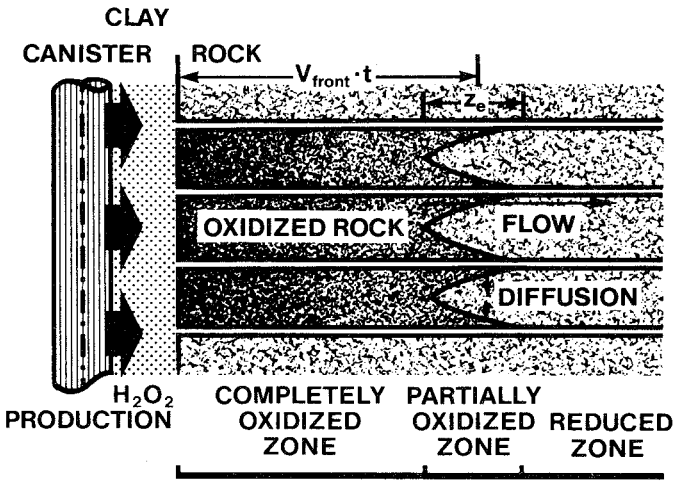

Figure 13-4. Propagation of the radiolysis front downstream of a canister. The hydrogen peroxide and other oxidizing substances move with the water in the fractures, but also diffuse from the fractures into the rock, where the bivalent iron is oxidized to trivalent iron.

iron /13-20/. When all available divalent iron in a zone has been oxidized, conditions in the water become oxidizing and many actinides become more soluble than under the reducing conditions that normally prevail in rock where there is still divalent iron. Thus, an oxidizing zone can be formed nearest the canister, which slowly expands as more oxidizing substances are transported out.

Calculations of the propagation of this so-called "redox front" have been carried out /13-12, 13-21/. In these calculations, it is assumed that all produced hydrogen peroxide or an equivalent quantity of other oxidizing species penetrate out to the clay and rock. When all iron in the clay has been consumed, the hydrogen peroxide diffuses into the rock and reacts with the iron there. In fractured rock, the hydrogen peroxide is also carried away with the flowing water in the fractures, but diffuses from there out into the microfissures in the rock and oxidizes a rock volume downstream of the canister. Figure 13-4 illustrates this propagation.

The propagation of the front downstream of a canister can reach a maximum of some 50 metres in one million years in relatively iron-poor rock (0.2% Fe(II)) /13-21/ if the greatest possible radiolysis is assumed to take place and all hydrogen peroxide goes out into the rock. Swedish crystalline rock contains 1-10% divalent iron /13-20/. In the calculations, it has been assumed that the radiolysis front does not propagate across the flow direction, so the

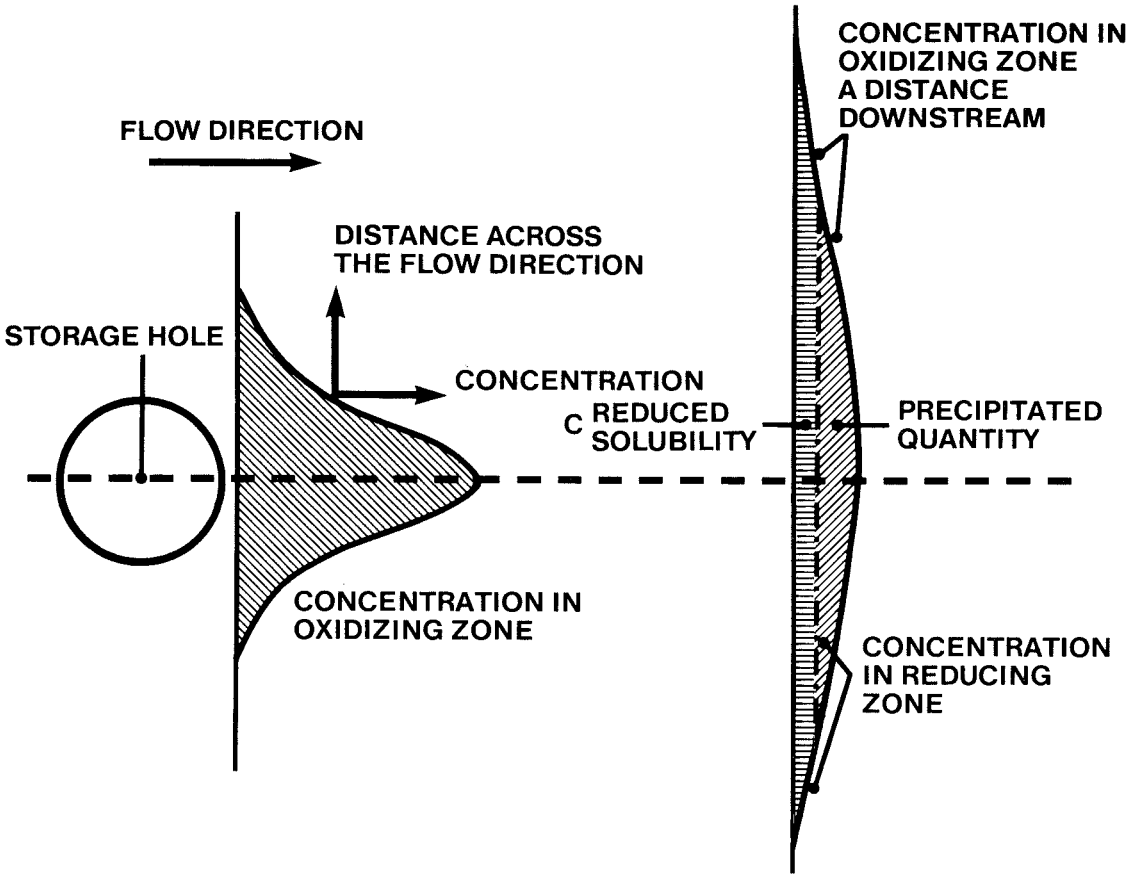

Figure 13-5. The concentration of a nuclide in the water in a fracture plane. A radionuclide with high solubility under oxidizing conditions precipitates at the redox front. The water downstream of the redox front has a low concentration C_{sol}^{red}, but the front has broadened and a larger water flow transports the nuclide.

distance downstream is exaggeratedly large for this reason as well. In practice, the front only moves a few metres /13-18/. The transverse propagation of the front has one negative consequence, however. Radionuclides that are readily soluble under oxidizing conditions spread out in the oxidized region. When these radionuclides come to the redox front and precipitate, the water in a much larger cross-sectional area of the rock will be saturated with the radionuclide than the very limited cross-sectional area in the vicinity of the canister. If the redox fronts from many canisters reach each other, most of the water that passes the total cross-sectional area of the repository will be saturated with the nuclides to the concen-

tration to which they can dissolve under reducing conditions /13-22/. Figure 13-5 illustrates the propagation of the radiolysis front sideways in a fracture and how a radionuclide that is highly soluble under oxidizing conditions precipitates to the lower solubility at the redox front and is transported further at the maximum concentration C_{sol}^{red}. Under unfavourable circumstances, all water downstream of the repository can become saturated to this concentration. Since, on the average, 150 m^2 of the repository's cross-sectional area can be ascribed to each canister, the water flow per canister can be:

$$Q_{eq}^{red} = 150 \cdot U_o \left[m^2\right] \cdot \left[1/(m^2 \cdot year)\right].$$

Since the radiolysis will in practice be much less than the maximum possible, the transverse propagation of the radiolysis front is far less. Calculations show /13-23/ that only a small portion of the water downstream of the repository will become saturated in the manner previously described. In the further calculations, however, it assumed that all water will be saturated.

13.3.3 Hydrogen evolution during radiolysis

Hydrogen that evolves during radiolysis dissolves in the water to some extent and diffuses out through the corrosion products and the clay. At high hydrogen production, it is possible that hydrogen gas will be formed locally when its solubility is exceeded. The gas then displaces the water, and hydrogen evolution decreases. However, the gas can displace the water in the large pores in the corrosion products and the clay and flow out through these pores at the same time as water is sucked in through the smaller pores due to capillary action. These conditions have been analyzed /13-12/ and gas permeability has been measured in wet bentonite /13-24/.

The hydrogen evolved during radiolysis dissolves in the water and diffuses out through the buffer to the passing water. Transport capacity by means of diffusion has been calculated in the same manner as for the steady-state phase of the radionuclide diffusion and is about 0.01 moles of H_2/year and canister at the solubility that exists at 50 bar of hydrogen pressure. The hydrogen can also

be transported by diffusion in the rock's water-filled microfissures /13-25/. This transport capacity is somewhat greater, about 0.08 moles of H_2/year and canister. If more hydrogen is generated, it is not able to dissolve into the water, forming gas bubbles instead. These bubbles can displace the water in the large pores in the clay and in the rock and flow out. At the same time, however, water may be sucked in by the capillary forces in the finest pores. The possibility can therefore not be exluded, at the present time, that hydrogen flows out at the same time as water flows in, in sufficient quantity to sustain at least a moderate radiolysis /13-12/. The outward transport of hydrogen in gaseous form is able to carry away the gas without the gas pressure in the canister ever exceeding the rock stresses at the depth in question. In the rock, the hydrogen can also be transported in the form of gas bubbles. A hydrogen flow of 0.1 moles/year corresponds to a gas volume of about 0.04 l/year at the prevailing hydrostatic pressure, 50 bar. This flow should displace an equivalent volume of water. Since the flow is less than the natural water flow past the canister, the transport takes place without any appreciable pressure increase.

13.3.4 Hydrogen-forming corrosion - the copper canister

Corrosion of the canister and the metals incorporated in it can potentially produce hydrogen. The fuel assemblies are constructed of zircaloy, inconel and stainless steel. In one of the canister alternatives, lead is included as a fill between the fuel rods. Hydrogen production from copper corrosion can be estimated at just under one mmol/year /13-26/. If the canister is penetrated, the material in the fuel assemblies and the lead (if any) will become accessible for corrosion. Zircaloy, inconel and stainless steel are highly resistant to corrosion. Lead also corrodes extremely slowly in oxygen-free groundwater /13-27/. According to a reasonable estimate of corrosion rates and exposed surface, the hydrogen production from the metal inside the canister should not exceed 0.1 mol/y /13-28/. Lead will undergo any hydrogen-forming corrosion under prevailing conditions /13-27, 13-28/.

13.4 RELEASE OF NUCLIDES FROM THE NEAR FIELD

A radionuclide with high solubility under oxidizing conditions precipitates at the redox front. The water downstream of the redox front has a low concentration C_{sol}^{red}, but the front has been broadened and a larger water flow is transporting the nuclide.

In the case of those nuclides that are not affected by the redox front, leaching takes place as previously (section 13.2.2) with a flow of:

$$N_i = Q_{eq} \cdot C_{oi} \qquad (13.2)$$

and

$$N_i = Q_{eq} \cdot C_{i,sol} \qquad (13.4)$$

and the two expressions distinguish the case where the outward transport is not limited (13.2) from the case where the outward flow is limited by the solubility of the nuclide (13.4).

In the case of those nuclides that precipitate at the redox front, the flow beyond the redox front is:

$$N_i = Q_{eq}^{red} \cdot C_{i,sol}^{red} \qquad (13.5)$$

Thus, the release to the far field can be determined by:

1) The outward transport rate of the uranium oxide; equation (13.2) (or possibly the oxidation rate),

2) The fact that some nuclides have low solubility and do not dissolve when the fuel (UO_2) is transported away or altered; equation (13.4); the release of these nuclides may be less than by mechanism 1),

3) Those nuclides that precipitate at the redox front - equation (13.5) - will be released at a lower rate than that due to mechanisms 1) or 2).

Table 13-5. Releases of certain radionuclides to the far field. Based on 1.4 tonnes of uranium, Q_{eq} = 0.57 l/y, Q_{eq}^{red} = 15 l/y.
Underlined values are limiting.

Column 1	2		3	4	5	6	7
Nuclide	Quantity per canister 10^5-year-old fuel		Congruent dissolution (6.8×10^6 years dissolution (time)	Solubility limit under oxidizing conditions	Solubility limit at redox front	To far field. Min. of col. 3, 4, 5 as activity	To far field. co-precipitation with uranium
	g	Bq	g/y	g/y	g/y	Bq/y	Bq/y
^{238}U	1.4×10^6	1.66×10^{10}	0.21	0.21	$\underline{1.5\times10^{-4}}$	1.8	=
^{234}U	a)	9.8×10^{10}				10.5	=
^{235}U	a)	1.24×10^9				0.13	=
^{236}U	a)	1.92×10^{10}				2.1	=
^{239}Pu	386	8.81×10^{11}	5.7×10^{-5}	$\underline{1.41\times10^{-6}}$ b)		3 200	94
^{242}Pu	862	1.24×10^{11}	1.3×10^{-4}	3.15×10^{-6} b)		460	4.9
^{237}Np	2 960	7.77×10^{10}	4.3×10^{-4}		1.2×10^{-4}	3 100	3.3
^{230}Th	86	6.22×10^{10}	1.3×10^{-5}	$\underline{2.3\times10^{-7}}$		170	1.8
^{241}Am	4.19×10^{-5}	5.18×10^6	$\underline{6.2\times10^{-12}}$			0.76	5.6×10^{-4}
^{243}Am	1.91×10^{-2}	1.45×10^8	$\underline{2.9\times10^{-9}}$			21	0.016
^{99}Tc	895	5.70×10^{11}	1.3×10^{-4}		3×10^{-6}	1 900	=
^{129}I	c)	1.86×10^9				270	=
^{135}Cs	c)	1.97×10^{10}				2 900	=

a) Follows uranium-238
b) Sum of Pu-239 and Pu-242 is $4.56 \cdot 10^{-6}$ g/y
c) No solubility limit
= Same as in column 6

Table 13-5 presents the inflow to the far field for some important nuclides for a fuel that is 100 000 years old. Solubilities from section 12.9 have been used.

Trivalent and tetravalent actinides at low concentrations will probably be precipitated together with uranium when uranium precipitates at the redox front. This has been shown experimentally for plutonium /13-19/. An equally large fraction of the actinide precipitates as of the main component, uranium. The following actinides can be expected to be precipitated: Pu, Np, Th, Am. They will be transported to the far field in quantities reported in the right-hand column (7) in table 13-5.

With this precipitation mechanism, the plutonium isotopes, neptumiun and thorium would deliver a nuclide flow to the far field that is 30-1 000 times lower than their own solubility permits.

Since this mechanism has as yet only been shown experimentally to apply for plutonium, it is not used in the further treatment.

13.5 RELEASES FROM REPOSITORY FOR METAL COMPONENTS

13.5.1 General

Boxes (fuel channels) and boron glass rods from the reactors are embedded in cement in concrete moulds, which are placed in a rock repository at great depth. The rock cavern is filled with concrete. Altogether, about 900 tonnes of zircaloy and 160 tonnes of stainless steel will be deposited. It is primarily the radionuclides nickel-59 and niobium-94 that must be prevented from reaching the biosphere. The half-life of nickel-59 is 80 000 years, while that of niobium-94 is 20 000 years. The total quantity of nickel metal in the repository is about 17 tonnes, and of niobium about 60 kg. Only a small portion of this is radioactive.

When the repository has been sealed, groundwater will eventually reach the waste. The metals can then corrode, go into solution and subsequently be transported out to the surrounding groundwater.

13.5.2 Chemical environment in the repository

The quantity of concrete in the sealed repository will be about 100 tonnes per metre of tunnel. The concrete will determine the groundwater's pH in and immediately around the repository, see section 7.4.1. If the repository is located in rock with water flows up to 1 $l/(m^2 \cdot year)$, it will take at least 40 000 years to leach out all calcium hydroxide and at least 4 million years to leach out all aluminates and silicates. It is then assumed that the concrete has cracked or weathered so that the water can flow freely through it, and that dissolution takes place to full saturation in the flowing water.

It is hereby assumed that the flow of water through the tunnel per square metre is twice as high as that through the undisturbed rock. The total flow through the tunnels is 2 900 l/y.

13.5.3 Corrosion

The stainless steel possesses good resistance to corrosion at high pHs and will corrode very slowly in the oxygen-poor environment in the repository. Nickel, which is incorporated here as an alloying metal, is relatively inert and may remain stable in the repository environment.

Zircaloy alloys are also resistant to corrosion and rather insensitive to pH. The tests that have been conducted with zircaloy embedded in cement show no sign of corrosion of metals /13-29/.

Niobium is present in small quantities (about 1%) in alloys. Metallic niobium is very chemically resistant, but is attacked by strong alkaline solutions with a pH above 13. For this reason, niobium corrodes in a concrete environment, at least at the high pHs that prevail in the initial phase, when the alkali hydroxides are dissolved /13-30/.

With a reasonable estimate of the corrosion rate for the metal components in the repository and the surface area that is exposed to corrosion, hydrogen production will lie below 70 m^3 NTP per year /13-28/. Radiolysis also contributes towards hydrogen formation,

but the quantities are insignificant and can be neglected here /13-28/. The stated quantity of hydrogen gas is too great to be transported out through diffusion and water flow. Gas bubbles may form and be pressed out through the water-bearing fractures in the rock, whereby the water is partially displaced. The volume of water that must make way for gas in this manner will be less than 2 m^3/y, since the hydrogen is compressed by the hydrostatic pressure at great depths. This flow is of the same size as the natural flow, and there will therefore not be any appreciable pressure increase in the repository due to the displacement.

13.5.4 Solubility of nickel and niobium

Oxidized nickel will be bivalent in the repository environment. Bivalent nickel forms poorly soluble compounds with hydroxide, phosphate, sulphide and carbonate. The fulvic and humic acids in the groundwater may possibly form strong complexes with nickel and raise its concentration in the water. Phosphate and sulphide are present in such small quantities that they are not enough to precipitate any oxidized nickel. The solubility of the nickel will therefore be determined by the hydroxide. Within the pH range 10-13 that exists in the water in and around the concrete moulds, the solubility of the hydroxide limits the nickel concentration to max. 0.1 mg/l /13-31/. If the organic substances in the groundwater - humic and fulvic acids - form complexes with nickel only, solubility can amount to about 0.003 meq/l (see section 7.6) i.e. about 0.1 mg/l. However, this is improbable since there are larger concentrations of other metal ions, including Fe(II), in the water.

Since the concrete releases calcium ions into the water in the repository, the concentration of dissolved niobium in the repository will be limited by the solubility of calcium niobate, which is very low. The concentration of dissolved niobium will be lower than 10 µg/l /13-30/. Complexing with humic and fulvic acid should not be of any importance compared to other metals present in the repository, e.g. iron, chromium, nickel, cobalt etc. In the first place, the concentration of dissolved niobium ions will be extremely low, and in the second place, most of these ions will be present in the form of negatively charged niobate ions with little tendency to be bound in a complex.

13.5.5 Outward transport of nickel and niobium

If the repository is located in as good rock as that in which the fuel is stored, it will take about 30 million years for all nickel to be transported out. This applies at water flows in the rock of 1 l/(m^2 · year) and if the solubility of nickel is 0.2 mg/l. It has then further been assumed that the concrete has cracked or weathered apart, so that the diffusion resistance in the concrete and the transfer resistance from the repository to the water in the rock can be neglected, and that all water that reaches the tunnel is saturated with nickel /13-31/.

Due to the low solubility of niobium, it will take at least two million years to transport out all niobium from the repository. The assumptions are then the same as for nickel, with the exception of solubility, which is set at 10 µg/l for niobium /13-30/.

The release of nickel-59 from the repository will be a maximum of 10^6 Bq/y and the nickel-63 release will be a maximum of 10^8 Bq/y. The niobium-94 release will be at most 10^6 Bq/y. Since the quantity of both the nickel isotopes and niobium-94 is small in relation to the inactive isotopes, the latter will determine the rate of dissolution. The release of the active isotopes therefore decreases as they decay.

13.6 MODELS AND DATA

The calculations of the unsteady-state phase when the nuclides penetrate into and through the clay are based on Fick's law for unsteady-state diffusion and take into account the fact that the nuclides are enriched in the clay due to sorption. The model has been described in /13-10, 13-13/. A large number of measurements of the diffusion of different species in compacted bentonite have been carried out and have been published and analyzed in /13-10/. Sorption data are published in /13-8, 13-9/.

The model that describes the transport of dissolved species during the steady-state phase has been described in /13-11, 13-15/ in simplified form. The model is fully described in /13-12/, where the

solution that requires numerical methods has been compared with the simplified model. These models are used to calculated the water flow Q_{eq} that transports dissolved substances.

13.7 REFERENCE DATA

The following data have been used in the calculations:

Thickness of bentonite barrier	0.38 m
Diffusivity in water (all ions)	$D_v = 2 \times 10^{-9}$ m^2/s
Diffusivity in compacted bentonite (all ions, steady-state diffusion)	$D_e = 4 \times 10^{-11}$ m^2/s
Diffusivity under unsteady-state conditions	D_a table 13-1
Water flow in rock	$U_o = 0.1$ l/(m^2. year)
Average surface area per canister	150 m^2
Fracture width	0.1 mm
Fracture spacing	1 m
Number of fractures in a hole	6
Solubility data for nuclides	table, section 12.9
Penetration of clay into fractures	0 m

14 NUCLIDE DISPERSAL IN THE ROCK

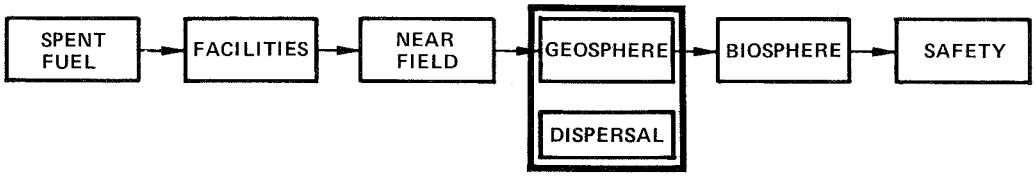

This chapter deals with the transport of released radionuclides in the geosphere. The model and data used are discussed. A further dispersal of radionuclides in the biosphere is dealt with in chapter 15.

14.1 RETARDATION MECHANISMS, GENERAL

The radionuclides are transported dissolved in the water, which moves slowly through the fractures of the rock. The velocity of the water in the fractures can vary from very low values up to several metres or tens of metres per year. All important nuclides, except iodine, react chemically or physically with the minerals present on the fracture faces. These reactions include ion exchange, adsorption, precipitation and various chemical reactions, such as mineralization. Taken together, these reactions are often called sorption. Hereinafter, the term sorption strictly refers only to adsorption and ion exchange.

When radionuclides sorb on the fracture face, their concentration in the water decreases accordingly. Only when the fracture face has assumed equilibrium with the water can the nuclide be transported further along the fracture. Most important nuclides sorb very strongly. At equilibrium, the fracture face can hold hundreds to tens of thousands of times as large quantities of nuclide as the water in the fracture. The water gives up a large portion of its nuclide content to the fracture faces it passes. It therefore takes a much longer time for a nuclide to move a given distance than it does for the water. The ratio between the velocity of the water and the velocity of the nuclide due to surface sorption is called the "retention factor due to surface sorption" (R_a). For a nuclide with

a retention factor of R_a = 100, it takes 100 years to move the same distance the water moves in one year.

Some fractures contain fracture-filling material and porous secondary fracture minerals which sorb the radionuclides and contribute towards further retarding their migration.

Crystalline rock types, such as granites and gneisses, have microscopically small fissures between the crystals. These fissures comprise an interconnected pore system containing water. The radionuclides are much smaller than the microfissures and can diffuse into this pore system. The inner surfaces in the rock matrix are many times (thousands and more) larger than the surfaces in the fractures in which the water flows. Penetration into and sorption on the inner crystal surfaces retards the radionuclides far beyond the retardation caused by sorption on the fracture faces. Even non-sorbing nuclides will move slower than the flowing water, since they diffuse into the stagnant water in the pores.

Since the radionuclides decay with time, certain nuclides with high retention and short half-lives will decay to negligible levels before the water reaches the biosphere (e.g. ^{90}Sr, ^{137}Cs, ^{241}Am). Other nuclides with low retention and long half-lives (e.g. ^{129}I) will only have lost a small fraction of their activity.

Certain nuclides, including the actinides, can form radiocolloids or sorb on colloidal particles in the water (pseudocolloids). Due to their size, the colloids are not able to the same extent to penetrate into the micropores and are therefore less affected by this retardation mechanism. Neither the true colloids nor the pseudocolloids are completely stable; they slowly dissolve. With long travel times, the colloids will dissolve and therefore be retarded by the previously described mechanisms. The same applies to nuclides that have been complex-bound to fulvic or humic acids in the water, since these complexes are also broken up with time.

Certain transport paths are faster than others, partly because the fracture widths differ in size and partly because the paths are more or less tortuous. Some of the nuclide quantity will therefore move faster and some slower than the average. This phenomenon is

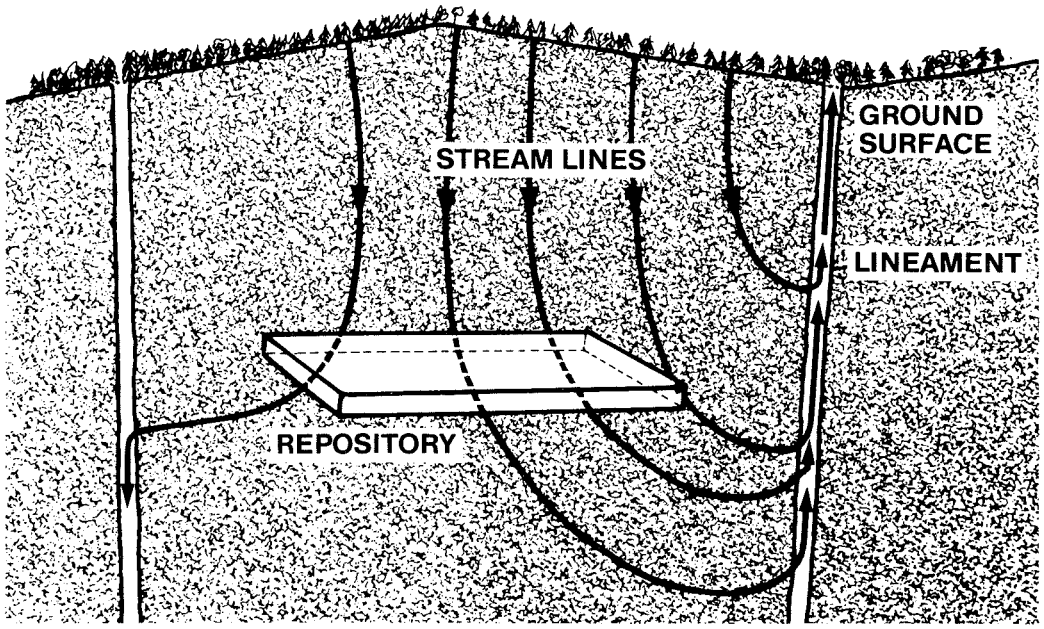

Figure 14-1. The figure illustrates the principles for location of the repository and some stream lines which run to a nearby lineament and up through it to the ground.

called dispersion. Dispersion leads to spreading of the release over a longer period of time.

In the case of stable substances, dispersion also reduces the maximum concentration that reaches the biosphere. In the case of radionuclides, however, the effect of decay must also be taken into account. Certain nuclides that would have decayed considerably if they had remained in the geosphere during the mean travel time reach the biosphere earlier and therefore at higher concentrations due to dispersion. Under the conditions being considered here, a large dispersion generally leads to higher release levels than a low dispersion.

14.2 PHYSICAL MODEL

14.2.1 Introduction

The repository is situated in rock of relatively low hydraulic conductivity. Water flows in the rock's fractures from places with higher potential to places with lower potential. Figure 14-1 illustrates the situation of the repository and how stream lines intersect it on their way to outflow areas. In the figure, outflow through a lineament with higher hydraulic conductivity is illustrated. Here, the flow can go almost vertically upward if the lineament goes through a low point on the ground.

When the water passes the repository, radionuclides from the canisters that have corroded can enter it. The quantity of escaping nuclide "i" at every point in time, $N_{tot,i}$, is the product of the number of leaking canisters n, the equivalent water flow Q_{eq} each canister has been able to deliver a nuclide to, and the concentration in this water flow C_{oi}:

$$N_{tot,i} = nQ_{eq} C_{oi} \qquad (14.1)$$

The transfer of nuclides to the water is described in chapter 13.

This quantity of nuclide is transported with the water in the rock. The quantity of nuclide that sorbs on the rock is proportional to its concentration in the water at the low concentrations that prevail for most important nuclides, which means that retardation due to sorption is not affected by any dilution due to transverse dispersion. An exception is cesium, which has relatively higher sorption at lower concentration. /14-1/. This element is therefore retarded more the lower its concentration is.

14.2.2 Water flow rates and velocities

The water flow rates in the rock are calculated from the rock's hydraulic conductivity and the hydraulic gradient (see chapter 6).

$$U_o = K_p i \qquad (14.2)$$

Hydraulic conductivity has been measured in a number of areas and in many deep boreholes. Mean values of K_p vary at repository depth (approx. 500 m) between about 4×10^{-11} and 2×10^{-9} m/s between the different areas. The hydraulic gradient - i - is determined partly by variations in the level of the water table at the ground surface and partly by how the forces of friction associated with the water's flow in the rock level out and reduce the variations on the surface.

Local variations of the water table at the surface are greatly levelled out with increasing depth. A 10% local gradient at the surface can typically decrease to 0.1% at a depth of 500 m /14-2/. Only in exceptional cases does the gradient at a depth of 500 m exceed 1%. This can occur if two closely-spaced nearly parallel lineaments have different potentials and thereby drive the water through the intervening rock mass. At a depth of 500 m, a gradient of i = 1% gives a water flow of:

$U_o = 0.1$ l/(m^2.year) for rock with $K_p = 3 \times 10^{-10}$ m/s

Hydraulic conductivity is greater in the lineaments at the same depth, and the flows can be accordingly higher. Hydraulic conductivity increases closer to the ground surface and can be 100 to 1 000 times greater. The gradient also increases closer to the surface, so that the water flow near the ground surface can be thousands to tens of thousands times higher. This means that a water volume that passes the repository may be diluted thousands to tens of thousands of times as it approaches the ground surface.

It is possible to calculate in detail the water flow in the rock that surrounds a repository. This has been done for a number of areas (see chapter 18). At repository depth, the variations are relatively small. However, changes in the topography can alter the direction and flow at a point in the repository. It has therefore been deemed better to use somewhat conservative flows and flow paths in general than to follow the individual flow lines through the repository for some special case.

The water flow U_o is assumed to be equal everywhere at repository level. The water's retention time from a canister to the lineament can be estimated from:

$$t = \frac{Z_o}{U_o} \varepsilon_f \qquad (14.3)$$

where Z_o = distance between lineament and canister
ε_f = flow porosity
For U_o = 0.1 l/(m^2.year)
and with $\varepsilon_f = 10^{-4}$, the retention time t
obtained for Z_o = 100 m is 100 years for the water

The water's retention time for a given flow U_o has no direct influence on the retention time of the sorbing nuclides, since their retention factors are inversely proportional to ε_f. However, the travel time of non-sorbing substances is equal to the travel time of the water.

14.2.3 Nuclide transport in the fractures

The nuclides exist either as charged ions, charged or uncharged complexes or colloids. One and the same nuclide can exist simultaneously in all forms and alternate between them. The dissolved positively charged species, for example cesium and strontium, react by means of ion exchange and adsorption with the minerals along the flow path and can also penetrate into the rock's micropore system and adhere to the inner surfaces in the rock. Uncharged and charged complexes can be adsorbed on the surfaces in the rock and on fracture walls. (Many of the actinides, e.g. uranium, plutonium, neptunium are complex-bound (see section 12.1)).

Complexes with fulvic and humic acids can reduce sorption of the nuclides, see section 12.8.3.

True colloids and pseudocolloids can be transported with the velocity of the water, but - given time (several to tens of years) - they dissolve when the water passes mineral surfaces on which little of the nuclide has yet sorbed. With long travel times, all

of the nuclides therefore behave as if they were dissolved in the groundwater. Measured sorption data can therefore be used even if colloids should have been formed through precipitation at the redox front or through adsorption on natural mineral particles in the groundwater. In the calculations, however, the consequences of irreversible sorption of the pseudocolloids are dealt with. See chapter 20.

Most of the nuclides that are transported with the mobile water in the fractures react with the minerals on the fracture faces. Reaction takes place both with the minerals that make up the rock itself, such as quartz and feltspar, and with secondary minerals that have been precipitated on the fracture face such as calcite, chlorite etc. Some fractures also contain small quantities of clays, e.g. smectite, with which the nuclides react.

Ion exchange and physical adsorption are rapid, reversible reactions and have, with few exceptions, constant distribution factors at low concentrations. This means that the concentration C_s on the fracture face is proportional to the concentration C_f in the water in the fracture.

$$C_s = K_a C_f \qquad (14.4)$$

K_a = the surface sorption coefficient m^3/m^2

The nuclides can also adhere to the surface by means of reversible precipitation and by means of irreversible reactions. Precipitation due to the fact that the solubility of the nuclide has been exceeded is an important mechanism to limit radioactive releases from the near field, but is of no importance in the far field unless the composition of the water is greatly altered. Irreversible reactions such as mineralization occur and can be of importance in practice and reduce releases. Since the kinetics of these reactions are not fully known, these effects are disregarded.

The reversible surface reaction retards the migration of the nuclides with the water by a factor of R_a (the retention factor), which is dependent on the surface sorption coefficient and the ratio between fracture surface area and water volume in the fracture.

$$R_a = 1 + K_a a \tag{14.5}$$

where a = fracture surface area available for sorption per volume of water in the fracture m^2/m^3

For a plane fracture,

$$a = \frac{2}{\delta} \tag{14.6}$$

where δ = fracture width, m

For a rock where the fracture spacing is S m, the porosity of the fracture is obtained as:

$$\varepsilon_f = \delta/S \tag{14.7}$$

At known water flow rates U_o in the rock, the velocity of the water U_f can be calculated from:

$$U_f = U_o/\varepsilon_f \tag{14.8}$$

The migration velocity for nuclide "i" is then:

$$U_i = \frac{U_f}{R_a} = \frac{U_o}{\varepsilon_f R_a} = \frac{U_o}{\varepsilon_f + K_a a \varepsilon_f} \tag{14.9}$$

By inserting equations (14.6) and (14.7) in (14.9), we obtain

$$U_i = \frac{U_o}{\varepsilon_f + 2\ K_a/S} \tag{14.10}$$

For sorbing nuclides, $\varepsilon_f << K_a \frac{2}{S}$

and ε_f can be neglected in equation (14.10). The migration velocity of the nuclide is then independent of the velocity of the water in the fracture and of the porosity of the fracture system.

$$U_i = \frac{U_o S}{2\ K_a} \tag{14.11}$$

The migration velocity is proportional to the water flow rate and the fracture spacing, which determine the available sorption surface area per volume of rock. At the same water flow rate, a more highly fractured rock gives a lower nuclide migration velocity. For example,
for S = 5 m,
U_o = 0.1 l/(m^2.year) and K_a = 0.2 m (typical actinide value)
U_i = 1.3 mm/year

Surface sorption is not the only important retardation mechanism, however.

14.2.4 Penetration in the rock matrix

Gneisses and granites in Swedish Precambrian rock have a continuous pore system consisting of the microfissures between the crystals in the rock matrix. The porosity in this pore system varies between 0.1 and 0.5% /14-1, 14-3, 14-4/ for the rock matrix. Fracture minerals and rock in crush zones have higher porosities. Values between 1 and 9% have been measured. Substances dissolved in the water can diffuse into this pore system and sorb on the inner surfaces. Figure 14-2 shows penetration and sorption in the rock matrix.

The penetration depth increases with time. Non-sorbing nuclides penetrate far into the matrix, while sorbing nuclides are retarded since they also have to fill up the sorption sites before they migrate further. The sorption capacity of the inner surfaces is normally expressed as a mass-based sorption coefficient, K_d, or as a volume-based sorption coefficient, $K_d \rho_p$, where ρ_p is the density of the rock. The concentration of nuclide per volume of rock at equilibrium with a liquid content C_p in the pores is:

$$q = K_d \rho_p C_p \qquad (14.12)$$

The penetration depth can be calculated with the aid of Fick's laws for diffusion, if diffusivity is known, and by taking retardation due to sorption into account /14-5/. Examples of penetration depths for some different nuclides at different times are given in table 14-1.

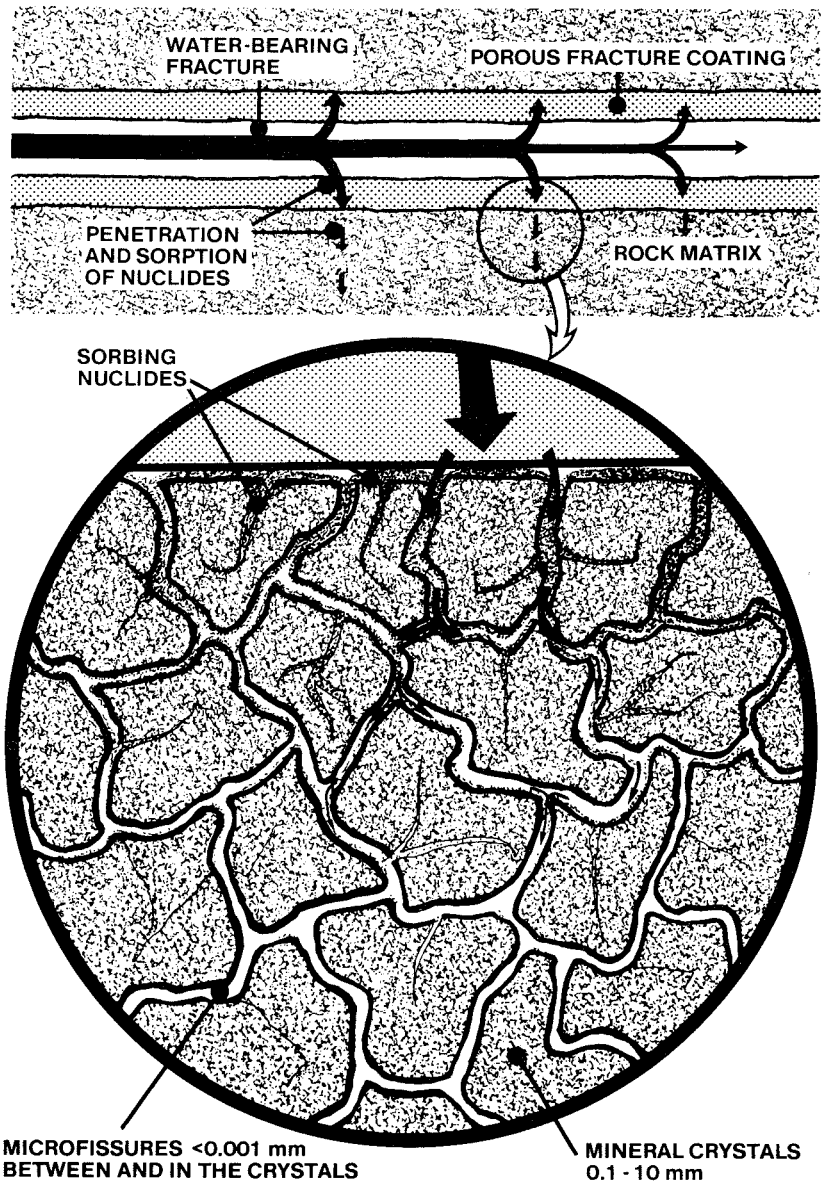

Figure 14-2. The figure shows the penetration and sorption of the nuclides in the microfissures in the rock matrix.

By "penetration depth" is meant the distance from the surface at which the nuclide has 1% of its concentration at the surface.

It is evident from table 14-1 that non-sorbing substances can penetrate far into the rock and completely saturate the rock sections between the fractures. The actinides, which sorb very strongly, reach penetration depths after long periods of time (millions of years) of several tens of mm. The rock nearest the fractures constitutes a powerful sink for the nuclides, since they are removed from the mobile water through diffusion into the matrix.

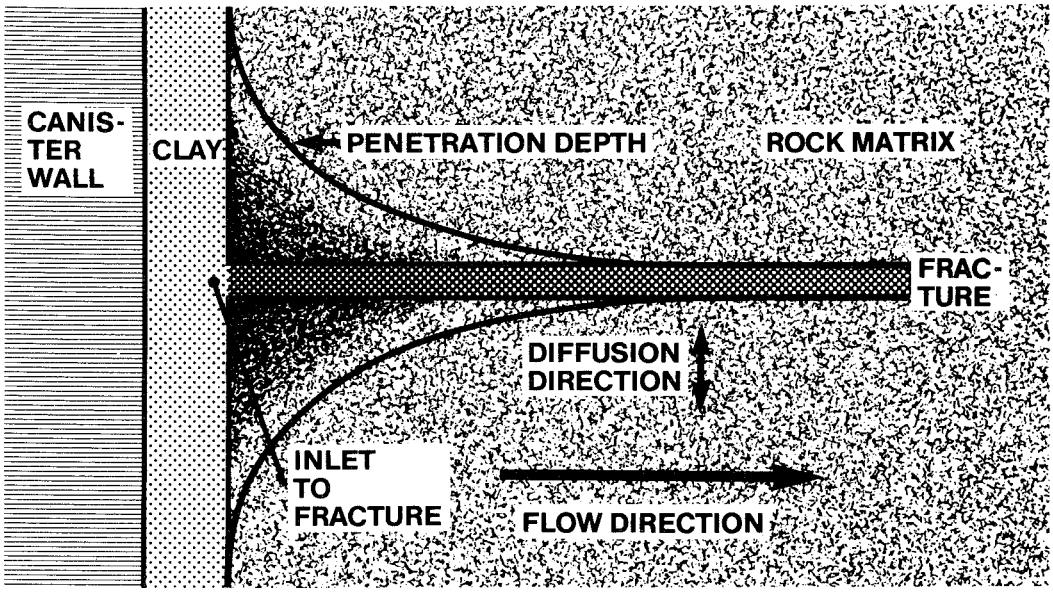

Figure 14-3. Nuclides carried by the water in a fracture diffuse into the rock matrix.

A penetration depth of about 0.1 mm corresponds to a retardation that is as great as that due to surface sorption. This means that retardation of the radionuclides due to penetration in the matrix is of great importance at long contact times.

Figure 14-3 shows how a nuclide is sucked into the rock matrix along a fracture downstream of the repository. The penetration depth will vary along the flow path. It is not possible to specify a constant retention factor, as for the surface sorption case, since the nuclide velocity varies with the contact time.

In the same manner as for surface sorption, the migration velocity of the sorbing nuclides is not dependent on the water velocity U_f, but rather on the flow rate U_o and the fracture frequency (or the fracture spacing /14-5, 14-6/). A heavily fractured rock, for example a crush zone, can be advantageous from the viewpoint of retardation if the water flow is not affected. It provides larger surface areas for surface sorption and for penetration into the micropores.

Talbe 14-1. Penetration depth $Z_{0.01}$ m of some different nuclides at different contact times. $Z_{0.01} = 4\sqrt{D_a t}$.

Element	K_{d_3p} (m^3/m^3)	D_a [2] (m^2/s)	10^2 years	10^4 years	10^6 years
I	0.002 [1]	2.5×10^{-11}	1.12	11.2	112
Cs	16 [3]	1×10^{-13}	0.071	0.71	7.1
Am [5]	1.35×10^{4}	3.7×10^{-18} 4)	0.43×10^{-3}	4.3×10^{-3}	43×10^{-3}

1) Equal to the porosity for non-sorbing substances.
2) Finnsjö granite /14-1/.
3) Finnsjö granite /14-1/ and at nuclide concentrations of 3 mg/l.
4) Calculated from the diffusivity for non-sorbing substance and the sorption coefficient (eqn. (14.13)).
5) The same values apply for Pa, Np, Th, Pu and U under reducing conditions.

The diffusivity of different substances in rock has been measured /14-1, 14-3, 14-4/. Diffusion takes place in the water in the micropores - pore diffusion - but also on the surface of the minerals - surface diffusion - for some sorbing substances /14-7/. Surface diffusion has been measured for strontium and cesium to be more than ten times as fast as can be explained by pore diffusion alone /14-8/. Only a few results are available for the actinides /14-9/. They show such small penetration depths that it cannot be concluded with certainty that any transport has taken place by means of surface diffusion. It is therefore assumed in the following that the movement of the actinides is dependent on pore diffusion alone. This underestimates the surface area available for sorption.

A sorbing substance's matrix diffusivity D_a during the unsteady-state phase can then be estimated from the diffusivity for non-sorbing substances with the same mobility in water and from retardation due to sorption:

$$D_a = \frac{D_v \, \varepsilon_p \, \delta_D}{K_d \rho_p \tau^2} \qquad (14.13)$$

D_v = the sorbing nuclide's diffusivity in pure water.

δ_D / τ^2 includes effects of constrictivity (δ_D) in the pores and tortuosity effects (τ^2)

ε_p = porosity that takes into account the fact that only a fraction equal to ε_p of the rock volume is available for diffusion transport.

The product

$$\varepsilon_p \frac{\delta_D}{\tau^2}$$

has been determined for a number of crystalline Swedish rock materials /14-4/ by means of diffusion measurements using iodide ions and tritiated water as well as by means of electrical conductivity measurements.

14.2.5 Dispersion mechanisms

Dispersion is a collective term for the various mechanisms that cause a dissolved substance to spread out to larger and larger liquid volumes as the liquid flows in a medium. Dispersion is caused by spreading by means of diffusion, random or deterministic variations in velocity in a channel (such as in the case of turbulent or laminar flow in a pipe) and random velocity variations between different channels in a network of channels. This dispersion is often called hydrodynamic dispersion. The concept of dispersion is also often extended to cover spreading due to the fact that the substance reacts with the solid matter by diffusing into and out of stagnant liquid volumes (e.g. micropores) and spreading due to channelling. The latter three mechanisms are termed dispersion in cases where their influences cannot be described separately. This is usually the case in connection with field measurements of tracer transport. The transport path is almost never known in sufficient detail to be able to treat these mechanisms separately.

Besides in the direction of flow - axial dispersion - dispersion also occurs across the flow direction. This transverse dispersion causes a concentrated nuclide plume to be diluted by mixing with water outside of the stream lines that have passed through the repository. In some cases, the nuclide concentration can be reduced considerably due to this dilution /14-10/. At present, however, no results are available from field tests where transverse dispersion has been measured in connection with flow in crystalline fractured rock. It could be quite low when flow takes place in a few well-defined channels, but could also be very great in rock where the main fracture directions run at large angles to the mean principal direction of flow. Owing to a lack of data, it is therefore assumed that no transverse dispersion takes place. This assumption prevents an underestimation of the nuclide concentration released to the surface water.

Field tests generally show that the dispersion coefficient D_L increases with the observation distance /14-11, 14-12/. The reasons for this are many. The network of fractures may be such that the mixing of water between different fractures does not take place sufficiently randomly. In this case, channelling occurs, which means that the water in some flow paths moves independently of the flow in other channels. Channelling causes a pulse to be dispersed more than it would be with random velocity variations alone. The dispersion coefficient increases in proportion to the flow distance /14-13/.

Available data on dispersion in crystalline rock are very limited. In Studsvik, tests have been conducted over 22 and 51 m /14-12/ and over 12 m /14-14, 14-15/. In Finnsjön, tests have been conducted over 30 m /14-16/. In Stripa, the flow distances studied are 3.5 and 5 m /14-17/, and laboratory tests have been conducted in natural fractures up to 0.3 m in length /14-26/. These tests, in which the water has mainly flowed in a fracture or an interconnected fracture system, show that the dispersion coefficient increases with length. Since the dispersion coefficient is proportional to the velocity /14-18/, these factors can be related in an expression:

$$U_f \cdot Z/D_L = \text{constant} = Pec$$

where U_f = velocity

Z = flow length

D_L = dispersion coefficient

Pec is an abbreviation for Peclet's number.

In the studies in crystalline rock mentioned above, Pec values of between 5 and 20 are obtained for the most part. The first part of the penetration curves is used for the determination. (This part is important for the nuclides that decay appreciably less if they have a shorter travel time.) The contact time for these tests is so short that the non-sorbing substances that are used in the tests have been affected little by matrix diffusion.

14.2.6 Decay

The radionuclides decay during their migration through the fracture system. Short-lived nuclides decay to negligible levels before they reach the biosphere. Many nuclides decay to other radionuclides. The decay chains may contain 3-4 nuclides with such long half-lives that the whole chain's migration and decay must be considered simultaneously. When the parent nuclide that has penetrated into the rock matrix decays, it leaves a daughter nuclide behind. This nuclide penetrates further into the matrix while also diffusing out to the fracture with the moving water. The daughter nuclide can in turn leave a daughter of its own. The different nuclides in a chain may have different diffusivities and sorption coefficients. Their migration can therefore not be described in a simple expression. Many chains have one nuclide with a much longer half-life than the others. This nuclide often dominates the whole chain.

14.3 VERIFICATION OF PHYSICAL MODEL

14.3.1 Introduction

The most important retardation mechanism is micropore diffusion and sorption on the micropore surfaces. It is such a slow process,

however, that it has not been possible by means of laboratory experiments alone to show that the strongly sorbing nuclides (actinides) penetrate tens of mm. (This would take 100 000 years or so.) It has therefore been necessary to use different approaches. Laboratory experiments have been used to demonstrate that the pores are interconnected over long distances. Field tests have been used to verify that the pores found in the laboratory also exist in rock subject to natural stress at great depths. Evidence for the migration of different substances in rock matrices under natural conditions has been sought and used to verify the fact that matrix diffusion occurs in nature and over long distances.

Flow paths and patterns in crystalline rock have been studied in natural fractures and fracture systems in the field over distances of up to 50 m and in the laboratory in up to 30 cm long fractures. In those tests where sorbing tracers have been used, it has also been possible to use the results to shed light on retardation mechanisms.

14.3.2 Laboratory tests

Few studies of pore systems in crystalline rock have been done before. During the years 1965-1977, Brace carried out a series of studies of electrical conductivity in the pore water in granites under pressure as a means of attempting to determine hydraulic conductivity /14-19, 14-20, 14-21/. Since electrical conductivity and diffusion of ions are analogous processes in aqueous systems, an idea of diffusion in the pore system as well as its dependence on the stress in the rock can be obtained from these studies. Heard /14-22/ and Trimmer et al /14-23/ have measured electrical and hydraulic conductivity in, inter alia, granite under very high stresses.

Skagius et al /14-1, 14-3, 14-4, 14-8/ have measured diffusion of iodide and tritiated water through 10 mm thick pieces of granites and gneisses. They have also measured electrical conductivity for saltwater-saturated rock pieces both with and without applied stress. Öquist and Jämtlid /14-24/ have measured porosity and electrical conductivity for different granites. Bradbury et al /14-25/ have measured iodide diffusion in granites.

The studies cited above show that interconnected pore systems of at least 10 or so cm exist. The porosity of the rock varies between 0.1 and 1%, and diffusivity in the pore systems is from thousandths to tenths of the values in free water. Increasing rock stress reduces both porosity and diffusivity in the pores. At a rock stress of 250 bar, Brace /14-19/ has measured the reduction of electrical conductivity to be a factor of about 2 compared to values at 50 bar. Skagius and Neretnieks /14-4/ find that at a rock stress of 220 bar, electrical conductivity has been reduced by about 30% compared to unstressed rock.

Torstenfelt et al /14-9/ show that cesium has penetrated a 0.2 mm thick natural fissure coating and 2.5 mm further into the granite. Two other granites show similar and deeper penetration depths for a contact time of 3 months. Diffusivities derived from these tests give D_a = 0.53 - 17 x 10^{-13} m^2/s for three different granites. These values agree well with those obtained by Skagius and Neretnieks /14-8/ using another measuring method for two different granites. In the latter study, the diffusivity of strontium was also obtained as D_a = 2.5 - 5 x 10^{-13} m^2/s.

These results show that both cesium and strontium have much higher diffusivity in the rock matrix than can be explained by diffusion in the pore liquid alone.

Tracer tests with both non-sorbing (tritiated water and high-molecular-weight lignosulphonate ions) and sorbing substances (strontium and cesium) in a 30 cm long natural fracture from the Stripa mine have been carried out /14-26/. The non-sorbing substances are used to characterize the flow (dispersion, fracture width). With knowledge of this, retardation due to sorption can be singled out.

The retardation of the sorbing substances can only be explained if both surface sorption and penetration in the matrix are taken into account. Sorption and diffusion data obtained from independent measurements agree with those obtained from the fracture tests. Raber et al /14-27/ have conducted similar tests on much smaller rock pieces and with fresh fractures.

Penetration tests have also been carried out with Tc and Am by Torstenfelt et al /14-9/. These tests reveal high sorption and very short penetration depth for Am in agreement with what can be expected in view of the high sorption.

Tracer tests with active Eu, Np, Pu have been carried out in the laboratory in natural fractures /14-28/. In the Europium test, it is found that a small fraction - per mill to per cent - of the activity comes out with the velocity of the water. This is a particle-bound fraction that does not have time to dissolve or sorb during its short retention time in the fracture (< 10 minutes). All the rest of the activity is found on the surface of the first few centimetres after the inlet, even after months of water flow. Figure 14-4 shows where Eu has sorbed in a flow test along a natural fracture.

In the test with plutonium, none could be detected in the outlet. All plutonium was found within a few mm of the inlet.

14.3.3 Field tests

Field tests in crystalline rock with tracers have been conducted in France /14-29/ and at many places in Sweden. The results of the French test do not seem to have been fully evaluated yet. In the tracer tests conducted in Sweden with I^-, Br^- and Sr^{2+} between two flow paths 22 and 51 m long at a depth of 60 m /14-12/, strontium was retarded with a retention factor of 6, which is more than twice as much as can be predicted with surface sorption alone.

More recent tests in Sweden over 11.8 m at a depth of about 100 m /14-14, 14-15/ with I^- tritiated water and Sr^{2+} show a retention factor of at least 15 for Sr^{2+}. Laboratory tests with crushed material show a retention factor of 30-35. These retention factors are not directly comparable, however, since the two tests have had different ratios between water volume and rock surface area.

Gustavsson and Klockars /14-16/ have carried out tracer tests with I^-, Blue Dextran and Sr^{2+}, among other species, in granitic rock at Finnsjön. The distance between the injection hole and the measure-

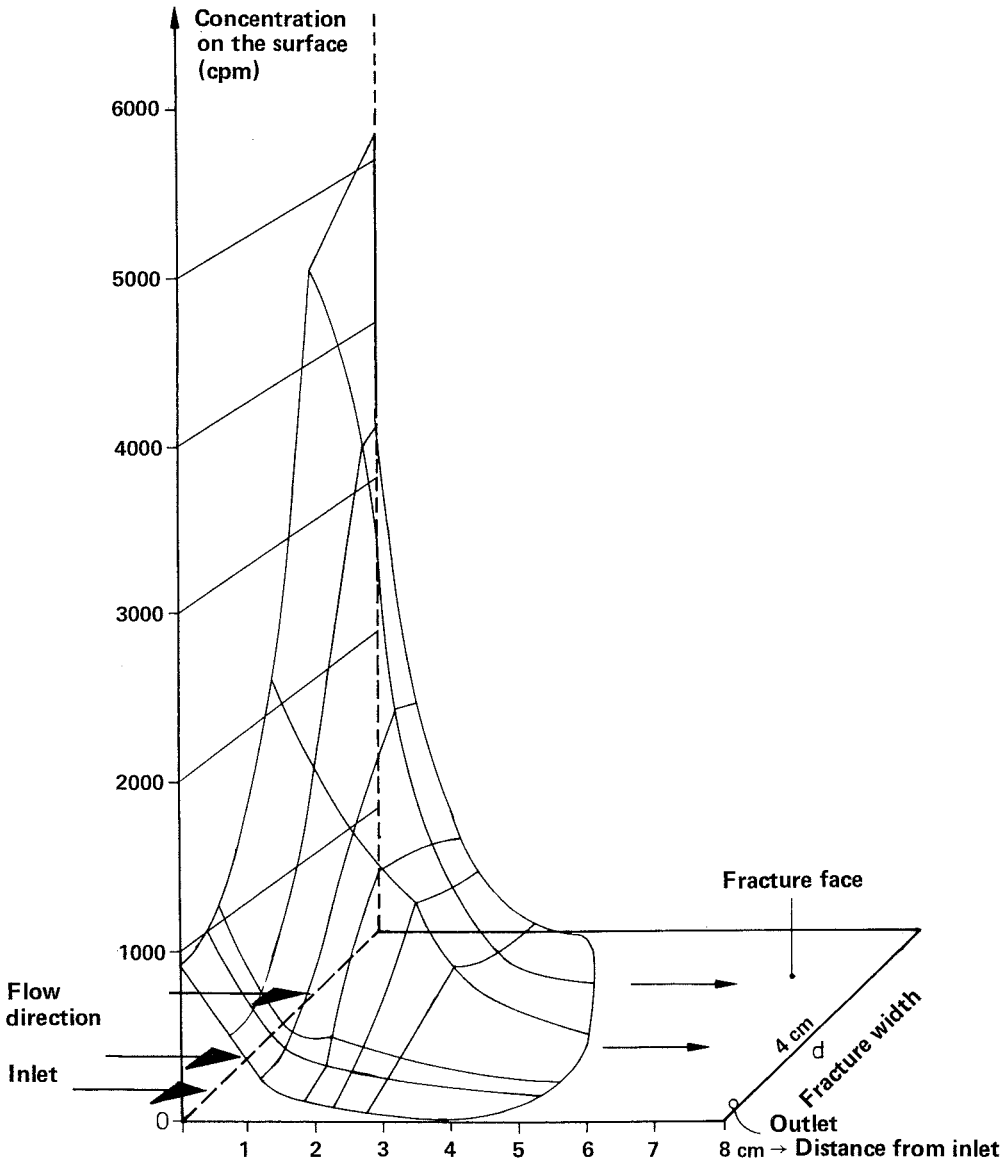

Figure 14-4. Europium solution that has flowed through a natural fracture has left sorbed Eu on the surface. The fracture has been opened and the concentration of Eu on one side has been measured and plotted upwards in the figure.

ment hole was 30 m and the depth about 90 m. Sr^{2+} was retarded very little in this test, but about 40% of the injected quantity failed to arrive at the collection hole. These tests have been interpreted by Hodgkinsson and Lever /14-30/ and Moreno et al /14-31/. Both attempts at interpretation find that the retardation is less than is expected on the basis of independent laboratory measurements of diffusivity and sorption coefficients on Finnsjö granite. The concentration of Sr^{2+} was 100-1 000 times higher in this test than the concentration used in laboratory measurements, which means that

the sorption coefficient is probably considerably lower in the field test than the one used for the interpretation. The poorer retardation in this flow path may also be due to the fact that there are low-sorbing fracture coatings on the fracture face, while the laboratory measurements were done on pure granite. Calcite is a material with low ion exchange and sorption capacity for Sr^{2+} /14-32/. This is a common fracture-filling mineral in Finnsjön /14-33/.

Field tests at great depth (360 m) in the Stripa mine have shown that an interconnected micropore system also exists in undisturbed rock with natural rock stresses /14-34, 14-35/. Both the laboratory tests and the field tests mentioned above show that even many mm thick fracture coatings allow dissolved species to pass through to the rock matrix. The coatings often have considerably higher porosity than the rock.

An attempt has been made to separate the dispersion due to channeling from other causes in /14-16/. It was found that if the field tests over 30 m in granite in Finnsjön were interpreted as flow in three channels instead of one channel, the dispersion coefficient was reduced to very low values. Hodgkinsson and Lever /14-30/ and Moreno at al /14-31/ evaluated the same tests with other assumptions and found that the hydrodynamic dispersion can be very small if matrix diffusion, channeling or diffusion in stagnated water volumes occurs. Tests in a natural fracture in the laboratory /14-26/ and two tests in the field in the Stripa mine /14-17/ show that channeling occurs and can be an important cause of dispersion. Channeling particularly affects the early arrival of the nuclides.

Lallemand-Barrès and Peaudecerf's /14-11/ review reports the results from many tests in more than ten geological media, but only a few tests in fractured crystalline rock. The scatter in the results is very great. The Peclet numbers obtained mainly fall within the interval 2-50, with only a few results falling outside of this interval. The mean is Pec=10. In determining these data, dispersion due to diffusion into the matrix has not been taken into consideration. These data therefore exaggerate the importance of the hydrodynamic dispersion.

The field data that are available from fractured crystalline rock were obtained over a maximum observation distance of 51 m. In order to extrapolate these data over longer distances, it is assumed that Pec = constant instead of that the dispersion coefficient D_L = constant. This ensures that any influence of channeling will not be underestimated. Further, the value Pec = 2 is used as a central value in the calculations for the safety analysis. This is probably an exaggeratedly low value, since matrix diffusion is particularly accounted for, but ensures that an early arrival of an important nuclide is not underestimated. The influence of early arrival and matrix diffusion has been discussed both quantitively and qualitively /14-36, 14-37/.

14.3.4 Natural evidence for the migration of dissolved substances in crystalline rock

Certain natural phenomena exist that shed light on some of the migration phenomena discussed above. These natural phenomena have, in some cases, been going on for a very long time and over longer distances than those that can be achieved in artificial tests.

Several natural uranium reactors were active in Oklo in Gabon about 1.8 billion years ago. This has been thoroughly described in a number of publications /14-38, 14-39/.

Analyses of the remaining uranium ore body, which is surrounded by clay and sandstone, show that the actinides still remain for the most part in the uraninite crystals and that several important fission products Ru, Tc and Nd or their daughters can be found for the most part within some 10 or so metres of the reactor. Cs and I are largely gone. During the operation of the reactor, which lasted for about 300 000 years, water flowed through the reactor, and it has been wet more recently as well. It is not possible to reconstruct the chemical conditions in detail, but judging from the presence of different minerals (Fe(II), Fe(III) minerals), it can be concluded that some of the most important parameters, pH and redox potential, have been very similar to those expected in a Swedish repository.

Crystalline rocks such as granite and gneiss contains small quantities of uranium and thorium mineral. Smellie /14-40/ has been able to show that uranium (^{234}U) has moved up to 60 cm over a period of about 1/2 million years into the rock matrix from a uranium mineralization in a fracture in the "Björklund" deposit by studying the relative occurrence of ^{238}U, ^{234}U and ^{230}Th.

14.4 MATHEMATICAL MODEL

14.4.1 Introduction

In order to permit quantification of the transport and sorption mechanisms described previously, they have been given a mathematical description. It has the following structure:

In a small volume element of the mobile water, an account is kept of how much of a nuclide is supplied and removed by means of the different mechanisms.

The nuclide is supplied and removed by means of:

- flow
- diffusion (dispersion) in the mobile liquid
- diffusion in the micropores in the rock
- surface sorption (and desorption)

Nuclides are also supplied through radioactive decay from the parent nuclide and are removed through their own decay.

The nuclide that is present inside the rock matrix, which belongs to the element with mobile water, is accounted for in the same way:

- Diffusion further to/from nearby volume elements of rock matrix or mobile water
- Sorption on micropore surfaces
- Supply and removal through decay

Since transport of nuclides occurs between nearby volume elements, transport away from one element is accounted for as transport into another. If a difference arises between supply and removal in an element, the nuclide concentration in this element increases or decreases to a corresponding degree.

14.4.2 Equations

For the sake of simplicity, and since most of the calculations are carried out for the one-dimensional case, the equations are written here in one-dimensional form.

The following is obtained for the mobile liquid:

$$\underset{(1)}{\frac{\partial c_f^i}{\partial t}} + \underset{(2)}{U_f \frac{\partial c_f^i}{\partial z}} - \underset{(3)}{D_L \frac{\partial^2 c_f^i}{\partial z^2}} = \underset{(4)}{a D_p \varepsilon_p \frac{\partial c_p^i}{\partial x}\bigg|_{x=0}} - \underset{(5)}{\lambda^i c_f^i} + \underset{(6)}{\lambda^{i-1} c_f^{i-1}} \qquad (14.14)$$

c_f^i = concentration of nuclide "i" in the mobile liquid
t = time
U_f = mean velocity of the mobile liquid
z = distance in the flow directon
D_L = dispersion coefficient
a = sorption surface area per liquid volume
$D_p \varepsilon_p$ = effective diffusivity in the rock matrix
c_p^i = concentration of nuclide "i" in the pore liquid in the rock matrix
x = distance from the fracture face
λ^i = decay constant for nuclide "i"

if surface sorption occurs, terms 1 and 5 shall be multiplied by $1 + K_a^i a$ and terms 6 by $1 + K_a^{i-1} a$.

The terms stand for

1 accumulation in the liquid
2 difference between supplied and removed by flow

3 difference between supplied and removed by dispersion

4 supplied or removed from the rock matrix

5 decayed

6 supplied from decaying parent

The following is obtained for the rock matrix:

$$\underset{(7)}{\frac{\partial c_p^i}{\partial t}} = \underset{(8)}{D_a \frac{\partial^2 c_p^i}{\partial x^2}} - \underset{(5)}{\lambda^i c_p^i} + \underset{(6)}{\frac{K_d^{i-1}}{K_d^i} \lambda^{i-1} c_p^{i-1}} \qquad (14.15)$$

D_a = matrix diffusivitiy

K_d = sorption coefficient for the rock matrix

The terms stand for

7 accumulation in the pore liquid

8 difference between supplied and removed by diffusion

Term 8 has been written here for plane geometry.

The equations (14.14) and (14.15) are coupled to each other via term 4 ($c_p = c_f$ at $x = 0$) and the equations must therefore be solved simultaneously. In multinuclide chains, a set of equations must be used for each nuclide and all equations must be solved simultaneously. The equations do not assume that U_f, a, K_a, K_d or $D_p \varepsilon_p$ are constant along the flow path.

In addition to the equations, initial and boundary conditions are also required. These tell us what conditions exist at the beginning of the time span we wish to study, and how the radio nuclides are transported into and out of the space being considered, or alternatively what concentration the nuclides have at the limits of the considered space. The most essential initial condition is that the water and rock matrix do not contain any nuclides at the beginning (t=o).

14.4.3 Solution of equations and verification of solution method

The equations (14.14) and (14.15) and their properties have been studied.

It has been possible to solve simplified cases analytically. The analytical solutions are used to check the more general numerical solutions. They are also useful for studying the influence of different quantities on the nuclide transport.

For flow in an individual fracture without dispersion but with the diffusion into the rock matrix, there is a very simple solution for a single radionuclide /14-5/. The great importance of matrix diffusion for the retardation of radionuclides is demonstrated here. Grisak and Pickens /14-41, 14-42/ have dealt with this case in a very similar fashion. Glueckauf /14-43/ has also treated this case. This solution is also included in the solution for a case with pure channeling /14-44/. Tang et al /14-45/ have come up with an analytical solution for flow in a single fracture, where dispersion also occurs. Rasmuson and Neretnieks /14-46/ describe a solution for flow in a porous medium where the rock blocks are approximated with spheres. The solution includes axial dispersion.

The same authors have used this solution to study the influence of different parameters on radionuclide migration /14-6/. The case with matrix diffusion in spherical blocks and with both radial and axial dispersion has been treated by Rasmuson /14-10/.

Parameter studies have been carried out for a large number of radionuclides both for the case with matrix diffusion and axial dispersion /14-47/ and for the case with channeling and matrix diffusion /14-44/. Chambré et al /14-48/ have come up with analytical solutions for the case of flow in a fracture and micropore diffusion with diffusion both in and across the direction of flow. The same authors also present an approximate analytical solution for a multinuclide chain in a single fracture with micropore diffusion, but without dispersion.

For more general cases, where conditions along the flow path vary, numerical solutions are used. The three most flexible numerical methods are:

finite difference methods	FD
finite element methods	FE
integrated finite difference methods	IFD

They are used to solve the equations (14.14) and (14.15) in 1, 2 or 3 dimensions with micropore diffusion, dispersion in different directions and chain decay. The methods are very flexible and can take different boundary and initial conditions into consideration.

The methods have been compared in the INTRACOIN study /14-49/. There, they gave very similar results for problems that contained 3 nuclide chains, micropore diffusion and dispersion in one and two directions.

In the KBS program, the integrated finite difference method IFD /14-50/ has been used. The method is also described well by Narasimhan and Witherspoon /14-51/ with application to water flows in porous media. The method is very simple in principle and is very flexible, since the size and shape of the elements can be varied within wide limits.

The method has been tested with the aid of the analytical solutions described previously /14-46, 14-52/ as well as within the INTRACOIN project /14-49/.

Application of the method to conditions with widely varying water velocity and areas where there are widely varying sizes of rock blocks (e.g. crush zones) has been described by Neretnieks and Rasmuson /14-53/.

14.4.4 A central calculation case

The repository is placed at a depth of about 500 m below the ground surface. The canisters are situated so that no canister is located closer than 100 m from a lineament. A calculation case has been established on the basis of expected geological, hydrological and chemical conditions at the different study areas. Table 14-2 presents the data used in the calculations. The flow is assumed to take place over the shortest path from the canisters nearest the lineament and out to the lineament. The flow then proceeds straight

up through the lineament to the ground surface. It is assumed that the flow from all canisters in the repository travels this path.

Table 14-2. Data for central calculation case.

Water flow at a depth of 500 m	U_o	10^{-4} $m^3/(m^2 \cdot year)$
Flow porosity	ε_f	10^{-4}
Fracture frequency, water-bearing fractures	1/S	0.2 m^{-1}
Porosity of matrix	ε_p	0.002
Effective diffusivity for dissolved substances (all nuclides)	$D_p \varepsilon_p$	5×10^{-14} m^2/s
Peclet's number (gives dispersion coefficent)	Pec	2
Distance for nuclide migration in rock	Z_o	100 m

Sorption data for the different nuclides are presented in table 12-7. Surface sorption is not used in the calculations, since it has little effect on the results and since it is difficult to distinguish from experiments what has sorbed on the fracture face and what has sorbed due to short penetration into the matrix. Only for Cs and Sr are measurements available where surface and volume sorption have been able to be distinguished /14-1/. These show that the surface sorption is equivalent to the sorption at a penetration depth of a few tenths of a millimetre for measurements carried out on crushed rock.

The supply of radionuclides to the flowing water from leaking canisters is calculated with the aid of the near field model. See Chapter 13, table 13-5.

Figure 14-5 shows the release from the near field to the far field of the most important nuclides. Figure 14-6 shows the resulting release from the far field of the same nuclides /14-54/.

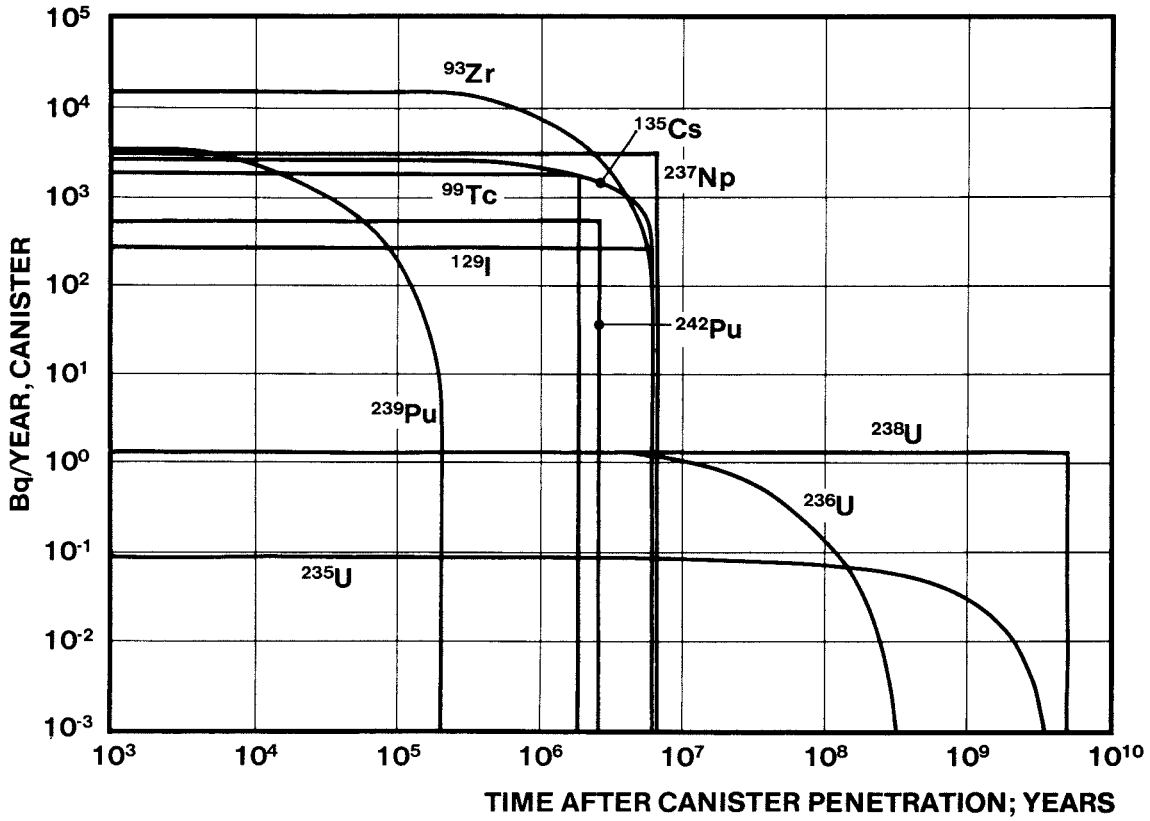

Figure 14-5. Release of radionuclides from the near field to the flowing water in the far field.

14.5 RELIABILITY OF THE BACKGROUND DATA

14.5.1 Model and data

The applicability of the equations to the reality that is to be described is judged by comparing calculated results with experimental results. For practical reasons, this cannot be done for the long time spans and over the great distances the predictions are intended to deal with. However, each transport mechanism can be verified independently by means of different methods, and the importance of uncertainty in the understanding of this mechanism can be evaluated.

The water velocity U_f is poorly known due to the fact that the porosity of the rock can vary and because virtually no porosity measurements have been made at great depths. However, it is of secondary importance for determining the transport velocity of the

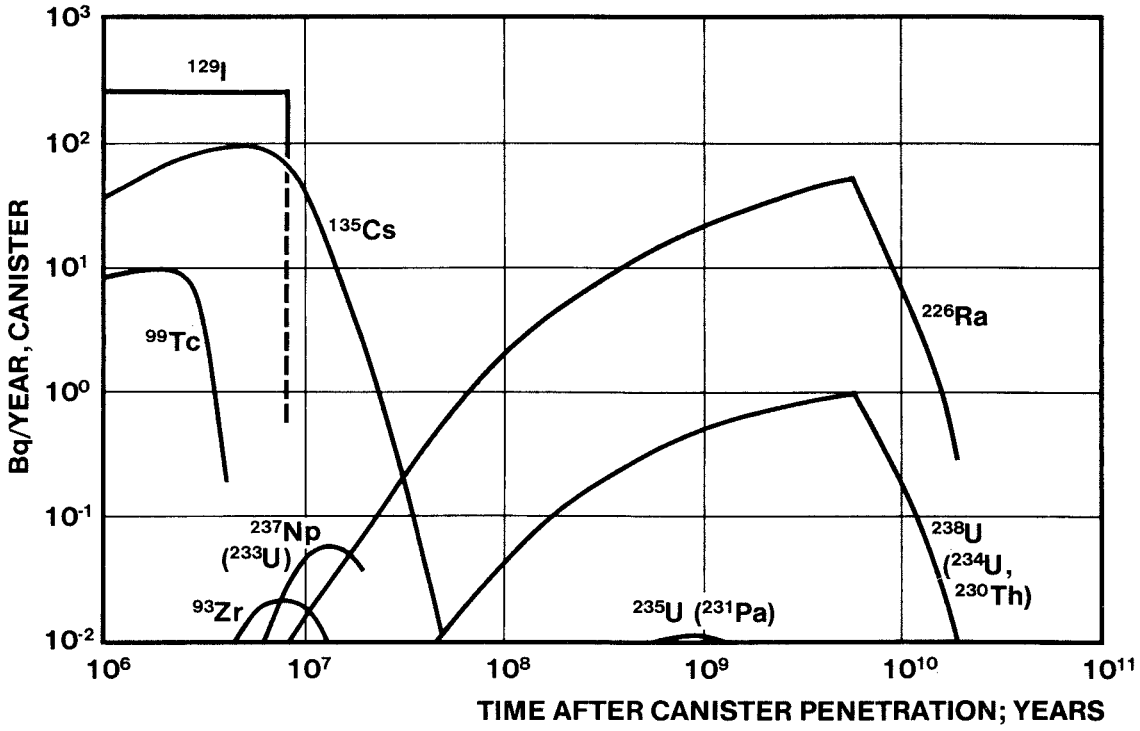

Figure 14-6. Release from the far field of the most common nuclides.

sorbing nuclides. For the non-sorbing nuclides, it is of no importance in determining the maximum release, since the possible water travel times do not provide enough time for decay for the interesting nuclides anyway. These matters have been dealt with by Neretnieks /14-5/ and Rasmuson and Neretnieks /14-6/. Dispersion D_L is a poorly known quantity and can be caused in part by channeling. Such large values of the dispersion coefficient are therefore used that they include both generous dispersion and the effect of channeling. The importance of channeling has been dealt with by Neretnieks /14-36/ and high dispersion coefficents by Rasmuson et al /14-37/. The use of a dispersion coefficient corresponding to Pec=2 means that high dispersion is assumed to prevail and that the dispersion coefficient increases with the flow distance. The latter assumption is equivalent to the effect of channeling. For some cases, a low dispersion (Pec=50) has also been used in order to ensure that the spreading of the release over a longer time due to high dispersion is not beneficial /14-54/.

In the same manner as for water velocity, available sorption surface area per mobile water volume does not directly influence the transport of sorbing nuclides at a given flow U_o. The quantity that determines the nuclide transport is the sorption surface area per rock volume a_v. This has been shown by Neretnieks /14-5/ and Rasmuson and Neretnieks /14-6/. The quantity a_v is in turn directly dependent on the fracture frequency 1/S where S = the mean fracture spacing. From the viewpoint of sorption, only those fractures that conduct water to an appreciable degree are interesting. The fracture frequency is therefore determined from water injection measurements in boreholes using the twin packer method (see section 6.1.3). Only those fractures which are water-bearing to a significant extent (fractures that transport as much or more than the mean fracture) are included in nuclide migration calculations. In many areas, this means that only about every 5th water-bearing fracture is included as making a contribution to the sorption surface area. Besides just to be generally cautious, this is done in order to allow for the fact that a fracture does not conduct water uniformly over its entire width, but sometimes conducts the water in "channels" in the fracture plane.

Observations in the Stripa mine indicate that less than half of a visible fracture conducts most of the water /14-55/. This type of channeling is not fully understood. This incomplete understanding is compensated for by using a high dispersion coefficient and by crediting only about 1/5th of the fracture face as being active for sorption as described above.

Effective diffusivity in the micropores $D_p \varepsilon_p$ and matrix diffusion D_a have been measured in many different crystalline rocks by several independent groups. The value used, $D_p \varepsilon_p = 5 \times 10^{-14}$ m^2/s, constitutes a conservatively chosen but realistic value. Compensation has therefore been made for the fact that the rock is heavily stressed at greater depths by the rock overburden. For all nuclides except cesium and strontium, where unambigious measurement data show that there is a strong contribution from surface diffusion, this possible contribution is neglected.

The sorption coefficients are discussed in chapter 12. They are chosen so that they constitute minimum values in groundwaters with

large but reasonable variations in pH, Eh and content of principal complexing agents - mainly carbonate.

14.5.2 Potential high-speed dispersal mechanisms

Most important radionuclides sorb on and in the rock matrix and are thereby retarded for such a long time that they decay to an appreciable extent before they reach the biosphere. Water at great depths contains some (ppm levels) organic substances in the form of fulvic and humic acids /14-56/. These can form strong complexes with many actinides and could constitute potential carriers of activity. The sorption coefficients of the trivalent nuclides (Pu, Am) can be reduced by up to a factor of 10, see chapter 12. This lower sorption coefficient still entails a considerable retardation of these nuclides.

As a result of precipitation processes, the actinides form radiocolloids. Owing to their greater mass, radiocolloids have lower diffusivity than single ions and can therefore not move as easily in the micropores. The radionuclides have been found to have a very high tendency to sorb on most available surfaces. This includes glass surfaces, various mineral surfaces and natural rock surfaces /14-57/. Moreover, the colloids are not stable, but exist in equilibrium with the dissolved nuclide. When this sorbs and is removed from the water, the colloid dissolves to a corresponding extent.

Nuclides dissolved in the water sorb on particles in the water. Natural waters contain low concentrations of particles - in the neighbourhood of less than one milligramme per litre /14-58/. Transport capacity via particle-bound activity is obtained by multiplying the particle concentration by K_d for the particles. For a particle concentration in the water on the order of 0.5×10^{-3} g/l and a K_d = 5 l/g, the concentration of nuclide bound to the particles is 0.0025 of the concentration of nuclide dissolved in the water.

The strongly sorbing nuclides that are bound to the particles thus constitute only 0.25% of the total quantity in the water. Since the nuclides are reversibly bound, they desorb from the particles at the same rate as the water is depleted of them. A special calculation (see chapter 20) deals with what would happen if the sorption were irreversible and the particles migrated at the velocity of the water to the biosphere, carrying with them the nuclides in a quantity determined by the transport mechanism described above.

Another source of particles is the clay in the buffer material around the canisters. The bentonite clay consists of very small particles, which can form colloids in water with low concentrations of dissolved ions. At concentrations of more than 20 mg/l of divalent cations, e.g. Ca^{2+}, the clay forms a stable gel /14-59, 14-60/. Sorption reactions on the bentonite particles are also reversible and any nuclides that are transported with the particles to a region with nuclide-free water desorb and sorb on the much larger surfaces of the microfissures in the rock.

15 DISPERSAL AND EXPOSURE IN THE BIOSPHERE

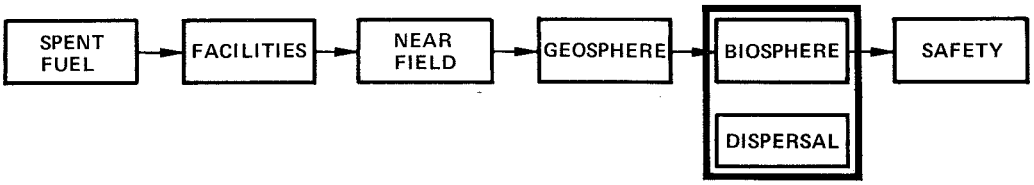

This chapter describes the premises for and results of the dilution and enrichment processes that occur in the biosphere. The mathematical model that serves as the basis for the calculations is presented.

The conversion factors between release and dose obtained from these calculations are given. A detailed discussion of the concept of radiation dose is presented in chapter 16.

15.1 THE IMPORTANCE OF DISPERSAL IN THE BIOSPHERE – GENERAL

The dispersal of radioactive substances from the repository can eventually lead to their coming into contact with man. Since dispersal from the repository takes place with the groundwater, the first contact of the radioactive substances with the biosphere takes place in a receiving body of water, or recipient.

Two different types of recipients have been studied as starting points for further dispersal in the biosphere.

- Well
- Lake

From the primary recipient, the substances are then further dispersed via the fresh and brackish water reservoirs out into a global cycle.

By "biosphere" is meant all living organisms, and in a broad sense their surrounding environment as well. The biosphere thus includes media in the environment which sustain the living organisms, i.e.

the entire hydrosphere and parts of the atmosphere and the upper ground layer.

The evaluation of the safety of a final repository is based on an analysis of the extent to which the population may be exposed to radioactive material from the repository. The analysis takes into account the long-range turnover of different radioactive substances in the biosphere and estimates radiation doses to man. Since the forecasts must be projected over very long spans of time, uncertainties of various kinds are introduced. The ambition has been to take these into account by analyzing the variations around a best estimate of a given factor, e.g. uptake in plants or in fish. When this has not been applicable, the description has been based on assumptions and choices of values that probably do not underestimate the radiation doses to man.

15.2 DESCRIPTION OF RECIPIENTS AND ECOLOGICAL MECHANISMS

The choice of primary recipient, lake or groundwater well, affects the paths of exposure that must be taken into account. The initial dilution in the recipient is of great importance for the individual doses.

In order to be able to calculate the activity dispersal, it is necessary that the ecosystems be studied with respect to local, regional, intermediary and global processes. The local and regional processes are thereby affected by data that are characteristic for the selected areas.

During the time spans discussed here, however, wells will be drilled and abandoned and lakes will be formed and die within time frames that are considerably shorter than the estimated duration of the releases. The environmental consequences of a repository site are therefore calculated here based on standardized recipients.

Water balance calculations and hydrological information concerning the rate of water turnover on a regional and global scale are utilized in those cases where transport takes place via the groundwater and surface water. Based on this premise and with the aid of

distribution coefficients determined by the ratio between the mobility of the nuclide and that of the water, nuclide-specific transfers are obtained for the soil-water turnover.

For turnover processes that take place during relatively short time spans, transport via a few dominant transport paths is critical. During longer time sequences, feedback mechanisms, for example from sediment to water, come into play.

15.2.1 Well

The final repository is sited in rock with low water flow. Typically, one or more rock formations in an inflow area are chosen. The formations are surrounded by geometrically well-defined fracture zones. The low permeability of the rock and the fracture zones in the study sites investigated render them unsuitable for wells with large water extractions. At the most, wells for single-family households or summer homes could conceivably be drilled in the area, mainly then in the outflow areas situated near the repository. Typical water extractions for such wells are 1.5-6 m^3/d with depths normally down to about 60 m.

In order to illustrate the effect of a well directly above the repository or in a nearby fracture zone, calculations have been carried out with data typical for the repository design and the study sites investigated /15-1, 15-2/. The results show that the natural groundwater flow through the repository is not affected by the existence of wells of the above-mentioned size subject to normal use.

If a well is frilled in an area with outflow from the repository, some of the water from the repository will enter the well. Calculations show that every volume of water in the well that has passed through the repository will be diluted with between 30 000 and several million volumes of water that has not passed through the repository /15-1, 15-2/.

A groundwater flow of 0.1 $l/(m^2 \cdot year)$ has been assumed at repository depth. With a minimum repository area of 0.5 km^2, the annual

nuclide flow from the repository will be diluted in at least 50 m^3 of water. In the well, then, a concentration is obtained that is equivalent to diluting the annual leakage in at least a million m^3 of water. A dilution equivalent to diluting the annual release in 500 000 m^3 of water is conservatively chosen for the further calculations.

15.2.2 Lake

Studies in the recipient areas in the study sites have shown that Morpa Lake at Fjällveden is a type of lake that has very low rates of water inflow and turnover. Since such conditions constitute unfavourable factors in the individual dose calculations, this lake has been chosen as the lake recipient on the study sites. areas. The characteristics of the lakes now existing on the study sites are described in chapter 18.

The water volume in the lake recipient has been selected in agreement with Morpa Lake at $3.2 \cdot 10^6$ m^3 and the turnover rate to once per 1 280 days.

15.3 DISPERSAL PROCESSES AND PATHS OF EXPOSURE

The turnover of radionuclides is controlled by the movement of different carriers in the various media. The nuclides are transported into the ground by irrigation and by dry and wet deposition, while resuspension and leaching transport substances out of the ground to the atmosphere, groundwater and surface water.

As the radioactive nuclides are transferred between the different natural reservoirs, activity can reach man via different paths of exposure: internal exposure through inhalation, intake of foodstuffs and drinking water and external exposure from material deposited on the ground. Bathing, activities on the beaches of lakes or seas where radioactive materials have accumulated and the handling of fishing tackle that has come into contact with the bottom sediment are other possible paths of external exposure.

The radioactive substances that may be present in various types of foodstuffs originate from uptakes via a varying number of transport paths:

- Crops take up radionuclides from the soil via their root systems and through direct deposition on leaf surfaces.

- The presence of radionuclides in meat and milk originates from the intake of contaminated feed or drinking water.

- Fish accumulate radionuclides via exchange with surrounding water and via foodstuffs.

The irrigation of vegetables, pasturage and crops in the local and regional areas constitutes a separate transport path.

15.4 MODEL PRINCIPLES

15.4.1 Mathematical model

Mathematical models have been developed to simulate the dynamic exchange of radionuclides in the biosphere.

The models, which are based on compartment theory, utilize a system of first-order linear differential equations with time-independent transfer coefficients plus a number of physically well-defined areas or volumes. The premises include that the reservoirs are instantaneously well-mixed. In this manner, the outflow of nuclides will be proportional to their concentration in the reservoir.

The relationship between the activities in the reservoir system is expressed in equations, where it is also possible to take decay chains into account.

15.4.2 Reservoirs in the model

For the turnover of radioactive substances in the air and water, reservoirs can be defined that satisfactorily fulfil the condition of instantaneous mixing. In a lake, for example, the bottom sediments also participate actively in the exchange of radionuclides - and the lake as a whole can therefore not be regarded as a homogeneous reservoir. In order to make allowance for this and obtain a better fit to real conditions, the lake is divided into separate water and sediment reservoirs between which an exchange takes place.

The premise that the outflow from a reservoir is only dependent on the quantity of activity in it can be regarded as valid in this study. The quantity of radioactive substances is consistently very low compared to the stable isotopes of the substances or chemically analogous carriers.

Constant transfer coefficients generally approximate the state of the system only during short time spans. Regarded over several annual cycles, the variations are evened out and constant coefficients can thereby provide a representative mean value.

15.5 CHOICE OF CALCULATION MODEL – BIOPATH

The BIOPATH model is based on the compartment principle dealt with in section 15.4.1 and describes the dispersal of radioactive substances released to the biosphere and resulting doses.

15.5.1 Model structure

BIOPATH is constructed /15-3/ with a division into zones at different levels:

- The local model calculates radiation doses to individuals in a critical group (nearby residents) around the source.

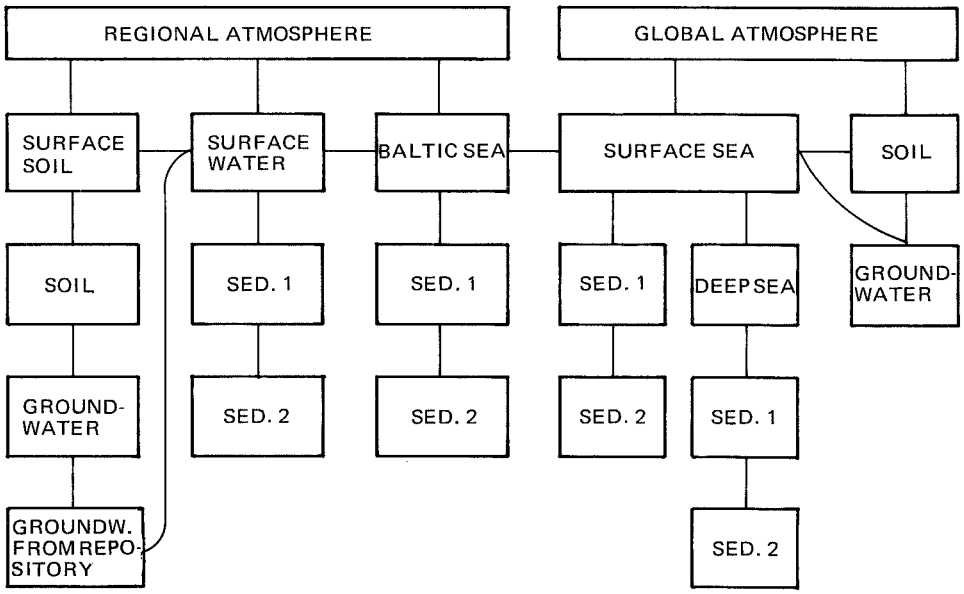

Figure 15-1. Schematic diagram of reservoirs in the BIOPATH model.

- The regional model takes into account dispersal in a wider area around the point of release. The local area is thus included in the regional area.

- The intermediary model constitutes a further step towards dispersal on a larger scale.

- The global model encompasses dispersal over the whole world.

A schematic diagram of the different reservoirs in the BIOPATH model is shown in figure 15-1.

These models COUPLED at different levels provide the framework for a study of exposure situations in limited ecosystems while also making it possible to follow the dispersal process through a gradual dispersal on an ever-widening scale.

Within the subsystems, the reservoirs have been designed /15-4, 15-5/ so that a representative picture is obtained of radioactive flows in the ecosystems.

The model is designed both to simulate important turnover and exposure processes and to describe doses to individuals and the population; for which international agencies and Swedish radiation protection authorities HAVE issued limits.

Different computer programs have been used to calculate the nuclide transport from a final repository to the biosphere. The results in the form of activity quantity released from the geosphere at different times (chapter 14) constitute source terms for BIOPATH.

15.5.2 Internal exposure

BIOPATH calculates the dose contributions via different paths of exposure to individuals and TO populations at the local and regional, intermediary och global levels.

Diet habits and consumption

The diet habits of the critical group and the population on a regional and global level as regards annual intake of drinking water, foodstuffs and respiration air have been standardized /15-6/.

The average consumption of water and feed has been calculated for those animals that form part of the transport path for radioactive substances and make contributions to human food in the form of meat, milk and egg products /15-7/.

Uptake in the food chains can go via the following links:

Uptake in green vegetables

Contribution from root uptake
" " direct deposition
" " irrigation

The sum of these contributions is multiplied by:

- annual consumption of green vegetables
- the dose factor for the nuclide

Transfer to meat and milk

Contribution from pasturage via root uptake and intake of soil
" " direct deposition on pasturage
" " drinking water

The sum of these contributions is multiplied by

- a distribution factor for the distribution of ingested radio nuclides in milk and meat

- annual consumption of meat/milk and the dose factor for the nuclide.

Uptake in fish

The activity concentration in water is multiplied by the concentration factor for fish and by

- annual consumption of fish and
- the dose factor for the nuclide.

Transfer coefficients describe the exchange between the reservoirs in the model.

In cases where groundwater or surface water serves as the transport medium, information on the water turnover rate on a regional and global scale is used. Iodine and technetium are examples of nuclides that follow the movements of the water quite well. In general, a distribution coefficient is used for other nuclides. This coefficient describes the nuclide's degree of mobility in relation to that of the water. In this manner, nuclide-specific transfer coefficients are obtained for turnover in soil and groundwater.

The transport of radionuclides atmosphere - ground is based on experimental studies of the average retention time of different substances in the atmosphere. The rate of resuspension of particle-borne activity back to the atmosphere is based on, among other things, estimates of the feedback of radioactive substances from the surface layer of the ground.

Salt is transferred to the atmosphere above the sea by evaporation of wave spray from the water. Some of this spray is deposited on land, which gives a transport sea - land.

A tabulation and discussion of parameter values used in the BIOPATH calculations is provided in /15-7/.

15.5.3 External exposure

The exposure times for the external paths of exposure (beach activities, bathing, handling of fishing tackle and radiation from the ground) are calculated for different population groups and area alternatives. The exposure time is multiplied by a dose factor, specific for each path of exposure, calculated according to the following principles.

External exposure from ground and beach

For calculating the external dose from radionuclides deposited in the ground and on beaches, it is assumed that all activity is accumulated in the uppermost surface layer.

External exposure from bathing

It is assumed that the bathers receive homogeneous radiation from all directions.

External exposure via handling of fishing tackle

The external dose that is obtained via the handling of fishing tackle is assumed to derive from activity in the form of a point source present in 10 kg of fishing tackle at a distance of 1 m.

15.5.4 Population and population growth

For calculation of the collective dose now and in the future, the program takes into account population distribution and population growth. Growth has been interrupted after the world population has reached 10 billion individuals.

15.6 DATA BASE AND UNDERTAINTIES

The reliability of the calculated doses is affected by uncertainties in the data base, the structure of the model, choice of paths of exposure, numerical approximations in the calculations and choice of transfer coefficients.

15.6.1 Data base

With the support of a large number of references, a revised data base containing the necessary input data to BIOPATH has been assembled during 1982 /15-7/.

In order to make it easier to carry out sensitivity analyses, an endeavour has been made to specify the interval of variation for the different parameters wherever possible.

The updated data base incorporates:

- Nuclide-independent transfer coefficients

  Deposition
  Resuspension
  Transport from the surface layers of the world oceans to the continents
  Water turnover in ground
  Water turnover on a global scale

- Nuclide-dependent transfer coefficients

  Sedimentation - fresh water systems
  Sedimentation - brackish water
  Sedimentation - surface sea
  Sedimentation - deep sea
  Turnover of nuclides in sediments
  Migration in ground
  Turnover of nuclides in groundwater

- Concentration and distribution factors for biological material in land and water areas.

- Diet and consumption parameters and yield values.

The data base for the nuclides that have been shown by analyses to dominate the doses is given in the following tables:

15-1 Nuclide-dependent transfer coefficients

15-2 Nuclide-independent transfer coefficients

15-3 Concentration and distrbution factors for transfer from reservoir to foodstuffs

15-4 Diet and consumption parameters

Table 15-1. Nuclide-dependent transfer coefficients of importance for calculaton of the individual dose for the dose-dominating nuclides.

Process	Transfer coefficient				
	I	Cs	Ra	Pa	Np
Turnover in surface soil	1.0×10^{-2}	2.1×10^{-3}	8.8×10^{-4}	5.3×10^{-5}	1.6×10^{-3}
Turnover in deep soil	2.4×10^{-4}	1.6×10^{-4}	6.7×10^{-5}	4.0×10^{-6}	1.2×10^{-4}
Turnover in ground water	2.0×10^{-1}	4.0×10^{-4}	1.7×10^{-4}	9.1×10^{-6}	2.9×10^{-4}
Transfer to sediment	3.0×10^{-2}	4.0×10^{-1}	1.8	1.4×10^{-1}	2.2×10^{-1}
Leakage from sediment	1.3×10^{-2}	1.1×10^{-3}	1.6×10^{-2}	1.3×10^{-2}	1.5×10^{-2}

Table 15-2. Nuclide-independent transfer coefficients of importance for calculation of the individual dose.

Process	Transfer coefficient
Turnover of groundwater	2
Irrigation from groundwater	2.4×10^{-4}
Turnover of surface water	3.0×10^{-1}
Irrigation from surface water	4.4×10^{-3}
Transport to deeper sediments	1.0×10^{-3}

Table 15-3. Concentration and distribution factors for transfer of activity from different reservoirs to foodstuffs.

Element	Concentration factors									Distribution factors		
	Pasturage-soil	Cereals-soil	Leafy veg.-soil	Root veg.-soil	Fish-fr.w.	Fish-br.w.	Fish-seawater	Aq. pl.-☆	Aq. pl.-☆	Milk d/kg	Meat d/kg	Eggs d/pc
Zr	$1,1x10^{-3}$	$1,7x10^{-4}$	$1,7x10^{-4}$	$1,7x10^{-4}$	$3,0x10^{2}$	$3,0x10^{2}$	$1,0x10^{2}$	$5,0x10^{-2}$	$5,0x10^{2}$	$5,0x10^{-6}$	$3,4x10^{-2}$	$6,0x10^{-5}$
Tc	1,0	$9,0x10^{-1}$	$1,0x10^{-1}$	$2,0x10^{-1}$	$3,0x10^{1}$	$3,0x10^{1}$	$1,0x10^{1}$	$4,0x10^{3}$	$4,0x10^{3}$	$1,0x10^{-3}$	$1,0x10^{-3}$	$9,0x10^{-4}$
I	$8,0x10^{-2}$	$2,0x10^{-3}$	$5,0x10^{-3}$	$1,0x10^{-3}$	$2,0x10^{1}$	$2,0x10^{1}$	$2,0x10^{1}$	$4,0x10^{3}$	$4,0x10^{3}$	$7,0x10^{-3}$	$8,0x10^{-3}$	$3,0x10^{-2}$
Cs	$1,0x10^{-1}$	$1,0x10^{-2}$	$2,0x10^{-2}$	$2,0x10^{-2}$	$1,3x10^{3}$	$2,0x10^{2}$	$1,0x10^{1}$	$1,5x10^{2}$	$2,0x10^{1}$	$7,0x10^{-3}$	$3,0x10^{-2}$	$2,0x10^{-2}$
Ra	$2,0x10^{-2}$	$1,0x10^{-2}$	$7,0x10^{-3}$	$3,0x10^{-3}$	$2,5x10^{1}$	$1,0x10^{1}$	$1,0x10^{1}$	$1,0x10^{2}$	$1,0x10^{2}$	$3,0x10^{-3}$	$7,0x10^{-4}$	$1,0x10^{-6}$
Th	$6,0x10^{-3}$	$6,9x10^{-4}$	$5,0x10^{-4}$	$1,0x10^{-3}$	$3,0x10^{1}$	$3,0x10^{1}$	$3,0x10^{3}$	$3,0x10^{3}$	$3,0x10^{3}$	$5,0x10^{-6}$	$7,0x10^{-4}$	$1,0x10^{-4}$
Pa	$3,0x10^{-3}$	$3,0x10^{-3}$	$3,0x10^{-4}$	$6,0x10^{-4}$	$1,0x10^{1}$	$1,0x10^{1}$	$1,0x10^{2}$	$5,0x10^{1}$	$5,0x10^{1}$	$5,0x10^{-6}$	$3,0x10^{-3}$	$1,0x10^{-4}$
U	$4,0x10^{-3}$	$1,2x10^{-3}$	$4,0x10^{-4}$	$8,0x10^{-4}$	5,0	5,0	1,0	$5,0x10^{1}$	$5,0x10^{1}$	$2,0x10^{-4}$	$1,0x10^{-2}$	$1,0x10^{-4}$
Np	$3,0x10^{-2}$	$4,0x10^{-4}$	$3,0x10^{-3}$	$6,0x10^{-3}$	$1,0x10^{1}$	$1,0x10^{1}$	$1,0x10^{1}$	$2,0x10^{3}$	$2,0x10^{3}$	$5,0x10^{-6}$	$3,0x10^{-3}$	$1,0x10^{-4}$
Pu	$6,7x10^{-4}$	$1,0x10^{-6}$	$1,0x10^{-4}$	$1,0x10^{-3}$	3,5	8,0	3,5	$1,8x10^{2}$	$1,0x10^{3}$	$1,0x10^{-7}$	$1,0x10^{-6}$	$1,0x10^{-4}$

☆ The concentration factor for aquatic plants applies to both algae and crustaceans.

15.6.2 Choice of paths of exposure

The paths of exposure included in the calculations cover what experience has shown to be the most relevant processes for doses to man. The paths of exposure consider both internal and external doses deriving from activity in the atmosphere, ground and water.

Table 15-4. Estimated consumption (in kg or litres) per person and year.

Food	Local case	Regional case	Global case
Drinking water	4.4×10^2	4.4×10^2	4.4×10^2
Milk	1.9×10^2	1.9×10^2	9.0×10^1
Meat	5.5×10^1	5.5×10^1	2.5×10^1
Green vegetables	2.5×10^1	2.5×10^1	9.0×10^1
Cereals	-	7.5×10^1	1.2×10^2
Root vegetables + potatoes	-	7.5×10^1	8.0×10^1
Fish	3.0×10^1	3.0×10^1	1.0×10^1
Eggs*	2.0×10^2	2.0×10^2	5.4×10^1
Algae + crustaceans	-	-	1.0×10^1

* Number per year.

The structure of the model also permits studies of future changes in foodstuff composition. Examples of possible changes that could shift importance to other paths of exposure are diet composition and food chains.

15.6.3 Numerical approximation

The numerical method used in the model provides a means to check the uncertainty that is introduced through approximations in the iterative processes. Error analyses have shown that the uncertainty in calculated doses stemming from numerical approximation is insignificant in relation to other sources of error and uncertainties /15-8/.

15.6.4 Variations in the exchange between the different reservoirs in the ecosystem

A model intended to describe the complex turnover in the biosphere includes a relatively large number of parameters, specified in the literature as recommended values or intervals. In certain cases, the spans of the intervals can be large.

By calculating statistical distributions, greater realism can also be obtained regarding dose or burden and the total uncertainty can be better quantified /15-9/. For this purpose, a programme has been used based on the Monte Carlo principle that takes into account the mutual dependence of the constituent parameters to as great extent as possible. In this manner, it has been possible to approximate the contributions of different parameters to the total uncertainty. A calculation for Ra-226-doses via milk has been carried out for parameters that experience has shown are of great importance for the calculation result. The calculations concern a case with irrigation of pasturage.

If the water concentration can be regarded as approximately constant, the distribution factor for intake/milk will dominate the uncertainty in the calculated doses with	approx. 60%
This is follwed by factors related to irrigation intensity, transport away from the root zone and the dose factor, each amounting to	approx. 10%
If, on the other hand, the water concentration is assumed to vary within a broader interval, the distribution factor for milk and the water concentration will each dominate with	approx. 30%
followed by irrigation intensity, dose factor and transport away from the root zone, each with	approx. 5%

As regards the first case, for which the water concentration could be assumed to be roughly constant, the frequency distribution for the dose has been obtained by varying the parameters used in BIO-

PATH. The calculation shows that the probability that the actual dose will be less than the dose obtained with the selected parameters lies in the interval of 60-65%.

No measure of the actual discrepancy between model prediction and reality is possible without testing the model prediction against observations. Comparisons have been made between the global distribution of tritium and carbon-14 obtained by means of measurements versus that obtained by means of model predicion. See section 15.6.7.

15.6.5 Variations in diet composition and uptake via food chains

The critical group is supposed to be representative of those individuals in the population who are expected to receive higher doses than average due to their diet and living habits.

For most nuclides, consumption of water, fish, milk, meat or green vegetables constitutes the dominant path of exposure.

Water consumption from local wells can scarcely increase substantially beyond the 440 l/y assumed. If the relatively high consumption of lake fish (30 kg/y) were halved, the dose from e g cesium-135 would be reduced nearly proportionally. The doses from radium, on the other hand, would be reduced by less than one third.

The critical group exposed through the use of water from the primary groundwater recipient generally receives the highest doses.

15.6.6 Daughter products in decay chains

In decay chains with radioactive daughter products, the distribution of daughter products between different parts of the biosphere depends to a certain extent on the turnover processes for the parent nuclide. In view of the relatively large dose contributions involved, the uranium-238 - uranium-234 - thorium-230 - radium-226 decay chain, the neptunium-237 - uranium-233 - thorium-229 decay chain and the uranium-235 - protactinium-231 decay chain are of particular interest.

The transfer rate between soil and groundwater reservoirs for both the parent nuclide uranium-235 and the daughter product protactinium-231 is manifest in the doses from protactinium-231 over paths of exposure with groundwater or surface water as an intermediary link.

15.6.7 Comparisons with states and process in nature

The dispersal of a substance in the biosphere is affected by certain factors that are specific for that substance. In general, however, dispersal on a large scale is affected by the movements of the water and the air, both of which constitute important carriers for the radioactive outflow to the biosphere. The radioactive isotope of hydrogen, tritium, faithfully follows the cycle of the water through the air, sea and biota after tritium has been incorporated in a water molecule.

The natural production of tritium in the stratosphere gives measurable activity levels in the biosphere. The global turnover of tritium from its natural source in the stratosphere has been simulated with the compartment model for the biosphere. Comparisons between equilibrium levels of tritium in different parts of the biosphere calculated in this manner and measured equilibrium levels can be used as a check of how well the model, with assumed movements for water in the atmosphere and the sea, can describe the distribution of tritium in nature. Such a comparison for the global distribution of tritium has shown that the deviation between results based on measurements and results based on calculation lies within a factor of 3 /15-10/. In a similar manner, comparisons have shown good agreement between forecasts and measurements for the global distribution of naturally produced carbon-14 /15-11/.

On the intermediary scale, the Baltic sea constitutes a link where fallout nuclides in the brackish water system and known salinity gradients have served as a basis for an analysis of the rate of exchange both between the Baltic Sea and the North Sea and between water and sediment.

15.7 LONG-RANGE PERSPECTIVE ON DISPERSAL

15.7.1 Long-term variations regarding ground and water

The description of different recipient areas is based on conditions that apply now or in recent time. In many cases, however, it will take millions of years before the activity will reach the surface water, and it is conditions at this time that should serve as a point of departure for the dose calculations. Assumptions concerning conditions in the future will of necessity, however, be associated with uncertainties.

Certain changes in external conditions can be expected to occur over long spans of tim, for example in

- The climate /15-12, 15-13/
- The water balance /15-14/
- Land use /15-15/

A radical change would be a new ice age. After the ice has melted, however, vegetation, animals and human beings will probably return and the main topographical features of the landscape will probably remain the same. (Cf. Section 8.9).

Some lakes will be choked with vegetation and die in the future. This process (known as eutrophication) has accelerated over the past decades due to an increased flow of nutrient salts to rivers and lakes. This means that former lake areas will be used as farmland or forest land. A gradual drying-up of the Baltic Sea can, for example, give rise to exposure from sediments that are used for agricultural production. However, changes in the paths of exposure through drying-up processes do not entail any essential change in the annual doses. Calculations show that the cultivation of agricultural products on contaminated sediments gives a dose contribution of the same order of magnitude as that obtained through the consumption of fish /15-16/.

Another type of change in land use is the exploitation of peat for different purposes. Since peat bogs exist within outflow areas,

they could become recipient areas for escaping radioactivity in the future.

Exposure could take place if:

- peat land is converted to agricultural land
- peat is used as a soil conditioner or
- peat is used for combustion.

The path of exposure via combustion should not have as great an effect as if peat is used as a soil conditioner or if the ground is eventually used for agricultural production.

The most important present-day process in the Swedish countryside is acidification. Increased combustion of fossil fuels has led to increased polution of the atmosphere, hydrosphere and ground, resulting in falling pH levels in many of Sweden's lakes. (Cf. Chapter 7.) Another important environmental process is the increased leaching of metals such as aluminium, cadmium, zinc, lead, iron, mercury and radium.

The paths of exposure included in the model are based on the present-day diet composition. In the long run, however, certain food resources may be further exploited, especially marine foods, and become important on a global scale. This has been taken into account in calculating population doses by including consumption of algae and crustaceans.

15.8 RESULTS

The results of the BIOPATH calculations are reported in table 15-5 as conversion factors between release and dose from different isotopes via the two initial recipients. Table 15-6 gives the calculation results for the so-called central calculation case. The same data are shown in curve form for the dominant nuclides and the lake recipient in figure 15-2 /15-6/.

As can be seen, the less retarded nuclides reach the biosphere first (the time in figure 15-2 is given in years after canister

penetration at 100 000 years). The dose from these nuclides is dominated by iodine-129 and cesium-135 ($2 \cdot 10^{-7}$ Sv and $2 \cdot 10^{-8}$ Sv, respectively). The releases of the heavy nuclides are dominated by radium-226, whose influence continues as long as the uranium dissolution continues. Neptunium-237 dominates at an early stage, but due to its decay, it reaches a maximum value around 10 million years after canister penetration. The dose from neptunium-237 is then $3 \cdot 10^{-10}$ Sv.

Table 15-5. Conversion factors between release from geosphere and dose via well and lake, continuous release of 1 Bq/y.

Nuclide	Individual dose (Sv/y) Well	Lake	Collective dose (ManSv/y)
^{93}Zr	$3.4x10^{-15}$	3.8x10-15	$1.0x10^{-13}$
^{99}Tc	$7.3x10^{-16}$	$5.5x10^{-16}$	$6.0x10^{-13}$
^{129}I	$1.7x10^{-13}$	$1.6x10^{-13}$	$1.4x10^{-8}$
^{135}Cs	$5.0x10^{-14}$	$5.0x10^{-14}$	$1.9x10^{-12}$
^{226}Ra	$6.1x10^{-13}$	$4.0x10^{-13}$	$3.3x10^{-12}$
^{229}Th	$1.1x10^{-12}$	$7.0x10^{-13}$	$2.0x10^{-11}$
^{230}Th	$1.0x10^{-13}$	$1.0x10^{-13}$	$7.9x10^{-12}$
^{231}Pa	$2.2x10^{-11}$	$1.0x10^{-11}$	$3.3x10^{-11}$
^{233}U	$7.8x10^{-14}$	$4.9x10^{-14}$	$1.9x10^{-11}$
^{234}U	$7.8x10^{-14}$	$4.9x10^{-14}$	$2.0x10^{-11}$
^{235}U	$8.0x10^{-14}$	$3.3x10^{-14}$	$2.6x10^{-10}$
^{236}U	$7.3x10^{-14}$	$4.5x10^{-14}$	$2.3x10^{-10}$
^{238}U	$6.9x10^{-14}$	$4.3x10^{-14}$	$2.4x10^{-10}$
^{237}Np	$1.6x10^{-12}$	$1.1x10^{-12}$	$4.0x10^{-8}$
^{239}Pu	$6.5x10^{-13}$	$2.6x10^{-13}$	$5.0x10^{-13}$
^{242}Pu	$1.2x10^{-13}$	$2.1x10^{-13}$	$4.7x10^{-13}$

Table 15-6. Doses from the central calculation case's nuclide inflows to the biosphere (4 400 canisters).

Nuclides	Max. ind. dose (Sv/y) Well	Lake	Max. coll. doses (ManSv/y)
^{93}Zr	3.0×10^{-13}	3.0×10^{-13}	8.9×10^{-12}
^{99}Tc	2.9×10^{-11}	2.2×10^{-11}	2.5×10^{-8}
^{129}I	2.1×10^{-7}	1.8×10^{-7}	1.0×10^{-2}
^{135}Cs	2.2×10^{-8}	2.2×10^{-8}	1.8×10^{-6}
^{226}Ra	1.0×10^{-7}	7.4×10^{-8}	6.4×10^{-7}
^{229}Th	3.0×10^{-10}	2.3×10^{-10}	8.4×10^{-8}
^{230}Th	7.4×10^{-10}	8.4×10^{-10}	1.4×10^{-7}
^{231}Pa	1.2×10^{-9}	4.4×10^{-10}	1.8×10^{-8}
^{233}U	2.2×10^{-11}	1.2×10^{-11}	1.8×10^{-8}
^{234}U	3.0×10^{-10}	1.8×10^{-10}	1.1×10^{-6}
^{235}U	4.1×10^{-12}	1.6×10^{-12}	1.4×10^{-8}
^{236}U	7.4×10^{-13}	3.3×10^{-13}	2.5×10^{-9}
^{238}U	2.7×10^{-10}	1.6×10^{-10}	1.0×10^{-6}
^{237}Np	3.9×10^{-10}	3.0×10^{-10}	9.2×10^{-6}

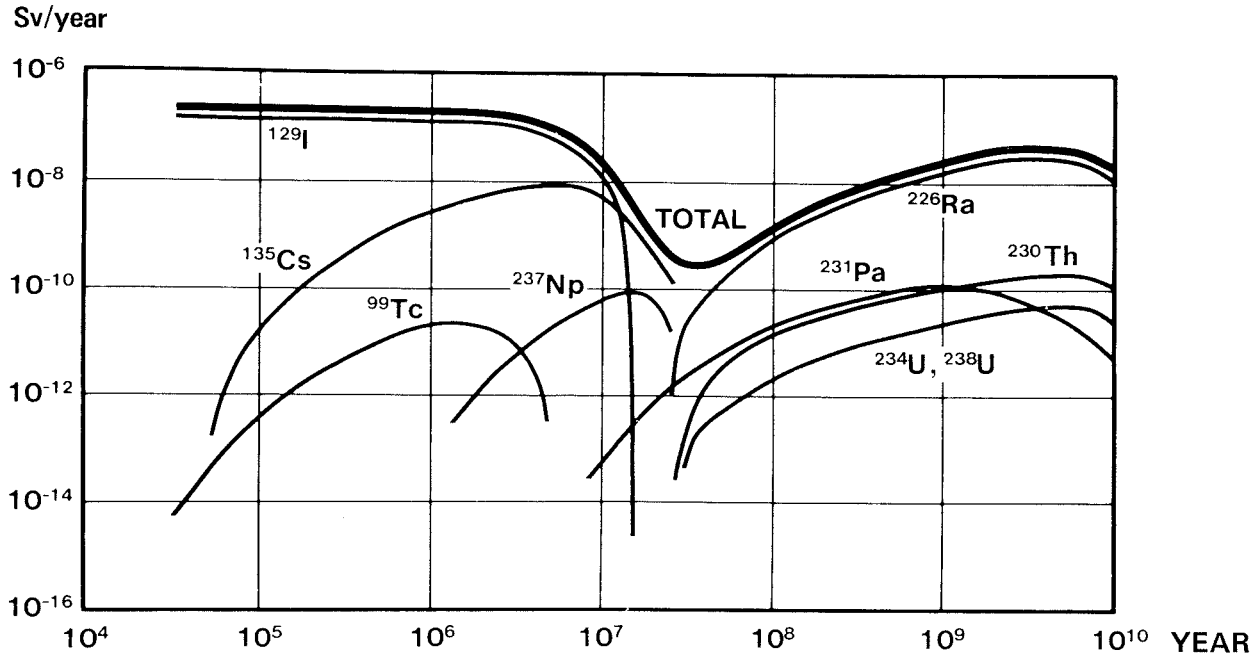

Figure 15-2. Calculated doses for the central case, 4 400 canisters and lake recipient. The time is given in years after the first canister penetration.

16 RADIATION DOSES AND HEALTH EFFECTS

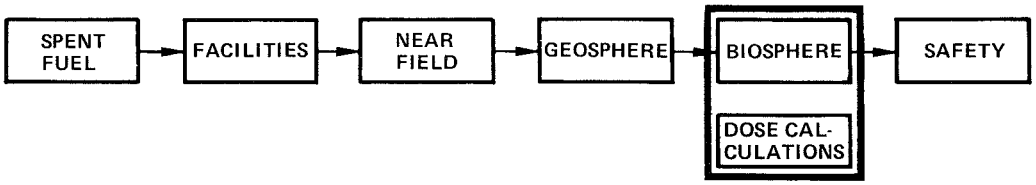

In this chapter, the implications of various radiation dose concepts are explained and methods and data to calculate them are described. The relationships between intake and dose used in the safety analyses are reported, as are the relationships between dose and effect on man.

16.1 DOSE BURDEN – GENERAL

The dispersal and turnover of radionuclides in the biosphere is calculated using mathematical models for ecosystems at the local, regional, intermediary and global level (see Chapter 15). Man's dietary habits and use of nature determine to what extent the radionuclide concentration in different parts of the biosphere will give rise to doses to man.

The consequences of the dispersal of radioactive substances are reported in the form of:

- dose to critical group (a limited number of individuals in the vicinity of the source) and

- dose to population - the collective dose, which gives rise to exposure of parts or all of the global population.

The accumulated dose over an infinite period of time - the dose commitment - or over a certain limited period of time is calculated for a release to the biosphere.

For a given nuclide, the maximum dose to the critical group and the maximum collective annual dose to the population can be obtained at different points in time.

16.2 DOSE TYPES

16.2.1 Individual dose

According to the radiological definition, the critical group shall represent a limited number of individuals that can receive higher doses than average.

According to government regulations /16-1/, the radiation doses from releases of different radioactive nuclides from a nuclear power station shall be calculated for the group of persons that form a critical group for each nuclide. The critical group does not necessarily have to be an existing group. Different nuclides can have different critical groups. The dose contribution for each nuclide in the group of persons that make up a critical group for that particular nuclide is calculated. The sum of these dose contributions is probably considerably greater than the dose to the group that receives the highest radiation dose in reality. By limiting the total dose, an extra factor of safety is therefore usually introduced.

16.2.2 Collective dose

The collective dose is the sum of the doses to all individuals in a given population.

Depending on the nuclide and the time after the inflow into the biosphere began, different population groups dominate the total collective dose.

The purpose of limiting the collective dose is to limit the future mean dose - and thereby the risk of delayed, random injuries.

The model for calculating the turnover of radioactive substances within and between different ecosystems permits the collective dose to different population groups to be calculated.

16.2.3 Dose commitment

The concept of dose commitment is intended to be used to estimate the long-range superimposition of doses from radioactivity released in different years. If the dose rate from a radioactive release is integrated over time, the dose commitment for an infinite period of time is obtained. Such calculations have been carried out.

16.3 DATA BASE AND CALCULATION MODELS

16.3.1 Data base and choice of model

The data base is very large, thanks largely to the extensive work carried out by the International Commission on Radiological Protection (ICRP) and published in the Commission's publications /16-2 to 16-6/.

The transport of radionuclides in the body is described by means of models of the compartment type and average turnover rates for healthy, adult individuals.

Such models have been developed for calculating the dose to different organs:

Dose to lung

When radioactive aerosols are inhaled, portions of the respiratory passages will be irradiated. Other organs and tissues are irradiated at the same time, both by activity in the lungs and from other tissues where inhaled material has been accumulated.

The ICRP Task Group on Lung Dynamics /16-7/ has calculated the distribution and retention of material in the respiratory tract.

The model takes into account particle size and defines three retention classes, which partially reflect the chemical form of the aerosol.

Dose to bone tissue

Those cells in the skeleton that are considered to be of the greatest interest in relation to cancer are located in the bone marrow or on the bone surfaces (endosteal surfaces) as well as certain epithelial cells near the bone surfaces /16-8/. For endosteal tissues and epithelial tissues adjacent to the bone surfaces, the ICRP recommends that the dose equivalent be calculated as a mean value over tissue to a distance of 10 μm from the surface of the bone.

Dose to gastrointestinal tract

The model is based on a biological model developed by Eve /16-9, 16-10/. For radiological purposes, the gastrointestinal tract is considered to consist of four sections, each represented by a compartment.

16.3.2 Dose conversion factors issued by the ICRP

Following an intake of radioactive substances, a number of organs and tissues will be irradiated. Organ doses can be converted to an equivalent whole-body dose according to ICRP 26 in such a manner that the total risk of cancer and hereditary diseases shall be less than or equal to the risk from uniform whole-body irradiation. Concerning principle for the weighting of organ doses, see Section 16.3.4.

The ICRP has defined 50 years as the length of an individual's occupational life. The total dose equivalent shall therefore be integrated over this period. The dose equivalent commitment from an intake of radioactive substances is the burden a person is subjected to during the period up to 50 years after the intake if no dose-abating measures are taken.

The calculations take into account both dose contributions resulting from radiation in the organ in question and dose contributions in organs and tissues at greater depth inside the body.

For individuals in radiological work, the highest permissible equivalent whole-body dose is 50 mSv per year. This is intended to limit stochastic, randomly occurring effects.

The dose equivalent commitment also includes the dose commitment from each daughter nuclide produced by the parent nuclide in the body. It is normally assumed that a daughter nuclide behaves metabolically in the same manner as the parent nuclide.

For each radionuclide and for different chemical forms, a secondary standard has been developed in ICRP 30 in the form of ALI (Annual Limit of Intake) values, which limit intake through ingestion and through inhalation. Furthermore, limits have been derived for air concentration, known as DAC (Derived Air Concentration) values.

16.3.3 Age dependence

The weighting factors used in calculating the effective dose equivalent have been derived for adult individuals with standardization of a number of age-dependent factors. The ICRP has, however, indicated that these values may be used for children as well, in lieu of better information /16-5/.

All ALI and DAC values pertain, however, to persons in radiological work and must be used with caution for other purposes.

The age dependence of the absorbed dose and the dose equivalent commitment has been studied /16-11/. Following is a brief summary of the results.

Children and newborns

Ionizing gamma radiation with an energy greater than 10 keV from an organ will irradiate other organs as well. In children, whose body size is smaller, the radiation will reach more organs than in adults, leading to a higher absorbed dose in these organs.

On the other hand, children's intake of food and water is less than that of adults, at the same time as which children often have a higher rate of metabolism, which means that the activity is eliminated faster than for adults. The increase of absorbed dose in children due to body size is compensated for in part through these effects.

In calculating the dose equivalent commitment that arises through intake early in the life cycle, the fact that children have a longer expected life must be taken into account. For nuclides with a long biological and physical retention time, it is therefore usually not sufficient to integrate over 50 years; instead, an integration time of 70 years should be applied.

A significant difference in the dose equivalent commitment due to differences in body size can be expected for technetium-99 and iodine-129. This difference can be roughly estimated at about a factor of 10 for a newborn individual compared to an adult. For radium and certain actinides, body size has only a small effect on the dose equivalent commitment. An important factor for certain actinides is the greater uptake via the gastrointestinal tract in newborn children.

The whole population

In calculating the consequences of a possible release of radionuclides to the biosphere, age dependence, uptake and an integration time of 70 years should therefore be taken into account in calculating the doses.

In order to take into account new data that has been obtained as well, a review has been carried out of the dose conversion factors for the nuclides of interest in connection with the final storage of nuclear waste /16-11/.

Table 16-1 presents the values obtained.

The limiting tissue for all isotopes except technetium-99 and iodine-129 is bone tissue. Technetium is distributed evenly in the body, so the whole-body dose itself is limiting; the limiting tissue for iodine is the thyroid gland.

The differences in the table stem primarily from the following changes:

^{239}Pu New data for uptake via the gastrointestinal tract and proposed revisions submitted to the ICRP.

^{237}Np New data for uptake via the gastrointestinal tract. Such a possible reduction has also been recommended in ICRP 30 for trace quantities of the nuclide.

^{231}Pa A weighing-together of available data.

The ICRP's values have been used for nuclides where the dose conversion factors have not been subjected to special scrutiny.

Table 16-1. Committed dose equivalent to limiting tissue and effective dose equivalent per unit intake (Sv Bq^{-1}). The values in this report have been integrated over 70 years, the ICRP 30 values over 50 years.

Nuclide	Values in this report		ICRP-30	
	Limiting tissue	Effective dose equiv.	Limiting tissue	Effective dose equiv.
^{239}Pu (soluble)	1.4×10^{-5}	7.0×10^{-7}	2.1×10^{-6}	1.2×10^{-7}
^{239}Pu (insoluble)	2.7×10^{-7}	1.4×10^{-8}	2.1×10^{-7}	1.2×10^{-8}
^{237}Np	2.5×10^{-5}	1.2×10^{-6}	1.9×10^{-4}	1.1×10^{-5}
^{226}Ra	7.5×10^{-6}	3.3×10^{-7}	6.8×10^{-6}	3.1×10^{-7}
^{230}Th	4.1×10^{-6}	1.6×10^{-7}	3.6×10^{-6}	1.5×10^{-7}
^{231}Pa	5.5×10^{-4}	2.2×10^{-5}	7.2×10^{-5}	2.9×10^{-6}
^{99}Tc	-	3.4×10^{-10}	-	3.4×10^{-10}
^{129}I	3.3×10^{-6}	9.8×10^{-8}	2.5×10^{-6}	7.4×10^{-8}

16.3.4 Other assumptions

Linear dose/effect relationship

One of the fundamental assumptions behind the ICRP's recommendations is that a linear relationship exists - without a threshold value - between dose and the probability of a harmful effect. See section 16.4.1.

This is the reason why it is possible to add doses that are obtained in different tissues or organs to obtain a measure of the total risk. The same applies to the use of the collective dose as an index of the total detrimental radiation effect in the population.

"Effective" or " weighted" whole-body dose

In previous recommendations, the ICRP has used the concept "critical organ" and the dose limit for the individual is determined by the dose limit for this organ. The ICRP now recommends instead a procedure that takes into account the total risk resulting from the exposure of all tissues. Thus, the concept "weighted" or "effective" whole-body dose has been introduced. The purpose of this is to gain a means to add together doses to different organs and normalize the risk to a single representative number. The risk can then be calculated in the same manner regardless of whether the whole body or a specific organ is being irradiated.

The value of the weighting factor recommended by the ICRP for different organs is given in the following table:

Tissue	Weighting factor
Gonads	0.25
Breast	0.15
Red bone marrow	0.12
Lung tissue	0.12
Thyroid gland	0.03
Bone tissue	0.03
5 next-most irradiated organs	0.30/5

16.4 EFFECTS OF IONIZING RADIATION

16.4.1 Health effects

The ionizing radiation is absorbed in body tissues and thereby gives rise to radiation doses. The radiation comes either from radioactive substances that decay in the body - internal irradiation - or from substances in the surroundings, external irradiation.

Acute injuries

Very high radiation doses on the order of 1 Sv or more cause acute injuries due to the fact that many cells in sensitive tissues are damaged or die. The blood-forming tissues are usually the most critical. Sensitivity varies, but around one of ten people that have received 2 Sv to the whole body during a short period of irradiation run the risk of dying within a couple of months without medical attention. The mortality rate resulting from acute radiation injury increases rapidly with rising doses above 2 Sv, but the risk is insignificant at radiation doses below 1.5 Sv.

Foetuses are much more sensitive to ionizing radiation than adult people. Some limited experience exists from their radiation of foetuses, partly from the nuclear bomb explosions over Hiroshima and Nagasaki and partly from irradiation in medical treatment. The body of statistics is rather small, so the results of animal studies must also be used. It is difficult to establish a dose limit for foetal damage on the basis of present-day knowledge. On the basis of radiological risk assessments the Swedish authorities recommend abortion for a pregnant woman who has been exposed to radiation for medical treatment only if she has been irradiated so much that the foetus has received more than 0.1 Sv. The risk is dependent on the age of the foetus.

Acute radiation injuries are sometimes referred to in radiation protection contexts as non-stochastic and the dose limit for these injuries for most organs is 0.5 Sv per year for personnel in radiological work.

Delayed injuries

Small radiation doses involve insignificant risks for acute radiation injuries, but can lead to delayed health effects in the irradiated individual or his descendents.

The quantitatively most important delayed effect of ionizing radiation is probably cancer. Cancer risk assessments can be made on the basis of a relatively large body of data from epidemiological studies of irradiated people, especially from survivors from Hiroshima and Nagasaki and persons who have been subjected to radiation treatment for certain non-mortal diseases. These cases mainly involve comparatively high doses, however.

From the radiation protection viewpoint, it is important to know what the relationship between radiation dose and risk of cancer looks like at very low doses. However, only a few studies within this low-dose interval permit risk assessments.

The ICRP recommends standards for radiation protection based on a risk philosophy whereby the risk increases in direct proportion to the dose, i.e. a linear dose-risk relationship without a threshold. Other relationships have been discussed, and it has been contended that the actual risk at low doses may be considerably lower than that given by a linear dose-risk relationship.

In the USA, a committee under the National Research Council (the Committee on Biological Effects of Ionizing Radiation) recently published a report that leaves the option open to evaluate the risks with assumptions of linear, quadratic or linear-quadratic dependence on the radiation dose.

Our Swedish radiation protection authority - like the ICRP - assumes a linear relationship between dose and risk.

It has been shown that ionizing radiation produces pronounced genetic effects in virus, bacteria, fungi, insects and certain mammals, e g mice. However, it has not been possible to demonstrate a higher incidence of genetic damage in irradiated people, including the large population that survived with relatively high

radiation doses in Hiroshima and Nagasaki. A number of mutations have almost certainly been induced, but the problem is of a statistical nature. They cannot be distinguished from the larger numbers of normally occuring genetic changes in a population.

It also appears to be clear that, from the viewpoint of injury - even if one integrates over a large number of generations - the genetic risks are not greater than the cancer risks.

16.4.2 Risk factors for organs and tissues

The risk factors for different tissues are based on estimated probabilities of certain serious life-threatening diseases - mainly cancer - i e stochastic (random) changes or pronounced genetic defects that can appear in offspring /16-5, 16-12/. See table 16-2.

Table 16-2. Risk factors given by the ICRP applying to exposure in radiological work.

Organ or tissue	Risk factor Sv^{-1}	Effct
Gonads	0.01	Heriditary effects in the first two generations
Red bone marrow	0.002	Leukemia, resulting in death
Bone	0.0005	Skeleton cancer, " " "
Lung	0.002	Lung cancer, " " "
Thyroid gland	0.0005	Thyroid cancer, " " "
Breast	0.0025	Breast cancer, " " "
Each other individual tissue	<0.001	Cancer, " " "
Other tissues, total	0.005	Cancer, " " "
Homogeneous whole-body irradiation	0.01	" " " "
"	0.004	Hereditary effects within the first two generations
"	0.008	Hereditary effects within all generations

The ICRP has introduced the concept of "detriment" to identify and quantify the harmful effect of ionizing radiation. In general, the detriment in a population is defined as the mathematical expectation of an injury that can arise from irradiation. This takes into

account both the probability of each injurious effect and the degree of severity.

According to the definition of "detriment", the injury is proportional to the value of the collective dose. The validity of this relationship between detriment and collective dose is dependent on the validity of the assumption of linearity - without a threshold value - between risk and dose. The ICRP has maintained that this is a cautious assumption.

16.5 REFERENCE DATA

In calculating the dose caused by the release of radioactive substances from a final repository, the factors given in table 16-3 have been used for converting intake to dose.

Table 16-3. Dose conversion factors (Sv/Bq) for inhalation and intake of food.

Nuclides	Inhalation	Ingestion
^{93}Zr	8.6×10^{-9}	4.2×10^{-10}
^{99}Tc	2.0×10^{-9}	3.4×10^{-10}
^{126}Sn	2.3×10^{-8}	4.7×10^{-9}
^{129}I	4.7×10^{-8}	9.8×10^{-8}
^{135}Cs	1.2×10^{-9}	1.9×10^{-9}
^{226}Ra	2.6×10^{-6}	3.3×10^{-7}
^{229}Th	5.7×10^{-4}	9.4×10^{-7}
^{230}Th	8.6×10^{-5}	1.6×10^{-7}
^{231}Pa	3.4×10^{-4}	2.2×10^{-5}
^{233}U	3.6×10^{-5}	7.2×10^{-8}
^{234}U	3.6×10^{-5}	7.1×10^{-8}
^{236}U	3.4×10^{-5}	6.7×10^{-8}
^{238}U	3.2×10^{-5}	6.3×10^{-8}
^{237}Np	1.3×10^{-4}	1.2×10^{-6}
^{239}Pu	1.4×10^{-4}	7.0×10^{-7}
^{242}Pu	1.3×10^{-4}	1.1×10^{-7}

REFERENCES

CHAPTER 9

9-1 PUSCH R
Swelling Pressure of Highly Compacted Bentonite.
University of Luleå.
KBS TR 80-13, 1980-08-20.

9-2 PUSCH R
Use of Clays as Buffers in Radioactive Repositories.
University of Luleå.
KBS TR 83-46, May 1983.

9-3 PUSCH R
Permeability of Highly Compacted Bentonite.
University of Luleå.
KBS TR 80-16, 1980-12-23.

9-4 PUSCH R
Stability of Deep-Sited Smectite Minerals in Crystalline Rock - Chemical Aspects. KBS TR 83-16, March 1983.

9-5 ANERSON D M
Smectite Alteration, Proceedings of a Colloquium at State University of New York at Buffalo, May 26-27 1982.
State University of New York at Buffalo.
KBS TR 83-03, February 15, 1983.

9-6 PUSCH R, ERIKSEN T, JACOBSSON A
Ion/Water Migration Phenomena in Dense Bentonites. Proc. Scientific Basis for Radioactive Management, Berlin 1982, Elsevier Publ. Co. (Werner Lutz Ed).

9-7 ERIKSEN T E, JACOBSSON A
Diffusion of Hydrogen, Hydrogen Sulfide and Large Molecular Weight Anions in Bentonite.
Royal Institute of Technology, Stockholm, University of Luleå.
KBS TR 82-17, 1982-07-02.

9-8 PUSCH R
Stress/Strain/Time Properties of Highly Compacted Bentonite.
University of Luleå.
KBS TR 83-47, May 1983.

9-9 PUSCH R
Stability of Bentonite Gels in Crystalline Rock-Physical Aspects.
University of Luleå.
KBS TR 83-04, February 1983.

9-10 PUSCH R, BÖRGESSON L, NILSSON J
Buffer Mass Test - Buffer Materials
University of Luleå, AB Jacobson & Widmark.
STRIPA PROJECT TR 82-06, August 1982.

9-11 KNUTSSON S
Värmeledningsförsök på buffertsubstans av kompakterad bentonit.
("Thermal conductivity tests on buffer material of compacted bentonite").
University of Luleå.
KBS TR 72, 1977-11-18.

9-12 PUSCH R, NILSSON J
Buffer Mass Test - Rock Drilling and Civil Engineering.
University of Luleå, AB Jacobson & Widmark
STRIPA PROJECT TR 82-07, September 1982.

9-13 PUSCH R
Borehole Sealing With Highly Compacted NA Bentonite.
University of Luleå.
KBS TR 81-09, 1981-12-07.

CHAPTER 10

10-1 LÖNNERBERG B, LARKER H, AGESKOG L
Encapsulation and Handling of Spent Nuclear Fuel for Final Disposal.
1. Welded Copper Canisters
2. Pressed Copper Canisters (HIPOW)

3. BWR Channels in Concrete
ASEA-ATOM, ASEA, VBB
KBS TR 83-20, May 1983

10-2 SANDERSSON A, SZLUKA T F, TURNER J
Feasibility Study of ED Welding of Spent Nuclear Fuel Canisters
Welding Institute Cambridge UK
KBS TR 83-25, April 1983.

10-3 TEKNISKA RÖNTGENCENTRALEN AB
Feasibility Study of Detection of Defects in Thick Welded Copper.
KBS TR 83-32, April 1983.

10-4 KJELLBERT N
Nuklidhalter i använt LWR-bränsle och i högaktivt avfall från återcykling av plutonium i PWR.
("Nuclide levels in spent LWR fuel and in high level waste from the recycling of plutonium in PWR.")
Stadsvik Energiteknik AB
KBS TR-111, July 1978

10-5 The Swedish Corrosion Research Institute and its Reference Group
Corrosion Resistance of a Copper Canister for Spent Nuclear Fuel.
KBS TR 83-24, April 1983.

10-6 WIKBERG P, GRENTHE I, AXELSEN K
Redox Conditions in Groundwaters from Svartboberget, Gideå, Fjällveden and Kamlunge.
Royal Institute of Technology.
KBS TR 83-40, April 1983.

10-7 BENJAMIN L A, HARDIE D, PARKINS R N
Investigation of the Stress Corrosion Cracking of Pure Copper
University of Newcastle upon Tyne, UK
KBS TR 83-06, April 1983.

CHAPTER 11

11-1 EKLUND U-B, FORSYTH R
Lakning av bestrålat UO_2-bränsle
("Leaching of irradiated UO_2 fuel")
Studsvik Energiteknik AB
KBS TR-70, Feb 1978

11-2 FORSYTH R
The KBS UO_2 Leaching Program
Summary Report: 1983-02-01.
Studsvik Energiteknik AB.
Studsvik/NF(P)-82/11.

11-3 VANDEGRAAF T T
Leaching of Irradiated UO_2 Fuel.
Atomic Energy of Canada Limited (AECL)
TR-100 (1980).

11-4 JOHNSON L H, SHOESMITH D W, LUNANSKY G E, BAILEY M G, TREMAINE P R
Mechanisms of Leaching and Dissolution of UO_2 Fuel.
Nucl. Techn, 56 (1982) 238.

11-5 JOHNSON L H
The Dissolution of Irradiated UO_2 Fuel in Groundwater.
Atomic Energy of Canada Limited (AECL).
AECL-6837 (1982).

11-6 JOHNSON L H, BURNS K I, JOLING H, MOORE C L
The Dissolution of Irradied UO_2 Fuel under Hydrothermal Conditions.
Atomic Energy of Canada Limited (AECL).
TR-128 (1981).

11-7 KATAYAMA Y B
Spent LWR Fuel Leach Tests.
Battelle Pacific Northwest Laboratory (PNL).
PNL-2982 (1979).

11-8 KATAYAMA Y B, BEADLEY D J, HARVEY C O
Status Report on LWR Spent Fuel IAEA Leach Tests.
Batelle Pacific Northwest Laboratory (PNL).
PNL-3173 (1980).

11-9 OGARD A E, BENTLEY G, BRYANT E, DUFFY C J, GRISHAM J, NORRIS A E, ORTH C, THOMAS K
Are Solubility Limits of Improtance to Leaching?
Ed.: John Moore
Plenum 1981.

11-10 WANG R
Spent-Fuel Special Studies Progress Report: Probable Mechanisms for Oxidation and Dissolution of Single-Crystal UO_2 Surfaces.
Battelle Pacific Northwest Laboratory (PNL).
PNL-3566 (1981).

11-11 JOHNSON L H, JOLING H H
The Dissolution of Irradiated Fuel under Hydrothermal Conditions.
in: The Scientific Basis of Nuclear Waste Management IV.
Ed.: Stephen V Topp.
Elsevier 1982.

11-12 GRENTHE I, PUIGDOMENECH I, BRUNO J B
The Possible Effects of Alfa and Beta Radiolysis on the Matrix Dissolution of Spent Nuclear Fuel.
Royal Institute of Technology.
KBS TR 83-02, January 1983.

11-13 PAQUETTE J, LEMIRE R J
A Description of the Chemistry of Aqueous Solutions of Uranium Plutonium to 200^{o}C Using Potential-pH Diagrams.
Nucl. Sci. Eng. 79 (1981)26.

CHAPTER 12

12-1 AHRLAND S, LILJENZIN J O, RYDBERG J
Solution Chemistry of the Actinides, Comprehensive.
Inorganic Chemistry Vol. 5, Pergamon Press, Oxford 1973.

12-2 GRENTHE I, FERRI D
Actinide Species in Groundwater Systems.
Proc. OECD Workshop on NEAR-field Phenomena in Geologic Repositories for Radioactive Waste, Seattle 1981, p 93.

12-3 ALLARD B
Solubilities of Actinides in Neutral or Basic Solutions.
Actinides in Perspective (Ed N M Edelstein), Pergamon Press, New York 1982, p 553.

12-4 ALLARD B
Actinide Solution Equilibria and Solubilities in Geochemical Systems.
Chalmers University of Technology.
KBS TR 83-35, April 1983.

12-5 LANGMUIR D, HERMAN J S
The Mobility of Thorium in Natural Waters at Low Temperatures.
Geochim Cosmochim Acta 44(1980) 1753.

12-6 LANGMUIR D
Uranium Solution-Mineral Equilibria at Low Temperatures with Application to Sedimentary Ore Deposits.
Geochim Cosmochim Acta 42(1978) 547.

12-7 PAQUETTE J, LEMIRE R J
A description of the Chemistry of Aqueous Solutions of Uranium and Plutonium to 200°C using Potential-pH Diagrams.
Nuclear Sci. Eng. 79(1981) 26.

12-8 POURBAIX M
Atlas of Electrochemical Equilibria in Aqueous Solutions.
Pergamon Press, Oxford 1966.

12-9 BAES C F, MESMER R F
The Hydrolysis of Cations.
John Wiley and Sons, New York 1976.

12-10 ANDERSSON K, TORSTENFELT B, RYDBERG J
Leakage of Niobium-94 from an Underground Rock Repository.
Chalmers University of Technology.
KBS TR 79-26, 1979-11-05.

12-11 ANDERSSON K, NERETNIEKS I
Utläckning av Ni-59 från ett bergförvar.
("Leakage of Ni-59 from a rock repository")
Royal Institute of Technology
KBS TR 101, 1978-04-24

12-12 ALLARD B, TORSTENFELT B
On the Solubility of Technetium in Geochemical Systems.
Chalmers University of Technology.
KBS TR 83-60, May 1983.

12-13 ALLARD B, TORSTENFELT B, ANDERSSON K, RYDBERG J
Possible Retention of Iodine in the Ground.
2nd International Symposium on the Scientific Basis for Nuclear Waste Management, Boston, November 1979, Proceedings Plenum 1980, p 673.

12-14 STARIK I E
Grundlagen der Radiochemie.
Akademie-Verlag, Berlin 1963.

12-15 KEPAK F
Adsorption and Colloidal Properties of Radioactive Elements in Trace Concentrations.
Chemical Rev. 71 (1971) 357.

12-16 JOHNSON G L, TOTH L M
Plutonium(IV) and Thorium(IV) Hydrous Polymenr Chemistry.
Oak Ridge Nat Lab.
ORNL/TM-6365, 1978.

12-17 OLOFSSON U, ALLARD B, BENGTSSON M, TORSTENFELT B, ANDERSSON K
Formation and Properties of Actinide Colloids.
Chalmers University of Technology.
KBS TR 83-08, January 1983.

12-18 OLOFSSON U, ALLARD B
Complexes of Actinides with Naturally Occurring Organic Substances - Literature Survey.
Chalmers University of Technology.
KBS TR 83-09, February 1983.

12-19 MARINSKY J
The Complexation of Eu(III) by Fulvic Acid.
State University of New York at Buffalo.
KBS TR 83-14, 1983-03-31.

12-20 MAYA L
Hydrolosis and Carbonate Complexation of Dioxoneptunium(V) in 1.0 M $NaClO_4$ at 25°C.
Inorg Chim Acta, 1983, under tryckning.

12-21 OSMOND J K, COWART J B
The Theory and Uses of Natural Uranium Isotopic Variations in Hydrology.
Atomic Energy Rev 14(1976) 621.

12-22 BENES P, MAJER V
Trace Chemistry of Aqueous Solutions.
Elsevier, Oxford 1980.

12-23 ALLARD B, ANDERSSON K, TORSTENFELT B
The Distribution Coefficient Concept and Aspects on Experimental Distribution Studies.
Chalmers University of Technology.
KBS TR 83-62, May 1983.

12-24 BIRGERSSON L, NERTNIEKS I
Diffusion in the matrix of Granite Rock. Field Test in the Stripa Mine.
Royal Institute of Technology.
KBS TR 82-08, July 1982.

12-25 LANDSTRÖM O, KLOCKARS C E, PERSSON O, ANDERSSON K, TORSTENFELT B, ALLARD B, TULLBORG E-L, LARSON S Å
Migration Experiments in Studsvik.
Studsvik Energiteknik AB, Swedish Geological, Chalmers University of Technology.
KBS TR 83-18, 1983-01-31.

12-26 ALLARD B, KIPATSI H, RYDBERG J
Sorption of Long-Lived Radionuclides in Clay and Rock. I.
KBS TR 55, 1977.

12-27 ERDAL B R, AGUILAR R D, BAYHURST B P, DANIELS W R, DUFFY C J, LAWRENCE F O, MAESTAS S, OLIVER P Q, WOLFSBERG K
Sorption-Desorption Studies on Granite.
Los Alamos Sci Lab.
LA-7456-MS, 1979.

12-28 ALLARD B
Sorption of Actinides in Granitic Rock.
Chalmers University of Technology.
KBS TR 82-21, 1982-11-20.

12-29 ALLARD B, OLOFSSON U, TORSTENFELT B, KIPATSI H
Sorption Behaviour of Actinides in Well-defined Oxidation States.
Chalmers University of Technology.
KBS TR 83-61, May 1983.

12-30 ANDERSSON K, ALLARD B
Sorption of Radionuclides on Geologic Media - A literature Survey.
I: Fission Products
Chalmers University of Technology.
KBS TR 83-07, January 1983.

12-31 ANDERSSON K, TORSTENFELT B, ALLARD B
Sorption of Radionuclides in Geologic Systems.
Chalmers University of Technology.
KBS TR 83-63, May 1983.

12-32 ALLARD B, KIPATSI H, TORSTENFELT B
Sorption of Long-Lived Radionuclides in Clay and Rock. II.
Chalmers University of Technology.
KBS TR 98, 1978-04-20.

12-33 SHEPPARD J C, CAMPBELL M J, KITTRICK J A, HARDT T L
Retention of Neptumium, Americium and Curium by Diffusible Soil Particles.
Environmental Sci & Techn 13 (1979) 680.

12-34 EISENBUD M, LEI W, BALLAD R, PENNA FRANCA E, MIEKELEY N, CULLEN T, KRAUSKOPF K
Studies of the Mobilization of Thorium from Morro do Ferro.
5th International Symposium on the Scientific Basis for Nuclear Waste Management, Berlin, June 1982. Proceedings Elsevier 1982.

12-35 YAMAMOTO M, TANII T, SAKANOUE M
Characteristics of Fall-out Plutonium in Soil.
Journ Radiation Res 22 (1981) 134.

12-36 BONDIETTI E A, REYNOLDS S A, SHANKS M H
Interactio of Plutonium with Complexing Substances in Soils and Natural Waters.
IAEA-SM 199/51.

CHAPTER 13

13-1 The Swedish Corrosion Institute and its reference group.
Copper as canister material for unreprocessed nuclear waste - evaluation with respect to corrosion.
KBS TR 90, 1978-03-31

13-2 PERRY R H, CHILTON C H
Chemical Engineers Handbook.
5th Ed McGraw Hill 1973 Chapter 3.

13-3 NERETNIEKS, I, SKAGIUS K
Diffusivitetsmätningar av metan och väte i våt lera.
("Diffusivity measurements of methane and hydrogen in wet clay")
Royal Institute of Technology
KBS TR 86, 1978-01-09

13-4 NERETNIEKS I, SKAGIUS K
Diffusivitetsmätningar i våt lera av Na-lignosulfonat, Sr^{2+}, Cs^{+}
("Diffusivity measurements in wet clay, Na-lignosulphonate, Sr^{2+}, Cs^{+}")
Royal Institute of Technology
KBS TR 87, 1978-03-16

13-5 ERIKSEN T
Diffusion of Hydrogen, Hydrogen Sulfide and Large Moelcular Weight Anions in Bentonite.
Royal Institute of Technology.
KBS TR 82-17, 1982-07-02.

13-6 ERIKSEN T, JAKOBSSON A
Ion Diffusion Through Highly Compacted Bentonite.
Royal Institute of Technology, University of Luleå.
KBS TR 81-06, 1981-04-29.

13-7 ERIKSEN T, JACOBSSON A
Ion Diffusion in Compacted Sodium and Calcium Bentonites.
Royal Institute of Technology, University of Luleå.
KBS TR 81-12, February 1982.

13-8 TORSTENFELT B, ANDERSSON K, KIPATSI H, ALLARD B, OLOFSSON U
Diffusion Measurements in Compacted Bentonite.
Scientific Basis for Nuclear Waste Management, Vol 4, Elsevier N Y 1982.

13-9 TORSTENFELT B, KIPATSI H, ANDERSSON K, ALLARD B, OLOFSSON U
Transport of Actinides through a Bentonite Backfill.
Scientific Basis for Nuclear Waste Management, Vol 5, Elsevier North-Holland NY 1982.

13-10 NERETNIEKS I
Diffusivities of some Dissolved Constituents in Compacted Wet Bentonite Clay-MX80 and the Impact on Radionuclide Migration in the Buffer.
Royal Institute of Technology.
KBS TR 82-27, October 1982.

13-11 NERETNIEKS I
Transport of Oxidants and Radionuclides through a Clay Barrier.
Royal Institute of Technology.
KBS TR 79, 1978-02-20.

13-12 ANDERSSON G, RASMUSSON A, NERETNIEKS I
Migration Model for the Near Field.
Royal Institute of Technology.
KBS TR 82-24, November 1982.

13-13 NERETNIEKS I
Retardation of Escaping Nuclides from a Final Repository.
Royal Institute of Technology.
KBS TR 30, 1977-09-14.

13-14 SNOW D T
Rock Fracture Spacings, Openings and Porosities.
J Soil Mech Found, Div Amer Soc Civ Eng 94, SMI(1968) 73-91.

13-15 NERETNIEKS I
Leach Rates of High Level Waste and Spent Fuel - Limiting Rates as Determined by Backfill and Bedrock Conditions.
Paper presented at the 5th International Symposium on the Scientific Basis for Nuclear Waste Management.
Berlin 1982 June Proceedings North-Holland 1982, p 559-568.

13-16 CHRISTENSEN H, BJERGBAKKE E
Radiolysis of Groundwater from HLW Stored in Copper Canisters
Studsvik Energiteknik AB
KBS TR 82-02, 1982-06-29.

13-17 CHRISTENSEN H, BJERGBAKKE E
Radiolysis of Groundwater from Spent Fuel.
Studsvik Energiteknik AB.
KBS TR 82-18, November 1982.

13-18 CURTIS D, GANCARZ A
Radiolysis in Nature: Evidence from the Oklo Natural Reactors.
KBS TR 83-10, February 1983.

13-19 GRENTHE I, PUIGDOMENECH I, BRUNO J
The Possible Effects of Alfa and Beta Radiolysis on the Matrix Dissolution of Spent Nuclear Fuel.
Royal Institute of Technology.
KBS TR 83-02, January 1983.

13-20 TORSTENFELT B, ALLARD B, ITTNER T
Iron Content and Reducing Capacity of Granite and Bentonite.
Chalmers University of Technology.
KBS TR 83-36, April 1983.

13-21 NERETNIEKS I. ÅSLUND B
The Movement of Radionuclides Past a Redox Front.
Royal Institute of Technology.
KBS TR 83-66, May 1983.

13-23 NERETNIEKS I, ÅSLUND B
Two Dimensional Movement of a Redox Front Downstream from a Repository for Nuclear Waste.
Royal Institute of Technology.
KBS TR 83-68, May 1983.

13-24 PUSCH R, FORSBERG T
Gas Migration through Bentonite Clay.
University of Luleå.
KBS TR 83-71, May 1983.

13-25 NERETNIEKS I
Some notes in Connection with the KBS Studies of Final Disposal of Spent Fuel. Part 2.
Royal Institute of Technology.
KBS TR 83-67, May 1983.

13-26 The Swedish Corrosion Research Institute and its Reference Group
Corrosion Resistance of a Copper Canister for Spent Nuclear Fuel
KBS TR 83-24, April 1983.

13-27 The Swedish Corrosion Institute and its reference group
Bedömning av korrosionsbeständigheten hos material avsedda för kapsling av kärnbränsleavfall
("Evaluation of corrosion resistance of material intended for encapsulation of nuclear fuel waste.")
Status report 1977-0929 and supplementary statements
KBS TR 31, 1977-09-29

13-28 HÜBNER W
Vätebildning i avfallsförvar
("Hydrogen formation in waste repositories")
Stage 1 problem inventory
Studsvik Work Report
Studsvik 79-10-04

13-29 Corrosion du zircaloy après enrobage dans le ciment. Bitumes et ciments. Etudes et essais.
Groupe CEA, Paris 1983-01-05 p 193.

13-30 ANDERSSON K, TORSTENFELT B, RYDBERG J
Leakage of Niobium-94 from an Underground Rock Repository.
Chalmers University of Technology.
KBS TR 79-26, 1979-11-05.

13-31 NERETNIEKS I, ANDERSSON K
Utläckning av Ni-59 från ett bergförvar
("Leakage of Ni-59 from a rock repository")
Royal Institute of Technology
KBS TR 101, 1978-04-24

CHAPTER 14

14-1 SKAGIUS K, SVEDBERG G, NERETNIEKS I
A Study of Strontium and Cesium Sorption on Granite.
Nuclear Technology 59, 2(1982)302.

14-2 NERETNIEKS I
Some Notes in Connection with the KBS Studies of Final Disposal of Spent Fuel. Park 2.
Royal Institute of Technology.
KBS TR 83-67, May 1983.

14-3 SKAGIUS K, NERETNIEKS I
Diffusion in Crystalline Rocks.
Paper Presented at the 5th International Symposium on the Scientific Basis for Nuclear Waste Management.
Berlin, June 1982.
Proceedings North-Holland 1982 p 509-518.

14-4 SKAGIUS K, NERETNIEKS I
Diffusion Measurements in Crystalline Rock.
Royal Institute of Technology.
KBS TR 83-15, March 1983.

14-5 NERETNIEKS I
Diffusion in the Rock Matrix: An Important Factor in Radionuclide Retardation?
J Geophys Res 85(1980) 4379.

14-6 RASMUSON A, NERETNIEKS I
Migration of Radionuclides in Fissured Rock - The Influence of Micropore Diffusion and Longitudinal Dispersion.
J Geophys Res 86(1981) 3749.

14-7 RASMUSON A, NERETNIEKS I
Surface Migration in Sorption Processes.
Royal Institute of Technology.
KBS TR 83-37, March 1983.

14-8 SKAGIUS K, NERETNIEKS I
Diffusion in Crystalline Rock of some Sorbing and Nonsorbing Species.
Royal Institute of Technology.
KBS TR 82-12, March 1982.

14-9 TORSTENFELT B, ITTNER T, ALLARD B, ANDERSSON K, OLOFSSON U
Mobilities of Radionuclides in Fresh and Fractured Crystalline Rock.
Chalmers Institute of Technology.
KBS TR 82-26, 1982-12-20.

14-10 RASMUSON A
Diffusion and Sorption in Particles and Two-Dimensional Dispersion in a Porous Medium.
Water Resources Res 17(1981) 321.

14-11 LALLEMAND-BARRÈS A, PEAUDECERF P
Recherche des relations entre la valeur de la dispersivité macroscopique d'un milieu àquifère, ses autres caractéristriques et les conditions de mesure.
Bulletin du B.R.G.M. Section III, 4(1978) 277.

14-12 LANDSTRÖM O, KLOCKARS C-E, HOLMBERG K-E, WESTERBERG S
In Situ Experiments on Nuclide Migration in Fractured Crystalline Rocks.
Studsvik Energiteknik AB, The Geological Survey of Sweden.
KBS TR 110, July 1978.

14-13 NERETNIEKS I
A Note on Dispersion Mechanisms in the Groundwater Resources Res 1983 (in print).

14-14 LANDSTRÖM O, KLOCKARS C E, PERSSON O, ANDERSSON K, TORSTENFELT B, ALLARD B, LARSON S Å, TULLBORG E L
A Comparison of In-Situ Radionuclide Migration Studies in the Studsvik Area and Laboratory Measurements.
Paper Presented at the 5th International Symposium on the Scientific Basis for Nuclear Waste Management.
Berlin, June 1982.
Proceedings North-Holland 1982 p 697-706.

14-15 LANDSTRÖM O, ANDERSSON K, TULLBORG E-L
Migration Experiements in Studsvik.
Studsvik Energiteknik AB, Swedish Geological.
KBS TR 83-18, 1983-01-31.

14-16 GUSTAFSSON E, KLOCKARS C-E
Studies on Groundwater Transport in Fractured Crystalline Rock under Controlled Conditions using Non Radioactive Tracers.
Geological Survey of Sweden.
KBS TR 81-07, April 1981.

14-17 ABELIN H, GIDLUND J, NERETNIEKS I
Migration in a Single Fissure.
Paper Presented at the 5th International Symposium on the Scientific Basis for Nuclear Waste Management.
Berlin June 1982.
Proceedings North-Holland 1982 p 529-538.

14-18 FRIED J J, COMBARNOUS, M A
Dispersion in Porous Media.
Advances Hydroscience 7 (1971) 1970.

14-19 BRACE W F, ORGANGE A S, MADDEN W T
The Effect of Pressure on the Electrical Resistivity of Water Saturated Crystalline Rocks.
J Geophys Res 70 (1965) 5669.

14-20 BRACE W F, WALSH J B, FRANGOS W T
Permeability of Granite under High Pressure.
J Geophys Res 73 (1968) 2225.

14-21 BRACE W F
Permeability of Granite under High Pressure.
J Geophys Res 82 (1977) 3343.

14-22 HEARD H C, TRIMMER D, DUBA A, BONNER B
Permeability of Generic Repository Rocks at Simulated In Situ Conditions.
Lawrence Livermore Laboratory.
UCRL-82609, April 1979.

14-23 TRIMMER D, BONNER B, HEARD H C, DUBA A
Effect of Pressure and Stress on Water Transport in Intact and Fractured Gabbro and Granite.
J Geophys Res 85 (1980) 7059.

14-24 ÖQUIST U, JÄMTLID A
Porositets- och resistivitestsbestämningar på borrkärnprov från Finnsjön och Sternö
("Porosity and resistivity determinations on drill core samples from Finnsjön and Sternö")
Report 1981-03-10
Geological Survey of Sweden

14-25 BRADBURY M H, LEVER D, KINSEY
Aqueous Phase Diffusion in Crystalline Rock.
Paper Presented at the 5th International Symposium on the Scientific Basis for Nuclear Waste Management.
Berlin June 1982.
Proceedings North-Holland 1982 p 569-578.

14-26 NERETNIEKS I, ERIKSEN T, TÄHTINEN P
Tracer Movement in a Single Fissure in Granitic Rock: Some Experimental Results and their Interpretation.
Water Resources Res 18, 4(1982) 849.

14-27 RABER E, TAILOR R, ISHERWOOD D, VANDERGRAAF T
Laboratory Studies of Radionuclide Transport in Fractured Climax Granite.
Lawrence Livermore National Laboratory, June 1982.

14-28 ERIKSEN T
Radionuclide Transport in a Single Fissure. A Laboratory Study.
Royal Institute of Technology.
KBS TR 83-01, 1983-01-19.

14-29 PEAUDECERF P, VAUBOURG P
Massif B, Reconnaissance du milieu et measures in situ des paramètres.
Commissariat à l'Energie Atomique, Bureau de Recherches géologiques et minières, Service Geologique National, Department Hydrogèologie, Avril 1980.

14-30 HODGKINSON D P, LEVER D A
Interpretation of a Field Experiment on the Transport of Sorbed and Nonsorbed Tracers through a Fracture in Crystalline Rock.
Theoretical Pysics Division, Atomic Energy Research Establishment, Harwell, England.
AERE-R-10702, October 1982.

14-31 MORENO L, NERETNIEKS I, KLOCKARS C-E
Evaluation of Some Tracer Tests in the Granitic Rock at Finnsjön.
Royal Institute of Technology, Swedish Geological.
KBS TR 83-38, April 1983.

14-32 ANDERSON K, TORSTENFELT B, ALLARD B
Sorption of Radionuclides in Geologic Systems.
Chalmers University of Technology.
KBS TR 83-63, May 1983.

14-33 LARSON S Å, TULLBORG E-L, LINDBLOM S
Sprickmineralogiska undersökningar
("Fracture-mineralogical investigations")
Prav report 4.20, April 1980

14-34 BIRGERSON L, NERETNIEKS I
Diffusion in the Matrix of Granitic Rock. Field Test in the Stripa Mine. Part 1.
Royal Institute of Technology.
KBS TR 82-08, July 1982.

14-35 BIRGERSON L, NERETNIEKS I
Diffusion in the Matrix of Granitic Rock. Field Test in the Stripa Mine. Part 2.
Royal Institute of Technology.
KBS TR 83-39, March 1983.

14-36 NERETNIEKS I
Prediction of Radionuclide Migration in the Geosphere. - Is the Porous Flow Model Adequate?
International Symposium on Migration in the Terrestrial Environment of Long-Lived Radionuclides from the Nuclear Fuel Cycle.
IAEA symposium, Knoxville, Tennessee, USA, July 1981.

14-37 RASMUSON A, NARASIMHAN T N, NERETNIEKS I
Chemical Transport in a Fissured Rock. Verfification of a Numerical Model.
Water Resources Res 18 (1982) 1479.

14-38 Natural Fission Reactors.
Vienna International Atomic Energy Agency, IAEA, 1978.

14-39 CURTIS D B, BENJAMIN T M, GANCARZ A J
The Oklo Reactors: Natural Analogs to Nuclear Waste Repositories
Los Alamos National Lab, Los Alamos.
LA-UR-81-3783, 1981.

14-40 SMELLIE J A T
Radioactive Disequilibria in Mineralized Drill Core Samples from the Björklund Uranium Occurrence, Northern Sweden.
Swedish Geological.
KBS TR 82-15, December 1982.

14-41 GRISAK G E, PICKENS J F
Solute Transport through Fractured Media. The Effect of Matrix Diffusion.
Water Resources Res 16 (1980) 719.

14-42 GRISAK G E, PICKENS J F
An Analytical Solution for Solute Transport through Fractured Media with Matrix Diffusion.
J Hydrology 52 (1981) 47.

14-43 GLUECKAUF E
The Movement of Solutes through Aqueous Fissures in Porous Rock
Atomic Energy Reserach Establishment, Harwell, England.
AERE-R 9823, June 1980.

14-44 NERETNIEKS I
Migration of Radionuclides in Fissured Rock: some Calculated Results Obtained from a Model Based on the Concept of Stratified Flow and Matrix Diffusion.
Royal Institute of Technology.
KBS TR 82-03, October 1982.

14-45 TANG D H, FRIND E O, SUDICKY E A
Contaminant Transport in Fractured Porous Media: An Analytical Solution for a Single Fracture.
Work done by University of Waterloo for Atomic Energy of Canada Limited.
AECL-TR 132, Nov. 1980.

14-46 RASMUSON A, NERETNIEKS I
Exact Solution of a Model for Diffusion in Particles and Longitudinal Dispersion in Packed Beds.
American Institute of Chemical Engineers, Journal 26 (1980) 686.

14-47 RASMUSON A, NERETNIEKS I
Migration of Radionuclides in Fissured Rock - Results Obtained from a Model Based on the Concepts of Hydrodynamic Dispersion and Matrix Diffusion.
Royal Instittue of Technology.
KBS TR 82-05, May 1982.

14-48 CHAMBRE P L, PIGFORD T H, FUIJITA A, KAUKI T, KOBAYASHI A, LUNG H, TING D, SATO Y, ZAVOSKY S J
Analytical Performance Models for the Geology Respositories.
Earth Science Div, Lawrence Berkeley Lab and Dept Nuclear Engineering, Univ Calif, Berkeley Calif.
LBL-UCB-NE-4017 UC70, Oct 1982.

14-49 LARSSON A, GRUNDFELT B, ANDERSSON K, HADERMANN J
Mathematicl Models for Nuclide Transport in Geologic Media - An International Intercomparison (INTRACOIN).
IAEA/CN-43/434, Seattle 16-20 May 1983.

14-50 EDWARDS A L
"TRUMP": A Computer Program for the Transient and Steady State Temperature Distributions in Multidimensional Systems.
National Technical Information Service, National Bureau of Standards, Springfield, 1972.

14-51 NARASIMHAN T N, WITHERSPOON P A
An Integrated Finite Difference Method for Analysing Fluid Flow in Porous Media.
Water Resources Res 12 (1976) 57.

14-52 RASMUSON A, BENGTSSON A, GRUNDFELT B, NERETNIEKS I
Radionuclide Chain Migration in Fissured Rock - The Influence of Matrix Diffusion.
Royal Institute of Technology, KEMAKTA Consultant Company.
KBS TR 82-04, April 1982.

14-53 NERETNIEKS I, RASMUSON A
An Approach to Modelling Radionuclide Migration in a Medium with Strongly Varying Velocity and Block Sizes along the Flow Path.
Royal Institute of Technology.
KBS TR 83-69, May 1983.

14-54 BENGTSSON A, GRUNDFELT B, MAGNUSSON M, NERETNIEKS I, RASMUSON A
Model Calculations of the Migration of Radionuclides from a Repository for Spent Nuclear Fuel.
KEMAKTA Consultant Company, Royal Institute of Technology.
KBS TR 83-48, May 1982.

14-55 ABELIN H, GIDLUND J, NERETNIEKS I
Migration Experiments in a Single Fissure in the Stripa Granite.
Paper presented at the OECD/NEA Symposium on Geological disposal of radioactive waste. In situ experimenets in granite.
Stockholm 25-27 October 1982.

14-56 MEANS J, HEDINGTON G L
The Analysis of Humic and Fulvic Acid in Groundwater Samples
Batelle Columbus Laboratories, Columbia, Ohio.
Topical Report 1982-12-06.

14-57 OLOFSSON U, ALLARD B, TORSTENFELT B, ANDERSSON K
Properties and Mobilities of Actinide Colloids in Geologic Systems.
Paper presented at the 5th International Symposium on the Scientific Basis for Nuclear Waste Management.
Berlin June 1982.
Proceedings North-Holland 1982 p 755-764.

14-58 ALLARD B, LARSSON S Å, TULLBORG E-L, WIDBERG P
Chemistry of Deep Groundwaters from Granitic Bedrock.
Chalmers University of Technology, Swedish Geological, Royal Institute of Technology.
KBS TR 83-59, May 1983.

14-59 LE BELL J
Colloid Chemical Aspects of the "Confined Bentonite Concept".
Institute for Surface Chemistry.
KBS TR 97, 1978-03-07.

14-60 NERETNIEKS I
Some Aspects on Colloids as a Means for Transporting Radionuclides.
Royal Institute of Technology.
KBS TR 103, 1978-08-08.

CHAPTER 15

15-1 CARLSSON L, GRUNDFELT B
Model Calculations of the Groundwater Flow at Finnsjön, Fjällveden, Gideå and Kamlunge.
Swedish Geological, Kemakta Konsult AB.
KBS TR 83-45, May 1983.

15-2 THUNVIK R
Calculation of Fluxes through a Repository Caused by a Local Well.
Royal Institute of Technology.
KBS TR 83-50, May 1983.

15-3 BERGSTRÖM U, RÖJDER B
BIOPATH-A Computer Code for Calculation of the Turnover of Nuclides in the Biosphere and the Resulting Doses to Man.
Studsvik Energiteknik AB.

15-4 SUNDBLAD B, BERGSTRÖM U
Description of Recipient Areas Related to Final Storage of Unreprocessed Spent Nuclear Fuel.
Studsvik Energiteknik AB.
KBS TR 83-11, February 1983.

15-5 EVANS S. LAMPE S, SUNDBLAD B
Natural Levels of Uranium and Radium in Four Potential Areas for the Final Storage of Spent Fuel.
Studsvik Energiteknik AB.
KBS TR 82-22, December 1982.

15-6 APPELGREN A
Consumption Habits. A Statistical Summary and Comparison.
Studsvik Energiteknik AB.
NW-82/311, App2 (1982).

15-7 BERGSTRÖM U, WILKENS A-B
An Analysis of Selected Parameters for the BIOPATH-Program.
Studsvik Energiteknik AB.
KBS TR 83-28, April 1983.

15-8 BERGSTRÖM U
Analysis of the Importance for the Doses of Varying Parameters in the BIOPATH-Program.
Studsvik Energiteknik AB
KBS TR 81-03, March 1981.

15-9 HOFFMAN F O, GARDNER R H, ECKERMAN K F
Variability in Dose Estimates Associated with the Food Chain Transport and Ingestion of Selected Radionuclides.
ORNL/TM-8099 (1982)

15-10 BERGMAN R, BERGSTRÖM U, EVANS S
Environmental Transport and Long-term Exposure for Tritium Released in the Biosphere.
IAEA-SM-232/47 (1979).

15-11 BERGMAN R, McEWAN C
Dose and Dose Commitment due to Carbon-14 from the Nuclear Industry.
AB Atomenergi, Studsvik, S-548 (1977).

15-12 LILJEQUIST GÖSTA
Klimatologi, 1970
("Climatology, 1970")
The General Staff's Lithographic Institute, Stockholm

15-13 BOLIN BERT
Vad gör vi med klimatet? 1979.
("What are we doing with the climate? 1979")
Förlaget Ordfront, Stockholm

15-14 MELIN RAGNAR
Hydrologi i Norden 1970.
("Hydrology in the Nordic Countries 1970")
Utbildningsförlaget, Stockholm

15-15 Monitor 1981. Försurning av mark och vatten.
("Monitor 1981. Acidification of land and water.")
National Environment Protection Ward Bulletin 3/1981.

15-16 BERGSTRÖM U, RÖJDER B, WIDEMO U
Dose and Dose Commitment Calculations from Groundwaterborne Radioactive Elements Released from a Repository for Spent Nuclear Fuel.
Studsvik Energiteknik AB.
KBS TR 83-49, May 1983.

CHAPTER 16

16-1 NATIONAL INSTITUTE OF RADIATION PROTECTION
Begränsning av utsläpp av radioaktiva ämnen från kärnkraftstationer.
("Limitation of releases of radioactive substances from nuclear power stations.")
SSI FS 1977:2

16-2 International Commission on Radiological Protection. The Metabolism of Compounds of Plutonium and other Actinides.
ICRP Publication 19 (1972).

16-3 International Commission on Radiological Protection. Alkaline Earth Metabolism.
ICRP Publication 20 (1973).

16-4 International Commission on Radiological Protection. Report of Task Group on Reference Man.
ICRP Publication 23 (1975).

16-5 International Commission on Radiological Protection. Recommendation of the International Commission on Radiological Protection.
ICRP Publication 26 (1977).

16-6 International Commission on Radiological protection. Limits for Intakes of Radionuclides by Workers.
ICRP Publication 30 Part 1-3.

16-7 ICRP Task Group Report on Lung Dynamics Deposition and Retention Models for Internal Dosimetry of the Human Respiratory Tract.
Health Physics 12, 173-207 (1966).

16-8 ICRP Task Group on Radiosensitivity of Tissues in Bone.
Publication 11 (1968).

16-9 EVE I S
A Review of the Physiology of the Gastrointestinal Tract in Relation to Radiation from Radioactive Materials.
Health Physics 12, 131-161 (1966).

16-10 DOLPHING G W and EVE I S
Dosimetry of the Gastronintestinal Tract.
Health Physics 12, 163-172 (1966).

16-11 JOHANSSON L
Oral Intake of Radionuclides in the Population. A Review of Biological Factors of Relevance for Assessment of Absorbed Dose at Long Term Waste Storage.
National Defence Research Institute KBS TR 82-14, October 1982.

16-12 RECOMMENDATIONS OF THE INTERNATIONAL COMMISSION ON RADIOLOGICAL PROTECTION
Nuclear Safety Vol 20, No. 3, p 335 (1979).